

Climate change impact and adaptation for wheat protein

Senthold Asseng¹  | Pierre Martre² | Andrea Maiorano^{2,3} | Reimund P. Rötter^{4,5} | Garry J. O'Leary⁶ | Glenn J. Fitzgerald^{7,8} | Christine Girousse⁹ | Rosella Motzo¹⁰ | Francesco Giunta¹⁰ | M. Ali Babar¹¹ | Matthew P. Reynolds¹² | Ahmed M. S. Kheir¹³ | Peter J. Thorburn¹⁴ | Katharina Waha¹⁴  | Alex C. Ruane^{15,*} | Pramod K. Aggarwal¹⁶ | Mukhtar Ahmed^{17,18} | Juraj Balkovič^{19,20}  | Bruno Basso^{21,22}  | Christian Biernath²³ | Marco Bindi²⁴ | Davide Cammarano²⁵  | Andrew J. Challinor^{26,27} | Giacomo De Sanctis^{28,†}  | Benjamin Dumont²⁹ | Ehsan Eyshi Rezaei^{30,31} | Elias Fereres³² | Roberto Ferrise²⁴ | Margarita Garcia-Vila³² | Sebastian Gayler³³ | Yujing Gao¹ | Heidi Horan¹⁴ | Gerrit Hoogenboom^{1,34} | R. César Izaurralde^{35,36} | Mohamed Jabloun³⁷ | Curtis D. Jones³⁵  | Belay T. Kassie¹ | Kurt-Christian Kersebaum³⁸ | Christian Klein³⁹ | Ann-Kristin Koehler²⁶ | Bing Liu^{40,1} | Sara Minoli⁴¹ | Manuel Montesino San Martin⁴² | Christoph Müller⁴¹ | Soora Naresh Kumar⁴³ | Claas Nendel³⁸ | Jørgen Eivind Olesen³⁷ | Taru Palosuo⁴⁴ | John R. Porter^{42,45,46} | Eckart Priesack³⁹ | Dominique Ripoche⁴⁷ | Mikhail A. Semenov⁴⁸ | Claudio Stöckle¹⁷ | Pierre Stratonovitch⁴⁸ | Thilo Streck³³ | Iwan Supit⁴⁹ | Fulu Tao^{50,44}  | Marijn Van der Velde⁵¹ | Daniel Wallach⁵² | Enli Wang⁵³ | Heidi Webber^{30,38}  | Joost Wolf⁵⁴ | Liujun Xiao⁴⁰ | Zhao Zhang⁵⁵ | Zhigan Zhao^{56,53} | Yan Zhu⁴⁰  | Frank Ewert^{30,38}

¹Agricultural & Biological Engineering Department, University of Florida, Gainesville, Florida

²LEPSE, Université Montpellier INRA, Montpellier SupAgro, Montpellier, France

³Current Address: European Food Safety Authority, Parma, Italy

⁴Tropical Plant Production and Agricultural Systems Modelling (TROPAGS), University of Göttingen, Göttingen, Germany

⁵Centre of Biodiversity and Sustainable Land Use (CBL), University of Göttingen, Göttingen, Germany

⁶Department of Economic Development Jobs, Transport and Resources, Grains Innovation Park, Agriculture Victoria Research, Horsham, Victoria, Australia

⁷Department of Economic Development, Jobs, Transport and Resources, Agriculture Victoria Research, Horsham, Victoria, Australia

⁸Faculty of Veterinary and Agricultural Sciences, The University of Melbourne, Creswick, Victoria, Australia

⁹UMR GDEC, INRA, Université Clermont Auvergne, Clermont-Ferrand, France

¹⁰Department of Agricultural Sciences, University of Sassari, Sassari, Italy

¹¹World Food Crops Breeding, Department of Agronomy, IFAS, University of Florida, Gainesville, Florida

¹²CIMMYT Int, Mexico D.F., Mexico

¹³Soils, Water and Environment Research Institute, Agricultural Research Center, Giza, Egypt

¹⁴CSIRO Agriculture and Food, Brisbane, Queensland, Australia

¹⁵NASA Goddard Institute for Space Studies, New York, New York

*Authors from P.K.A. to Y.Z. are listed in alphabetical order.

†The views expressed in this paper are the views of the author and do not necessarily represent the views of the organization or institution to which he is currently affiliated.

- ¹⁶CGIAR Research Program on Climate Change, Agriculture and Food Security, BISA-CIMMYT, New Delhi, India
- ¹⁷Biological Systems Engineering, Washington State University, Pullman, Washington
- ¹⁸Department of Agronomy, Pir Mehr Ali Shah Arid Agriculture University, Rawalpindi, Pakistan
- ¹⁹International Institute for Applied Systems Analysis, Ecosystem Services and Management Program, Laxenburg, Austria
- ²⁰Department of Soil Science, Faculty of Natural Sciences, Comenius University in Bratislava, Bratislava, Slovakia
- ²¹Department of Earth and Environmental Sciences, Michigan State University, East Lansing, Michigan
- ²²W.K. Kellogg Biological Station, Michigan State University, East Lansing, Michigan
- ²³Institute of Biochemical Plant Pathology, Helmholtz Zentrum München-German Research Center for Environmental Health, Neuherberg, Germany
- ²⁴Department of Agri-food Production and Environmental Sciences (DISPAA), University of Florence, Florence, Italy
- ²⁵James Hutton Institute, Dundee, Scotland, UK
- ²⁶Institute for Climate and Atmospheric Science, School of Earth and Environment, University of Leeds, Leeds, UK
- ²⁷Collaborative Research Program from CGIAR and Future Earth on Climate Change, Agriculture and Food Security (CCAFS), International Centre for Tropical Agriculture (CIAT), Cali, Colombia
- ²⁸GMO Unit, European Food Safety Authority, Parma, Italy
- ²⁹Department Terra & AgroBioChem, Gembloux Agro-Bio Tech, University of Liege, Gembloux, Belgium
- ³⁰Institute of Crop Science and Resource Conservation INRES, University of Bonn, Bonn, Germany
- ³¹Department of Crop Sciences, University of Göttingen, Göttingen, Germany
- ³²IAS-CSIC, University of Cordoba, Cordoba, Spain
- ³³Institute of Soil Science and Land Evaluation, University of Hohenheim, Stuttgart, Germany
- ³⁴Institute for Sustainable Food Systems, University of Florida, Gainesville, Florida
- ³⁵Department of Geographical Sciences, University of Maryland, College Park, Maryland
- ³⁶Texas A&M AgriLife Research and Extension Center, Texas A&M University, Temple, Texas
- ³⁷Department of Agroecology, Aarhus University, Tjele, Denmark
- ³⁸Leibniz Centre for Agricultural Landscape Research, Müncheberg, Germany
- ³⁹Institute of Biochemical Plant Pathology, Helmholtz Zentrum München-German Research Center for Environmental Health, Neuherberg, Germany
- ⁴⁰National Engineering and Technology Center for Information Agriculture, Key Laboratory for Crop System Analysis and Decision Making, Ministry of Agriculture, Jiangsu Key Laboratory for Information Agriculture, Jiangsu Collaborative Innovation Center for Modern Crop Production, Nanjing Agricultural University, Nanjing, China
- ⁴¹Potsdam Institute for Climate Impact Research, Member of the Leibniz Association, Potsdam, Germany
- ⁴²Plant & Environment Sciences, University Copenhagen, Taastrup, Denmark
- ⁴³Centre for Environment Science and Climate Resilient Agriculture, Indian Agricultural Research Institute, IARI PUSA, New Delhi, India
- ⁴⁴Natural Resources Institute Finland (Luke), Helsinki, Finland
- ⁴⁵Lincoln University, Lincoln, New Zealand
- ⁴⁶Montpellier SupAgro, INRA, CIHEAM-IAMM, CIRAD, University Montpellier, Montpellier, France
- ⁴⁷US AgroClim, INRA, Paris, France
- ⁴⁸Rothamsted Research, Harpenden, UK
- ⁴⁹Water & Food and Water Systems & Global Change Group, Wageningen University, Wageningen, The Netherlands
- ⁵⁰Institute of Geographical Sciences and Natural Resources Research, Chinese Academy of Science, Beijing, China
- ⁵¹Joint Research Centre, European Commission, Ispra, Italy
- ⁵²INRA UMR AGIR, Castanet-Tolosan, France
- ⁵³CSIRO Agriculture and Food, Canberra, Australian Capital Territory, Australia
- ⁵⁴Plant Production Systems, Wageningen University, Wageningen, The Netherlands
- ⁵⁵State Key Laboratory of Earth Surface Processes and Resource Ecology, Faculty of Geographical Science, Beijing Normal University, Beijing, China
- ⁵⁶Department of Agronomy and Biotechnology, China Agricultural University, Beijing, China

Correspondence

Senthil Asseng, Agricultural & Biological Engineering Department, University of Florida, Gainesville, FL.
Email: sasseng@ufl.edu

Funding information

National Research Foundation for the Doctoral Program of Higher Education of China, Grant/Award Number: 20120097110042; International Food Policy

Abstract

Wheat grain protein concentration is an important determinant of wheat quality for human nutrition that is often overlooked in efforts to improve crop production. We tested and applied a 32-multi-model ensemble to simulate global wheat yield and quality in a changing climate. Potential benefits of elevated atmospheric CO₂ concentration by 2050 on global wheat grain and protein yield are likely to be negated by impacts from rising temperature and changes in rainfall, but with considerable

Research Institute (IFPRI); Global Futures and Strategic Foresight project; CGIAR Research Program on Climate Change, Agriculture and Food Security (CCAFS); CGIAR Research Program on Wheat; EU Marie Curie FP7 COFUND People Programme; French National Institute for Agricultural Research; National High-Tech Research and Development Program of China; Priority Academic Program Development of Jiangsu Higher Education Institutions; National Natural Science Foundation of China, Grant/Award Number: 41571088, 41571493; German Ministry for Research and Education (BMBF); Rothamsted Research; Biotechnology and Biological Sciences Research Council; Innovation Fund Denmark; China Scholarship Council; Italian Ministry for Agricultural, Food and Forestry Policies; Ministry of Agriculture and Forestry (MMM); Academy of Finland; German Ministry for Research and Education (BMBF); Victorian Department of Economic Development, Jobs, Transport and Resources; Australian Department of Agriculture and Water Resources; University of Melbourne; Grains Research Development Corporation, Australia; Federal Ministry of Food and Agriculture; German Science Foundation

disparities between regions. Grain and protein yields are expected to be lower and more variable in most low-rainfall regions, with nitrogen availability limiting growth stimulus from elevated CO₂. Introducing genotypes adapted to warmer temperatures (and also considering changes in CO₂ and rainfall) could boost global wheat yield by 7% and protein yield by 2%, but grain protein concentration would be reduced by −1.1 percentage points, representing a relative change of −8.6%. Climate change adaptations that benefit grain yield are not always positive for grain quality, putting additional pressure on global wheat production.

KEYWORDS

climate change adaptation, climate change impact, food security, grain protein, wheat

1 | INTRODUCTION

If current trends in human population growth and food consumption continue (Bajželj et al., 2014), crop production must be increased by 60% by mid-century to meet food demands and reduce hunger (Godfray et al., 2010), but climate change will make this task more difficult (Olesen et al., 2011; Porter et al., 2014; Waha et al., 2013; Wheeler & Von Braun, 2013). Crop models are used to simulate crop growth and development from local up to global scales to assist in climate change impact assessments (Chenu et al., 2017) and to evaluate agricultural adaptation options (Ruiz-Ramos et al., 2017), for example, to investigate potential effects of altering crop management, like sowing crops earlier or later in the season (Porter et al., 2014) or growing cultivars with different crop traits (Semenov & Stratonovitch, 2015; Tao, Rotter, et al., 2017). A growing number of studies describe climate change impacts on crop yield, but the impacts on the nutritional value of the crops have received much less attention even though this is a critical aspect of food security (Haddad et al., 2016). Grain protein concentration, the ratio of grain protein amount to grain yield, is an important characteristic affecting the nutritional quality but also the end-use value and baking properties of wheat flour (Shewry & Halford, 2002). Globally, wheat provides 20% of protein for humans (Tilman, Balzer, Hill, & Befort, 2011). Grain protein concentration, like yield, depends on a combination of factors such as the crop

genotype, soil, crop management, atmospheric CO₂ concentration and weather conditions (Triboi, Martre, Girusse, Ravel, & Triboi-Blondel, 2006; Wieser, Manderscheid, Erbs, & Weigel, 2008). Elevated CO₂ concentration alone can increase the total amount of protein in grain (Broberg, Högy, & Pleijel, 2017), but reduces its concentration (Broberg et al., 2017; Myers et al., 2014). Grain protein concentration increases with drought stress and higher temperatures as a result of reduced starch accumulation (Triboi et al., 2006).

We aimed to systematically study the combined effects of CO₂, water, nitrogen (N) and temperature on wheat grain protein concentration in a changing climate for the world's main wheat producing regions as part of the Agricultural Model Intercomparison and Improvement Project (AgMIP) (Rosenzweig et al., 2013). This is the most comprehensive study ever done of the effect of climate change on yield and the nutritional quality of one of the three major sources of human food security and nutrition (the others being rice and maize). We previously demonstrated that large ensembles of wheat models accurately simulate wheat yield under different environmental conditions, and especially under high temperatures (Asseng et al., 2015). Here, we used a crop model ensemble to estimate the impact of climate change and a potential adaptation to such changes on global grain protein. To see if crop models can simulate the impact of climate change

adequately, we first tested whether an ensemble of 32 different wheat models could reproduce the effects of increased temperature, heat shocks, elevated atmospheric CO₂ concentration, water deficit and the combination of these factors on yield and particularly on grain protein. As there have been many climate change impact studies without adaptation and studies testing the sensitivity of hypothetical traits, here, we included a trait adaptation option based on realistic traits from a wide range of field observations that justify the existence of unique heat stress tolerance traits in wheat.

2 | MATERIALS AND METHODS

2.1 | Crop models

Thirty-two wheat crop models (Supporting Information Table S1) were compared within the Agricultural Model Intercomparison and Improvement Project (AgMIP; www.agmip.org), using two data sets from quality-assessed field experiments (sentinel site data) and then applied at representative locations across the world. 18 of these models simulated grain protein. All model simulations were executed by the individual modeling groups.

2.2 | Field experiments for model testing

Two field/chamber experiments (INRA, FACE Australia) were used for model testing.

2.2.1 | INRA temperature experiment

The response of the winter wheat cultivar *Récital* to heat shocks (i.e., 2–4 consecutive days with maximum air temperature of 38°C) during the grain filling period was studied during three winter growing seasons at INRA Clermont-Ferrand, France (45.8°N, 3.2°E, 329 m elevation) (Majoul-Haddad, Bancel, Martre, Tribol, & Branlard, 2013; Tribol & Tribol-Blondel, 2002). For details see Supporting Information Data S1.

2.2.2 | FACE Australia experiment (CO₂ × temperature × water)

FACE data were obtained from selected treatments from a designed experiment from Horsham, Australia (36.8°S, 142.1°E, 128 m elevation) (Supporting Information Table S3). Details presenting the experimental design (Mollah, Rm, & Huzzey, 2009), the experimental data (Fitzgerald et al., 2016), and modeling analyses (O'Leary et al., 2015) have previously been published. Data were collated from one cultivar (cv. Yitpi) under two water regimes (rain-fed and supplemental irrigation), two nitrogen fertilization regimes (53 or 138 kg N ha⁻¹), and two sowing dates to create two growing season temperature environments for both daytime ambient (365 ppm) and elevated (550 ppm) atmospheric CO₂ concentrations. For details see Supporting Information Data S1.

2.3 | Field experiments for adaptation

Asseng et al. (2015) recently suggested a combination of delayed anthesis with an increased grain filling rate as possible adaptation for wheat to increased temperature. Such trait combination has never been shown yet to exist in the current available genetic material. Therefore, here we first explored a wide range of existing field experiments. We selected field experiments where a number of cultivars were grown across different temperature environments to search for the existence of such trait combination and if such cultivars are indeed better adapted to a warming climate, that is, these cultivars yield higher than other cultivars under warmer conditions. In these data sets, we looked for pairs of cultivars where one or more had a delayed anthesis in a warmer environment combined with an increased grain filling rate, and yielded higher in the warmer environment than a control cultivar (without these traits). Only the cultivar pairs which fulfilled these conditions are mentioned here. Four field experiments were considered and included experiments from Egypt, Italy, USA and CIMMYT. In each experiment, cultivars were compared under growing environments with increasing temperatures (through delayed sowing or growing at warmer locations). The Egypt experiment included three cultivars grown over 3 years under full irrigation (and sufficient N) across four temperature environments along the River Nile with two sowing dates. The Italy experiment included two cultivars grown over 2 years under full irrigation (and sufficient N) at one location with two sowing dates. In the Italy experiment, the same experiment was repeated with N limitations. The USA experiment included four cultivars (three cultivars were used as a control) grown for 1 year under full irrigation (and sufficient N) across 11 temperature environments along a transect in the south-east US with one sowing date. The CIMMYT experiment included data from the International Heat Stress Genotype Experiment (IHSGE) (Reynolds, Balota, Delgado, Amani, & Fischer, 1994), with two cultivars grown over 2 years under full irrigation (and sufficient N) across six temperature environments (experiments in different countries) with two sowing dates. For details see Supporting Information Data S1.

2.4 | Global impact assessment

The two main scaling methods most commonly used in climate change impact assessment studies are sampling and aggregation (Ewert et al., 2011, 2015). In sampling, the simulated points are assumed to represent an area (van Bussel et al., 2016, 2015), while in aggregation, an area is simulated with grid cells (Porwollik et al., 2017) or polygons assuming a grid cell (or polygon) is equal to a point. Each method differs in uncertainties with respect to input information (high in gridded simulation (Anderson, You, Wood, Wood-Sichra, & WU WB, 2015), less in sampling as true point data are used) and representation of heterogeneity (high in gridded simulation, less in sampling which however depends on the sampling strategy (Zhao et al., 2016)). We have chosen stratified sampling, a guided sampling method which improves the scaling quality (van

Bussel et al., 2016), with several points per wheat mega region (Gbegbelegbe et al., 2017). During the upscaling, a simulation result of a location was weighted by the production a location represents (Asseng et al., 2015). Liu et al. (2016) recently showed that stratified sampling and weighted by the production with thirty locations across wheat mega regions resulted at country and global scale in similar temperature impact and uncertainty as aggregation of simulated grid cells. The uncertainty due to sampling decreases with increasing number of sampling points (Zhao et al., 2016). We therefore doubled the thirty locations from Asseng et al. (2015) to sixty locations (Figure 1; Supporting Information Table S4) covering contrasting conditions across all wheat mega regions. All models provided simulations for thirty high-rainfall or irrigated wheat-growing locations (Locations 1–30, simulated with no water or nitrogen limitations), representing about 68% of current global wheat production and thirty low-rainfall wheat-growing locations with wheat yields below 4 t DM ha⁻¹ (Locations 31–60), representing about 32% of current global wheat production (Reynolds & Braun, 2013). Each location represents an important wheat-growing area worldwide (Figure 1).

Additional details about the locations 1–30 can be found in (Asseng et al., 2015). In contrast to the high-rainfall locations 1–30, soil types and N management vary among the low-rainfall locations 31–60 (Supporting Information Figures S1–4). For details see Supporting Information Data S1.

2.5 | Climate scenarios

There were two steps in global impact simulations. In step 1, six scenarios were simulated for the sixty global locations and 30 years of climate. The six climate scenarios had a baseline climate (1981–2010) or baseline climate with main daily temperature increased by

2 or 4°C, crossed with two atmospheric CO₂ concentrations, 360 and 550 ppm (Table 1).

The baseline (1980–2010) climate data are from the AgMERRA climate dataset (Ruane, Goldberg, & Chrissanthacopoulos, 2015), which combines observations, data assimilation models, and satellite data products to provide daily maximum and minimum temperatures, solar radiation, precipitation, wind speed, vapor pressure, dew point temperatures, and relative humidity corresponding to the maximum temperature time of day for each location. These data correspond to carbon dioxide concentration ([CO₂]) of 360 ppm. The Baseline +2°C and Baseline +4°C scenarios were created by adjusting each day's maximum and minimum temperatures upward by that amount and then adjusting vapor pressure and related parameters to maintain the original relative humidity at the maximum temperature time of day. Observations and projections of climate change indicate that relative humidity is relatively stable even as this implies increases in specific humidity as temperatures increase (commensurate with the Clausius-Clapeyron equation; [Allen & Ingram, 2002]).

In a second step, wheat production in the sixty global locations was simulated under a climate change scenario corresponding to relatively high emissions for the middle of the 21st century (RCP8.5 for 2040–2069, using 571 ppm [CO₂] at 2055 from RCP8.5). Projections were taken from five global climate models (GCMs) (HadGEM2-ES, MIROC5, MPI-ESM-MR, GFDL-CM3, GISS-E2-R), with historical conditions modified to reflect projected changes in mean temperatures and precipitation along with shifts in the standard deviation of daily temperatures and the number of rainy days (Supporting Information Figures S7–8). These scenarios were created using the “Enhanced Delta Method” (Ruane, Winter, Mcdermid, & Hudson, 2015), and GCMs were selected to include models with relatively large and relatively small global sensitivity to the greenhouse gases that drive

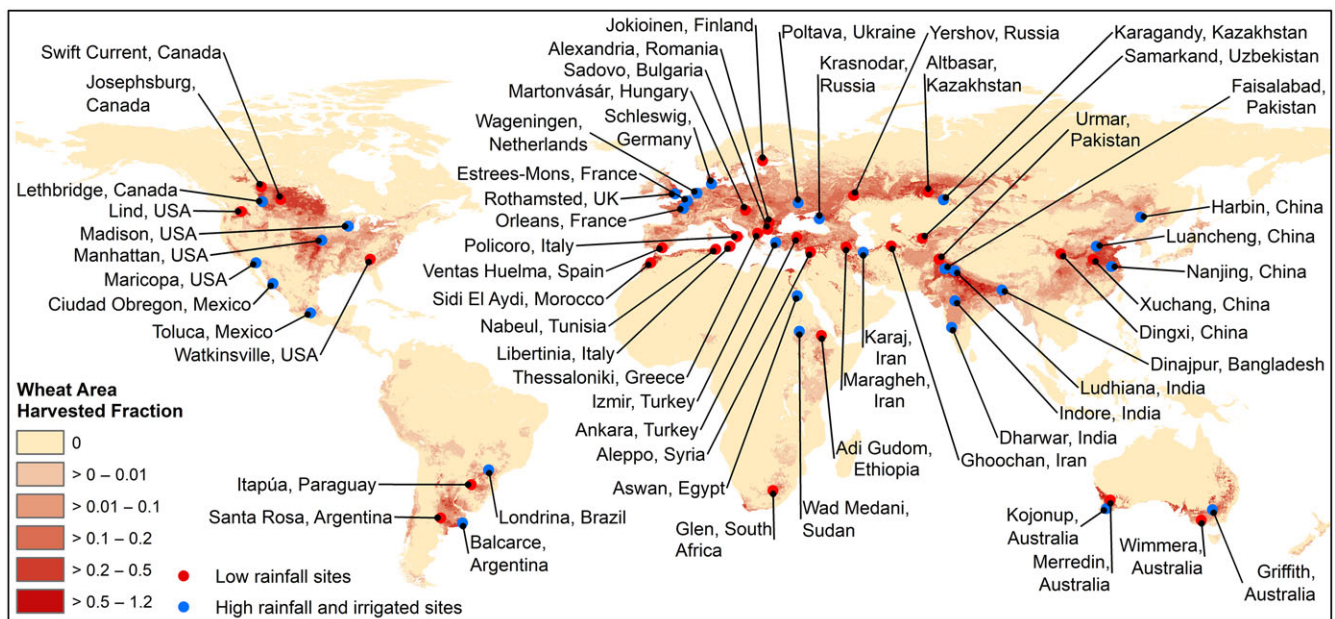


FIGURE 1 The thirty locations representing high-rainfall and irrigated wheat regions (blue) and thirty locations representing low-rainfall/low-input regions (red) of the world used in this study. Wheat area from (Monfreda, Ramankutty, & Foley, 2008)

TABLE 1 Outline of the baseline and climate change scenarios simulated in this study

Period	Scenario/GCM	CO ₂ (ppm)	Adaptation
1981–2010	Baseline	360	None
1981–2010	Baseline	360	2-traits combination
1981–2010	Baseline +2°C	360	None
1981–2010	Baseline +4°C	360	None
1981–2010	Baseline	550	None
1981–2010	Baseline +2°C	550	None
1981–2010	Baseline +4°C	550	None
2040–2069	HadGEM2-ES	571	None
2040–2069	MIROC5	571	None
2040–2069	MPI-ESM-MR	571	None
2040–2069	GFDL-CM3	571	None
2040–2069	GISS-E2-R	571	None
2040–2069	HadGEM2-ES	571	2-traits combination
2040–2069	MIROC5	571	2-traits combination
2040–2069	MPI-ESM-MR	571	2-traits combination
2040–2069	GFDL-CM3	571	2-traits combination
2040–2069	GISS-E2-R	571	2-traits combination

climate changes to account for the uncertainty of the fifth coupled model intercomparison project (CMIP5) GCMs ensemble (Ruane & McDermid, 2017).

Each scenario was examined with current management as well as under one possible trait adaptation, a cultivar combining delayed anthesis and an increased potential grain filling rate. Therefore, there were 11 treatments and each was simulated for 30 years at each of the sixty locations.

To consider the diversity of model approaches of the 32 participating wheat models and allow all modelers to incorporate their models, we proposed a simple but still physiological-based trait combination. The proposed traits were simulated in full combination only, to quantify the impact of such a trait combination. The aim of this study was not to analyze the contribution of various individual traits, nor to explore the full range of traits that could possibly assist in an adaptation strategy.

The proposed simple trait combination to minimize the impact of future increased temperatures on global yield production included (Supporting Information Table S6):

1. Delay anthesis by about 2 weeks under the Baseline scenario via increased temperature sum requirement, photoperiod sensitivity, or vernalization requirement. No change in the temperature requirement for grain filling duration was considered.
2. Increase in rate (in amount per day) of potential grain filling by 20% (escape strategy).

2.5.1 | Testing the climate change response of models without N dynamics

Simulation results from all 32 models were used in the grain yield impact analysis. When analyzing the impacts on grain protein yield

and protein concentration, only 18 crop models were used that had routines to simulate crop N dynamics leading to grain protein and had been previously tested with field measurements. The yield distributions and yield impacts simulated with the 32 models and the 18 models used in protein analysis were similar (Supporting Information Figures S10–11).

We also applied the Kolmogorov–Smirnov two-sample test to test the differences in the distributions of simulated yield impacts from the 18 models (used in the protein analysis) and the 32 models. The distributions of climate change impacts on grain yields were different for the two multi-model ensembles for the climate change scenarios with genetic adaptation, but not without the genetic adaptation and for the trait effect (Supporting Information Table S7).

2.5.2 | Aggregation of local climate change to global wheat production impacts

Before aggregating local impacts at sixty locations to global impacts (Figure 1), we determined the actual production represented by each location. The total wheat production for each country came from FAO country wheat production statistics for 2014 (www.fao.org). For each country, wheat production was classified into three categories (i.e., high rainfall, irrigated, and low rainfall). The ration for each category was quantified based on the Spatial Production Allocation Model (SPAM) dataset (<https://harvestchoice.org/products/data>). For some countries where no data were available through the SPAM dataset, we estimated the ratio for each category based on the country-level yield from FAO country wheat production statistics. The high-rainfall production and irrigated production in each country were represented by the nearest high-rainfall and irrigated locations (Location 1–30). Low-rainfall production in each country was represented by the nearest low-rainfall locations (Location 31–60).

The global wheat grain and protein production impact was calculated using the following steps:

1. Calculate the relative simulated mean yield (or protein yield) impact for climate change scenarios for 30 years (1981–2010) per single model at each location.
2. Calculate the *median across 32 models* (or 18 in case of protein simulations) *and five GCMs per location (multi-model [CMs and GCMs] ensemble median)*. Note that CMs and GCMs simulation results were kept separate only for calculating the separate CM and GCM uncertainties (expressed as range between 25th and 75th percentiles).
3. Calculate the absolute regional production loss by multiplying the relative yield (or protein yield) loss from the multi-model ensemble median with the production represented at each location (using FAO country wheat production statistics of 2014 from www.fao.org, the latest reported yield statistics available at the time of the study). Calculate separately for high-rainfall/irrigated and low-input rainfed production. This assumes that the selected simulated location is representative of the entire wheat-growing region surrounding this location.

4. Add all regional production losses to the total global loss.
5. Calculate the relative change in global production (i.e., global production loss divided by current global production).
6. Repeat the above steps for the 25th and 75th percentile relative global yield (or protein yield) impact from the 32 (or 18 in case of protein simulations) model ensemble.

The 18-model ensemble used for protein simulations simulated similar yield impacts compared to the 32-model ensemble (Supporting Information Table S7), but small yield differences between the two ensembles made it necessary to normalize the simulated impacts from the two ensembles for the calculation of impacts on grain protein concentration. The reported impacts on grain protein concentration are therefore the normalized numbers. The 32-model ensemble yield impacts and the simulated 18-model ensemble relative grain protein yield impacts are directly reported (i.e., without this normalizing). The calculation of changes in grain protein concentration is shown with equations below.

Yield change (y_c), due to climate change or the introduction of a trait, was calculated as: $y_c = \tilde{y}_{\text{future}}^{(32)} / \tilde{y}_{\text{baseline}}^{(32)}$

$$y_c = \tilde{y}_{\text{future}}^{(32)} / \tilde{y}_{\text{baseline}}^{(32)} \quad (1)$$

where $\tilde{y}_{\text{future}}^{(32)}$ and $\tilde{y}_{\text{baseline}}^{(32)}$ are respectively future (with or without adaptation) and Baseline yield as simulated by the median of 32 models. Grain protein yield change (p_c) is calculated as:

$$p_c = \tilde{p}_{\text{future}}^{(18)} / \tilde{p}_{\text{baseline}}^{(18)} \quad (2)$$

where $\tilde{p}_{\text{future}}^{(18)}$ and $\tilde{p}_{\text{baseline}}^{(18)}$ are respectively future (with or without adaptation) and baseline protein yield as simulated by the median of 18 models.

Impact on grain protein concentration uses global mean grain yield in 2014 as a baseline, reported as 3.31 t DM ha⁻¹ (FAO,) and a mean grain protein percentage of 13% (based on dry matter grain weight), which is a weighted average of the simulated results. While there are no global statistics on grain protein, the simulated global grain protein concentration appears reasonable, considering the protein content in the USDA World Wheat Collection has been reported to range from 7% to 22% of the dry weight (Vogel, Johnson, & Mattern, 1976), but generally varies from about 10%–15% of the dry weight for wheat cultivars grown under field conditions (Shewry & Hey, 2015). Observed grain protein content in temperate regions, like the Netherlands has been reported to range from 10% to 15% (Asseng, Keulen, & Stol, 2000)). An average of 13.2% (ranging from 10.5% to 16.3%) grain protein concentration has been reported across 330 wheat varieties from China grown during 2010–2011 (Yang, Wu, Zhu, Ren, & Liu, 2014) and an average of 13.4% was reported across wheat fields in Finland during 1988–2012 (Peltonen-Sainio, Salo, Jauhainen, Lehtonen, & Sievilainen, 2015).

In the simulated weighted average, the mean of the high-rainfall/irrigated locations 1–30 has a weight of about 2/3, and the mean of the low-rainfall/low-input locations 31–60 has a weight of about 1/3, according to their contribution to global production. The impact on grain protein concentration ($\Delta GP\%$) was calculated as follows:

$$\Delta GP\% = \frac{p_c \times 3.31 \times 0.13}{y_c \times 3.31} - \frac{3.31 \times 0.13}{3.31} = 0.13 \left(\frac{p_c}{y_c} - 1 \right) \quad (3)$$

This results in a change in grain protein concentration of –0.59 percentage point when using the changes in grain yield from 32 crop models as used in the analysis. Alternatively, using the changes in yield from the 18 crop models would result in a change in grain protein concentration of –0.36 percentage point (not used here).

3 | RESULTS

3.1 | Model testing

Results of crop model simulations were compared to observations from outdoor chamber and free-air CO₂ enrichment (FACE) experiments with increased temperature, heat shocks, and elevated CO₂ combined with increased temperature and drought stress. A statistical analysis on model ensemble performance for grain yield, grain protein yield and grain protein content is given in Table S4, showing RMSE for yield from 0.4 to 1.9 t/ha, with reasonable skill (EF) to simulate the variability for observed yield. RMSE for protein concentration ranged from 0.8% to 3.2% with poor skill due to the low variability in the observed protein concentration data (Table S4). Median predictions from this multi-model ensemble reproduced observed grain yields well including those affected by heat shock, high temperature or elevated CO₂ concentration (Figure 2a–c). Continuous high temperature conditions during the grain filling period (the period when the grain grows) reduced observed and simulated biomass growth and yield more than a 4-day heat shock, applied at different times during the same growth period, but elevated CO₂ increased biomass growth and yield in the observations and simulations. In addition, changes in grain protein yield and protein concentrations were captured well (i.e., similar response in simulations and observations) even under conditions where effects of temperature interacted with effects of CO₂ concentration and water (Figure 2d–i). The multi-model ensemble median and at least 50% of the simulation results for growth dynamics, final grain and protein yield, and protein concentration were generally within the uncertainty intervals of the measurements (Figure 2).

3.2 | Observed adaptation traits for climate change

Using datasets from observed field experiments (not simulations) at different locations in the world (in USA, Mexico, Egypt, Sudan and Italy), we found in these observations that existing genotypes with a trait of an extended growing period to delay anthesis (also called flowering), combined with a trait with a higher rate of grain filling (i.e., potential grain filling rate which is met when assimilates are available from photosynthesis and/or remobilization), are effective in countering some of the yield declines occurring in non-adapted cultivars when grown in warmer locations or during a warmer part of a season (Figure 3a). Other cultivars which had a delayed anthesis but not an increase grain filling rate (not shown here), did not yield

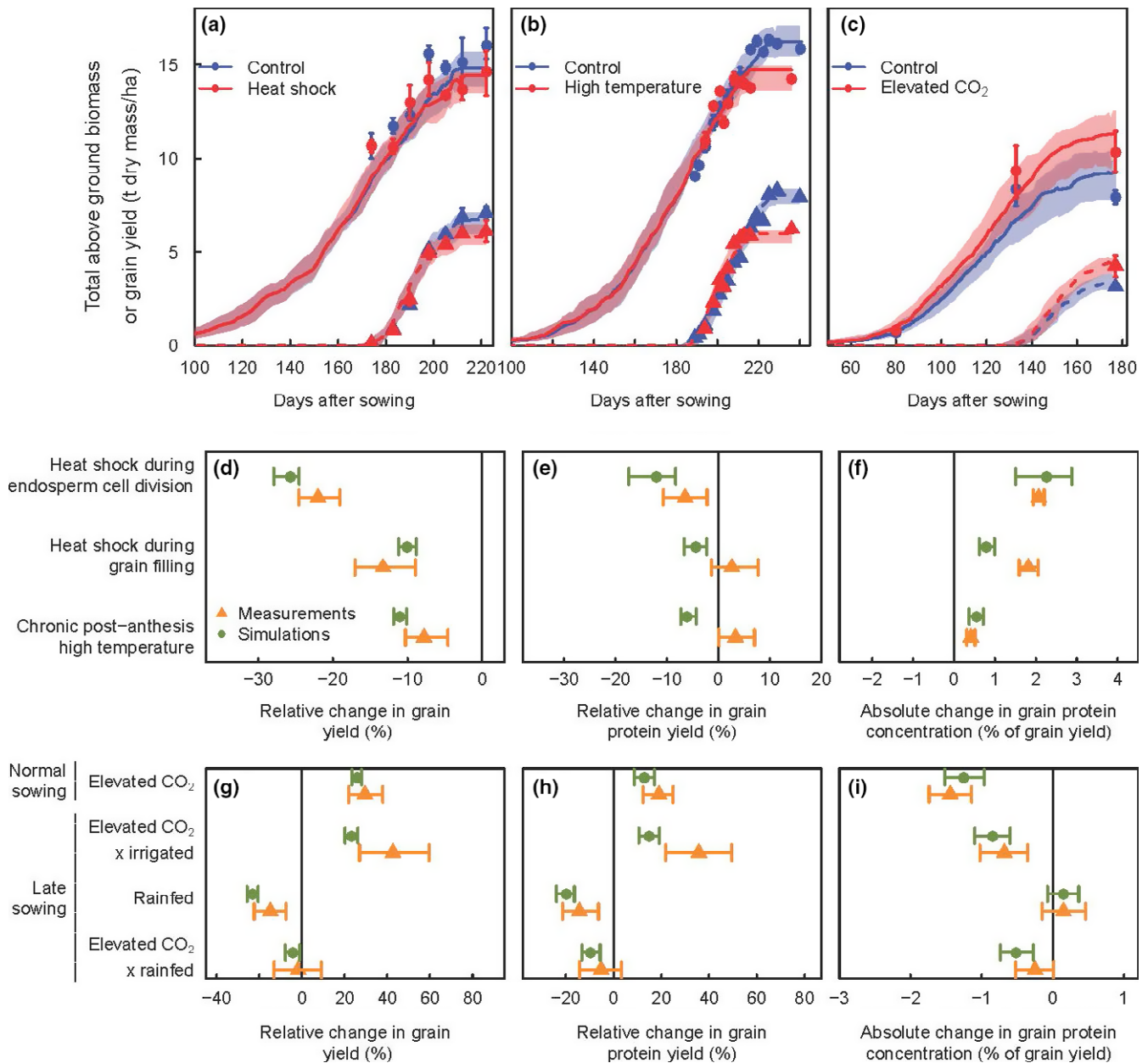


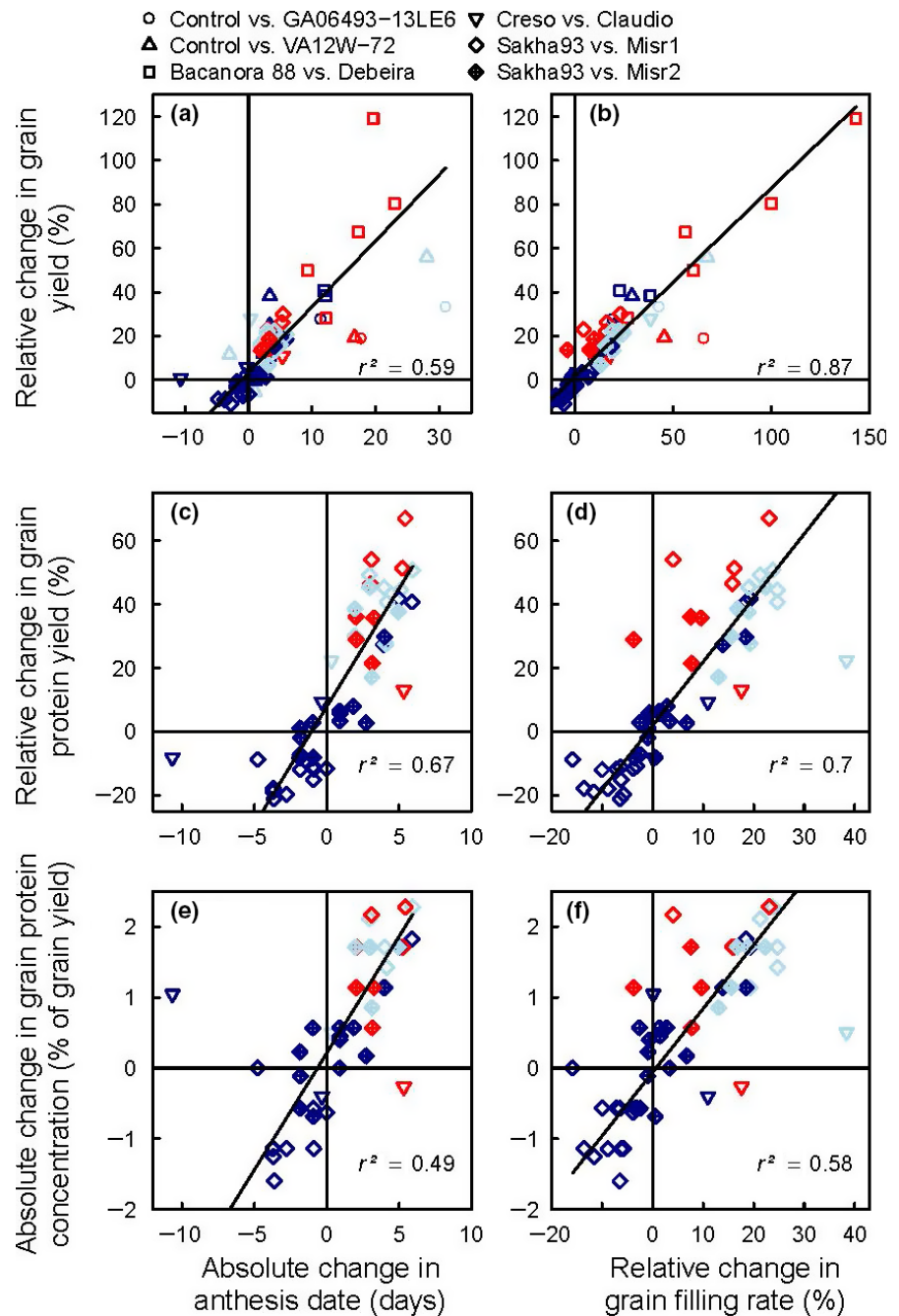
FIGURE 2 Measurements and multi-model simulations of total aboveground wheat biomass, grain yield, grain protein yield and grain protein concentration for wheat treated with heat shocks, higher temperature, elevated atmospheric CO₂ concentration, and different sowing times or irrigation. (a, b and c) Total aboveground biomass (circles, continuous lines) and grain yields (triangles, dashed lines) for wheat for three different experiments grown in control conditions or with (a) heat shocks of 38°C for 4 hr on 4 consecutive days during grain filling; (b) continuous +10°C/+5°C (day/night) temperature increase during endosperm cell division/early grain filling; and (c) elevated CO₂ (550 ppm). Multi-model ensemble medians (lines) and 25th to 75th percentile intervals (shaded areas) based on 32 simulation models are shown. Symbols indicate medians and error bars the 25th to 75th percentile intervals of measurements. (d to i) Percent changes in grain yield (d and g) and protein yields (e and h) and absolute changes in grain protein concentration (f and i) in response to chronic high temperature or heat shocks at different developmental stages (d, e and f) and different combinations of atmospheric CO₂ concentration, drought and sowing dates (g, h and i). Data are medians of measured or simulated changes and error bars show 25th to 75th percentile intervals. In all panels, simulations are the median of the 32 (grain yield) or 18 (grain protein) wheat model ensembles

higher than the non-adapted cultivars. For some locations, where observed grain protein data were available, the combination of delayed anthesis and higher rate of grain filling traits also increased grain protein yield in one cultivar compared to another cultivar (but for several cultivar pairs) when grown under warmer growing

conditions, although these traits were not fully expressed under cooler conditions (Figure 3b).

Observed grain and protein yield increased with this trait combination in warmer climates, but not when N supply was limited (Figure 4).

FIGURE 3 Comparison of the relative performance of measured wheat genotypes with or without both delayed anthesis and accelerated grain filling traits grown under field conditions at different temperatures. Changes in measured grain yield (a and b), grain protein yield (c and d), and grain protein concentration (e and f) vs. changes in traits. Symbol colors indicate mean temperatures during the growing season (from sowing to maturity) at each location in increasing order from deep blue, light blue, to red. The advanced wheat lines VA12W-72 and GA06493–13LE6 were compared to the standard cultivars AGS2000, Jamestown, and USG3120 in experiments at 10 locations in the United States. Mean values for AGS2000, Jamestown and USG3120 were used as the control to calculate changes in yield and protein. The modern cultivar Bacanora 88 and the standard cultivar Debeira were grown at one location in Mexico over two consecutive seasons, and at one location in Egypt and one in Sudan both for one season. The cultivars Creso and Claudio were grown at one location in Italy for two consecutive growing seasons. The modern elite cultivars Misr1 and Misr2 and the standard cultivar Sakha93 were grown at four locations in Egypt. Grain protein data were available for Italy and Egypt experiments only. Solid lines are standardized major axis regressions (all $p < 0.001$)



However, the relative change in observed grain yield was positively correlated with the change in grain protein concentration, even under limited nitrogen supply (Figure 5).

3.3 | Global climate change impact

Availing of a robust predictor with a multi-model ensemble (Figure 2) and evidence from field experiments for the existence for traits to counteract detrimental effects from raising temperature on crops (Figures 3–5), we assessed with crop models what impact climate change would have on overall wheat grain and protein yield and on protein concentration at other locations

and globally (Figure 1). The 32 tested crop models were applied with five bias-corrected global climate models (GCMs) for the representative concentration pathway 8.5 (RCP8.5) for the 2050 s. The multi-model median (crop models plus GCMs) impact of climate change and the variation across crop models and GCMs is shown for sixty locations around the globe representing major wheat producing regions and climate zones (Figure 6). In general, low- and mid-latitude locations show negative yield impacts from climate change, while high-latitude locations show some positive yield impacts. Negative impacts on protein yields were predicted at many locations, including high-latitude locations (Figure 6a).

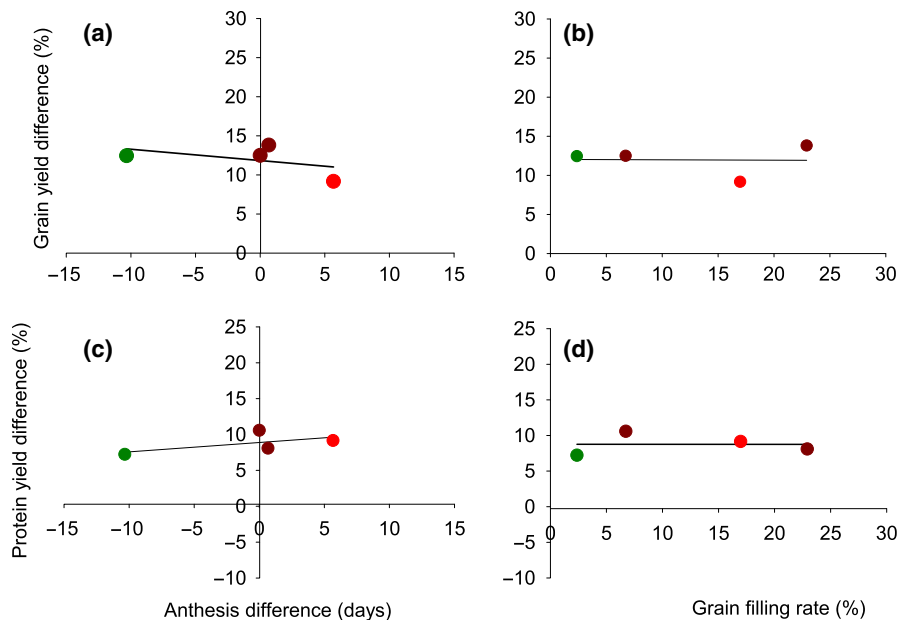


FIGURE 4 Comparison of cultivars with delayed anthesis and accelerated grain filling rate to standard cultivars in different temperature environments in Italy with limited nitrogen (60 kg N ha^{-1}). Relationship of observed (a and b) grain yield and (c and d) protein yield to (a and c) anthesis and (b and d) to grain filling rate. Green ($<13^\circ\text{C}$), dark red (13 to 15°C) and red ($> 15^\circ\text{C}$)

3.4 | Effect of adaptation

The field-identified trait combination of delayed anthesis and increased grain filling rate was introduced into the crop models (Supporting Information Table S6). Simulated yields did not improve in many of the low-rainfall/low-input locations due to a combination of terminal drought and N limitation (Figure 4). Protein yields that increased with the introduced trait combination were negatively affected by climate change for many locations, including those at high latitudes (Figure 6). But grain yields were improved in most locations with the trait combination of delayed anthesis and increased grain filling rate (Figure 6b).

The impact of climate change on grain protein concentration, which varies with both grain yield and protein yield, was more variable. Grain protein concentration varied between growing seasons and locations as did the response to climate change and the impact of the adapted trait combination (Figure 7). While the combined impact of increased temperature, elevated CO_2 concentration, and change in rainfall for RCP8.5 indicates that grain yield would increase for many seasons and locations, protein yield increase would not keep pace. This would result in a reduction in grain protein concentration for many situations (Figure 7). However, climate change and the adapted trait combination could lead to an increase in grain protein concentration for low-rainfall locations, particularly for those locations where yield is projected to decline (Figure 7).

We scaled the simulated impacts up from fields to globe by weighting each location with reported country wheat production data. Despite the stimulating effect of elevated CO_2 on crop growth, global wheat production would only increase by 2.8% (-7.4 to $+14.0\%$, 25th to 75th percentile range combining crop model and GCM uncertainty) by 2050 under RCP8.5. Most of the gains from elevated CO_2 on crop growth will be lost due to increasing

temperature. Simultaneously introducing the trait combination of delayed anthesis and increased grain filling rate could increase global yield to 9.6% (-7.8 to 27.0%) by 2050, with the impact from traits being 6.8%.

The growth stimulus from a 100-ppm increase in atmospheric CO_2 concentration is lost with an increase of about 2°C (increase of 1.0 to 4.2°C , 25th to 75th percentile range of crop model uncertainty) according to the simulated multi-model ensemble median (Figure 8).

However, when N limited growth, as is common for low-rainfall environments with low-fertilizer inputs, the growth stimulus was reduced. The multi-model ensemble median, averaged over 30 years, shows a CO_2 effect of 8.4% global yield increase (5.7% to 12.8% for 50% of crop models, weighted by production) per 100 ppm increase in CO_2 (Figure 8). Protein yields were estimated to change by -1.9% (-9.6% to $+5.5\%$ change, 25th to 75th percentile range combining crop model and GCM uncertainty) at the global scale with climate change, with many regions expected to be affected. Crop models account for a dilution of crop N and grain protein concentration at elevated CO_2 concentration (Figure 9). When the trait combination of delayed anthesis and increased grain filling was introduced, simulated global protein yield changed to -0.2% (-12.1% to $+12.0\%$ change) by 2050, with the impact from traits being 1.7%. Similarly, while extremely variable between locations and seasons (Figure 7), protein concentration is estimated to change by -0.6 percentage points, representing a relative change of -4.6% (-0.3% to -1.0% points, representing a relative change of -2.4% to -7.5%) by 2050 at the global scale. Greater losses in protein concentration would occur in many regions and seasons, amounting to -1.1 percentage points, representing a relative change of -8.6% (-0.6% to -1.5% points, representing a relative change of -4.7% to -11.8%), with the impact from traits being -0.5 points, representing a relative change of -4.1% .

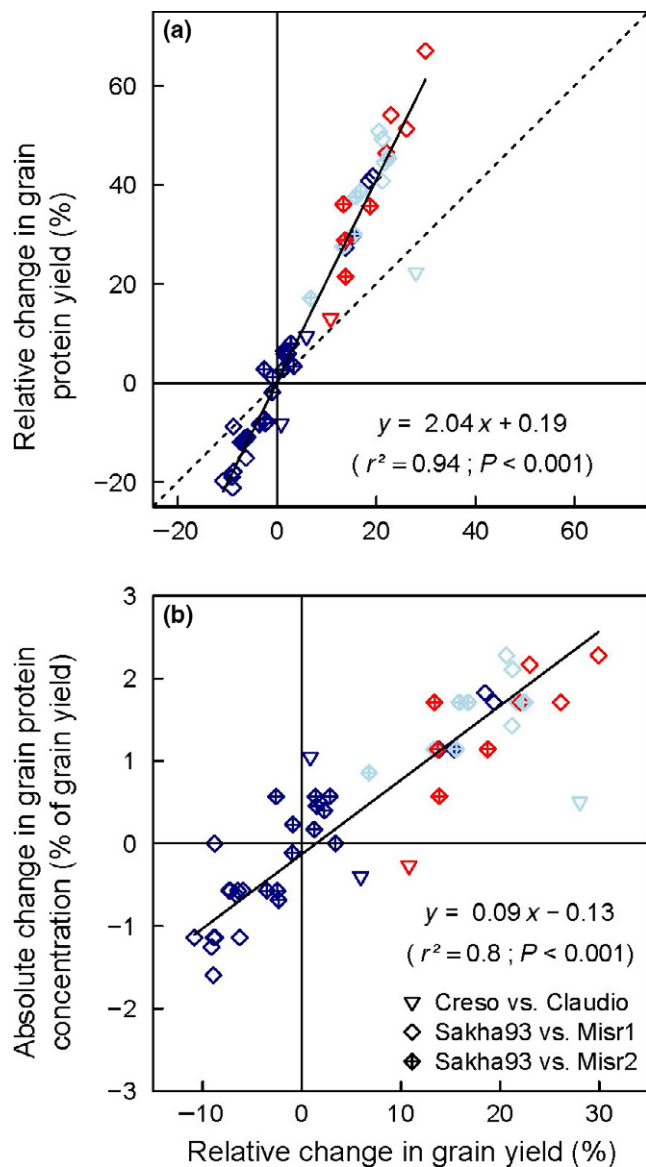


FIGURE 5 Comparison of wheat genotypes with delayed anthesis and accelerated grain filling rate compared to standard genotypes grown in the field in different temperature environments. Relative change in measured grain protein yield (a) and absolute change in grain protein concentration (b) against the relative change in grain yield. Symbol colors refer to mean temperature during growing season (planting to maturity) in increasing order from deep blue, light blue, to red for average temperatures at each location. The cv. Creso and the cv. Claudio were grown at one location in Italy for two consecutive growing seasons, and the modern elite cultivars Misr1 and Misr2 and the standard cultivar Sakha93 were grown at four locations in Egypt. Dashed line is 1:1 and solid lines are standardized major axis regressions

3.5 | Impact uncertainty

For the simulated impact estimates, the share of uncertainty from crop models was often larger than from the five bias-corrected GCMs (Supporting Information Figure S12). Uncertainties tended to increase with adaptation and were larger for impact estimates for

protein yield than for grain yield. The largest crop model uncertainties were for low- and mid-latitude areas (Supporting Information Figure S12).

4 | DISCUSSION

4.1 | Model testing

Median predictions from this multi-model ensemble reproduced observed grain yields well, consistent with other multi-model ensemble studies (Asseng et al., 2013; Bassu et al., 2014; Li et al., 2015; Martre et al., 2015), but here including those affected by heat shock, high temperature and elevated CO_2 concentration, a critical pre-request for simulating climate change impacts. Heat shock and high temperature interaction with elevated CO_2 concentration have never been tested with any impact model before. Multi-model ensemble simulations were recently compared with historical yields and showed that simulated yield impacts from temperature increase were similar to statistical temperature yield impact trends based on historical sub-country, country, and global yield records (Liu et al., 2016). This result suggests that interactions between climate and crop models can be insensitive to the methods chosen; thus, further supporting the use of the state-of-the-art multi-model ensembles such as the one used for this study.

Grain protein concentration is suggested by the simulation to decline globally by -1.1% points, representing a relative change of -8.6% , due to the simulated yield increase (for most locations) from elevated atmospheric CO_2 and the yield-improving trait adaptation. Attributing changes in observed protein trends is often hindered by many confounding factors in the field. For example, a study across fields in Finland from 1988 to 2012 showed a decline in grain protein concentration over this period of up to -0.7 grain protein % during the last third of this period (Peltonen-Sainio et al., 2015). Some of this declined has been attributed to plant breeding for higher yields and a declining response over time of grain protein concentration to N fertilizer (Peltonen-Sainio et al., 2015). In contrast, despite yield increases (by 51%) with variety releases since 1968 in North Dakota, USA, grain protein concentration has not changed during this time (Underdahl, Mergoum, Schatz, & Ransom, 2008).

Depending on the target market, required protein concentrations vary from 8% for pastries to $>14\%$ for pasta and bread, farmers grow specific wheat categories for specific markets. In addition, farmers might also attempt to manage N applications toward protein outcomes, but their effectiveness is often hampered by in-season variability in growing conditions (Asseng & Milroy, 2006). Recent trends in N fertilizer application (total amount of N fertilizer applied in agriculture) in the 20 major wheat producing countries, including China, India, Russia, USA and several European countries have leveled off or even declined like in France and Germany (FAO, 2018) and might further reduce wheat grain protein concentrations in the future.

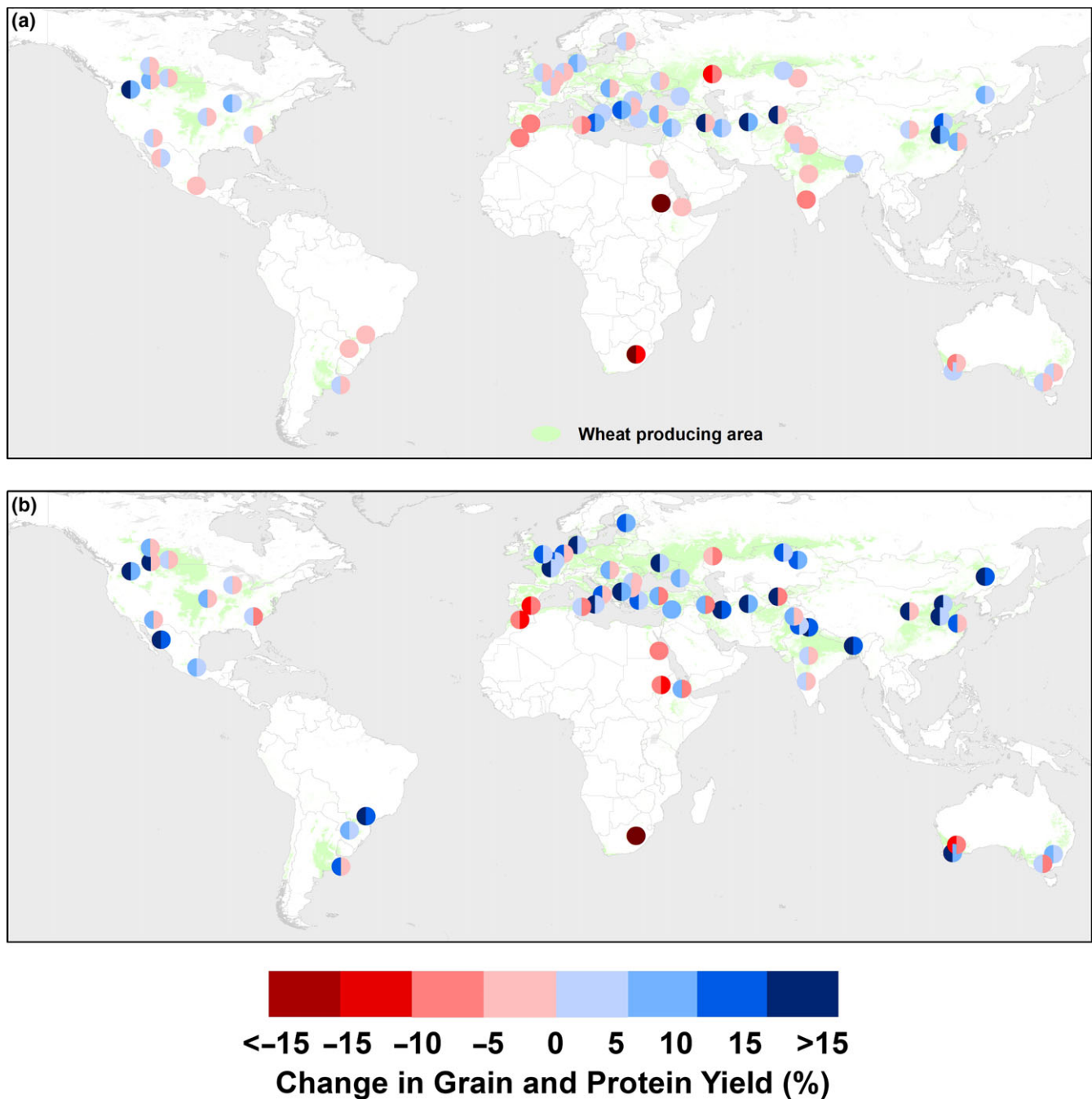


FIGURE 6 Simulated multi-model ensemble projection under climate change of global wheat grain yield (left half) and protein yield (right half), (a) without genotypic adaptation and (b) with genotypic adaptation. Relative climate change impacts for 2036–2065 under RCP8.5 compared with the 1981–2010 baseline. Impacts were calculated using the medians across 32 models (or 18 for protein yield estimates) and five GCMs (circle color) and the average over 30 years of yields using region-specific soils, cultivars, and crop management

4.2 | Adaptation traits for climate change

Rising temperatures are the main driver of projected negative climate change impacts on wheat yields (Porter et al., 2014). The shortening of the growing period (the time from sowing to maturity) with increasing temperatures has been identified as the main yield-reducing factor in another study, but not implemented (Asseng et al., 2015). In a warmer climate, the growing period is

shorter so there is less time to intercept light for photosynthesis resulting in less biomass accumulation and lower yields. To adapt crops to a warmer climate, the growing period could be extended by delaying anthesis. However, grain filling generally occurs during the relatively hot period of the season in most wheat-growing regions (Asseng, Foster, & Turner, 2011), so yield might be reduced due to the negative effect of even higher temperatures on the sensitive processes of grain set (time when the number of grains is

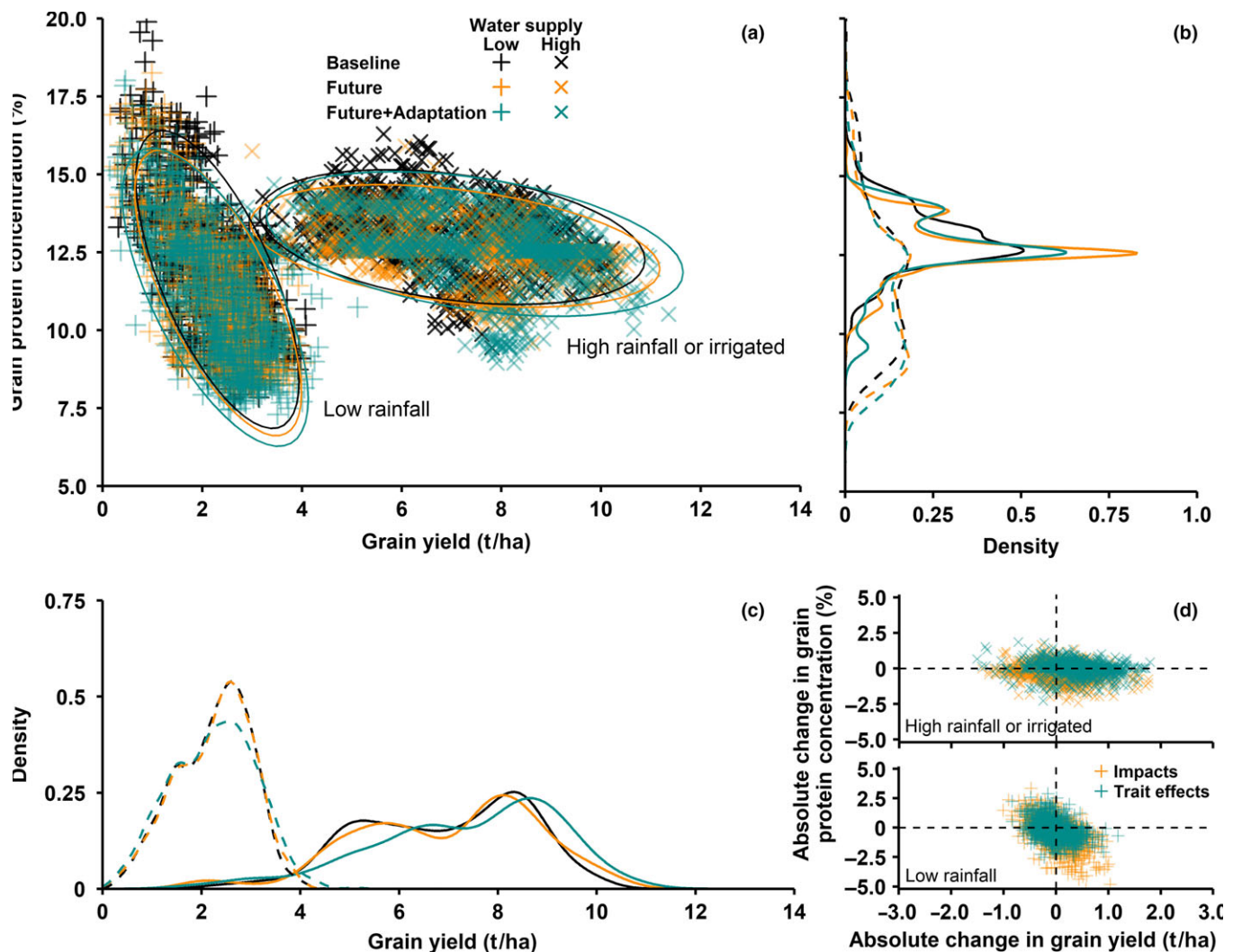


FIGURE 7 Multi-model impact of climate change with and without cultivar adaptation on the relationship between grain yield and protein concentration. Projections of annual wheat grain yield and grain protein concentration are shown for baseline period 1981–2010 (black) for RCP8.5 climate change impact in 2036–2065 with current cultivars (orange) or with genetic adaptation, that is, combined delayed anthesis with increased rate of grain filling (cyan) for 30 individual years across sixty locations using region-specific soils, cultivars and crop management. (a) Grain yield vs. grain protein concentration for individual years and locations. Medians across GCMs and 18 crop models are plotted. The ellipses capture 95% confidence levels of data in each treatment. Distributions of values for grain protein concentration (b) and grain yield (c) for thirty low-rainfall locations (dashed lines) and thirty high-rainfall or irrigated locations (solid lines). (d) Absolute changes in crop model ensemble medians for grain yield vs. grain protein concentration

set) and grain filling. Therefore, combining traits for delayed anthesis and higher rate of grain filling, as shown in our study, is an effective adaptation strategy for yield. While grain and protein yield increased with the newly introduced trait combination in warmer climates, grain protein concentration still declined in some cases when other growth restricting factors such as limited N supply also suppressed expression of these traits in a warmer climate. Applying additional N fertilizer application might not be a simple solution for climate change adaptation as major wheat-producing countries, such as France have been reducing N fertilizer application rates since the late 1980 s (Brissin et al., 2010).

A key message from our study is that, our results suggest that the combination of two simple traits through breeding can be used

to overcome the antagonism between grain yield and grain protein concentration. That antagonism has continuously reduced the nutritional and end-use value of wheat since the “green revolution” in the 1960 s with strongly increasing grain yields through the introduction of semidwarf genotypes combined with irrigation and fertilizers (Triboi et al., 2006). The field-observed positive correlation in field experiments between grain yield and protein concentration could be due to an increase in crop N accumulation at anthesis related to the extended duration of the vegetative phase and a more efficient translocation to grains during grain filling. But, it could also be due to a higher nitrogen remobilization rate and earlier leaf senescence. Hence, there is a need to improve the understanding of the physiological basis for the field-based observed positive correlation

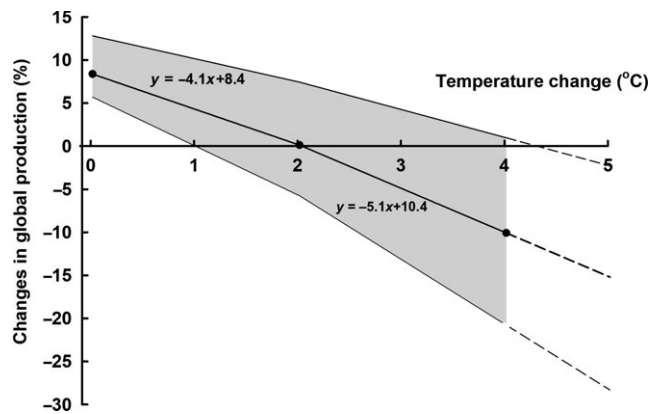


FIGURE 8 Simulated impacts of increasing temperature on global wheat grain production with 100 ppm increase in atmospheric CO_2 concentration. Relative grain yield impacts were calculated from simulated impacts of 550 ppm vs. 360 ppm CO_2 (linearly interpolated) and weighted by production. Center line shows crop model ensemble median of 32 crop models and mean of 30 years using region-specific soils, cultivars, and crop management. The shaded area indicates the 25th percentile and 75th percentile across crop models. Dashed lines are linear extensions to $+5^\circ\text{C}$ beyond simulated temperature range impacts. Equations show linear regression for before and after cross-point at 2°C

between grain yield and protein concentration through new targeted field experiments.

4.3 | Global climate change impact

While field experiments are critical for developing and testing hypotheses, these are limited to just a few sites and seasons. The application of a multi-model ensemble, combined with evidence from field experiments for the existence for traits to counteract detrimental effects from raising temperature on crops, enabled us to assess what impact climate change would have on overall wheat grain and protein yield and on protein concentration at other locations and globally. By applying the 32 tested crop models with five bias-corrected global climate models (GCMs), we covered a wide range of available GCM outputs (McSweeney & Jones, 2016). The chosen representative concentration pathway 8.5 (RCP8.5) for the 2050s is a high greenhouse gas concentration scenario with emissions continue to increase at current rates. Low- and mid-latitude locations show mostly negative yield impacts from climate change, while high-latitude locations show some positive yield impacts, consistent with other global studies and other crops (Rosenzweig et al., 2014), but

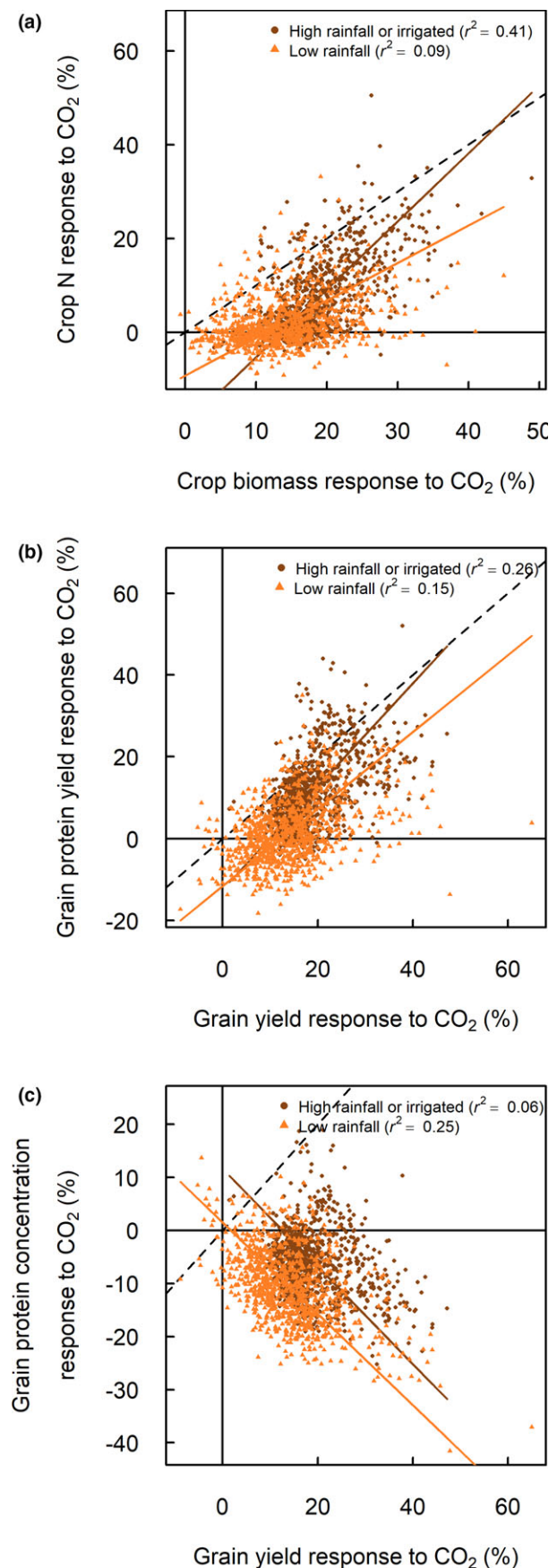


FIGURE 9 Simulated response to elevated CO_2 . In (a) relative crop N response vs. relative crop biomass response to elevated CO_2 . In (b) relative protein yield response vs. relative grain yield response to elevated CO_2 . In (c) relative grain protein concentration response vs. relative grain yield response to elevated CO_2 . Data are multi-model (18 models) ensemble median for 30 individual years during baseline period (1981–2010) across sixty global locations with 360 ppm (baseline) and 550 ppm (elevated) CO_2

negative impacts on protein yields were predicted at many locations, including high-latitude locations.

4.4 | Effect of adaptation

The combined impact of increased temperature, elevated CO₂ concentration, and change in rainfall for RCP8.5 indicates that grain yield would increase for many seasons and locations, but protein yield increase would not keep pace and would result in a reduction in grain protein concentration for many situations. However, climate change and the adapted trait combination could lead to an increase in grain protein concentration for low-rainfall locations, particularly for those locations where yield is projected to decline.

Most of the gains from elevated CO₂ on crop growth will be lost due to increasing temperature consistent with other simulation and field experimental studies (Asseng et al., 2015; Wheeler, Batts, Ellis, Hadley, & Morison, 1996). Simultaneously introducing the trait combination of delayed anthesis and increased grain filling rate could increase global yield. About a third of the impact on grain yields (2.1%) from this trait combination could be achieved globally by introducing the adaptation in the baseline climate, although yield would be reduced for many of the rainfed locations subject to terminal drought.

A simulated growth stimulus from a 100-ppm increase in atmospheric CO₂ concentration is suggested by our study to be lost with an increase of about 2°C according to the simulated multi-model ensemble median and is consistent with field experiments (Wheeler et al., 1996). Higher yield responses to elevated CO₂ have been reported in field experiments for wheat subject to drought stress compared to well-watered controls (Kimball, 2016; O'Leary et al., 2015). This did not hold true, however, when N limited growth (Kimball, 2016), as is common for low-rainfall environments with low-fertilizer inputs. The multi-model ensemble median here, averaged over 30 years, shows a CO₂ effect of 8.4% global yield increase per 100 ppm increase in CO₂. By comparison, observations from open top chamber and FACE field studies have shown 10%–20% increases in wheat yield per 100 ppm elevated CO₂ (Ainsworth & Long, 2005; Kimball, 2016; O'Leary et al., 2015), but less or even nil yield change when N is limiting (Kimball, 2016). Additional N supply for crop uptake could therefore become more important in the future. However, acceleration of soil organic matter turnover by higher temperature depletes soil carbon and N stocks, a process captured by some models. Crop models also account for the dilution of crop N and grain protein concentration at elevated CO₂ concentration, giving results similar to experimental wheat data (Pleijel & Uddling, 2012), but do not consider that nitrate assimilation in crops could be inhibited (Bloom, Burger, Rubio-Asensio, & Cousins, 2010), so likely underestimate the reduction in grain protein with climate change.

Other processes, like a possible effects of elevated CO₂ via stomata closure on canopy temperature (Kimball, Lamorte, & Pinter, 1999), not considered in the current models might also add to under- or overestimation of simulated impacts. The same applies to the poor understanding of genotype and CO₂ interactions that are

hence not included in the models (Myers et al., 2014). Other factors not included might also become important for future crop performance, such as rising ground-level ozone exposures, for example, in southern and eastern Asia (Tao, Feng, Tang, Chen, & Kobayashi, 2017) and dimming of light for photosynthesis in areas with high aerosol pollution.

Our analysis of the multi-location field trials suggests that crops with traits of delayed anthesis time and increased grain filling rate could be combined in wheat genotypes to combat the negative effects of increasing temperature on yield. The genetics of wheat anthesis time is determined by known genes so adaptations can be made through breeding or cultivar choice (Griffiths et al., 2009; Le Gouis et al., 2012). Although grain filling results from interactions between multiple physiological processes, some relevant major quantitative trait loci have been identified, and grain filling rate can be increased efficiently through breeding (Charmet et al., 2005; Wang et al., 2009). Some studies also showed that the rates of dry mass and N accumulation have common genetic determinisms (Charmet et al., 2005), so breeding for a higher rate of grain filling could improve both grain yield and protein concentration. Importantly, anthesis time and grain filling rate are mostly controlled by different loci (Wang et al., 2009) suggesting that these two traits can be improved concomitantly. The impact on yield and protein from this potential adaptation depends on the availability of nitrogen during the post-anthesis period (Bogard et al., 2011) and might require additional nitrogen remobilization into the grains (Avni et al., 2014; Uauy, Distelfeld, Fahima, Blechl, & Dubcovsky, 2006).

4.5 | Impact uncertainty

The share of uncertainty from crop models was often larger than from the five bias-corrected GCMs, suggesting a need for more research investments into impact models to reduce climate change impact uncertainty estimates, although the chosen GCMs only represent part of the overall available GCM uncertainties (McSweeney & Jones, 2016). The crop model uncertainty varied across locations, while the GCM uncertainty showed less spatial variation. Uncertainties tended to increase with adaptation and were larger for impact estimates for protein yield than for grain yield, partly because fewer crop models were available for the former. The largest crop model uncertainties were for low- and mid-latitude areas.

4.6 | Conclusions



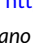






Our simulation results demonstrate that climate change adaptations that benefit grain yield are not necessarily positive for all aspects of grain quality for human nutrition (Myers et al., 2014), particularly in rainfed and low-input cropping regions. Many of the regions likely to be negatively affected are low- and mid-latitude regions that are less resilient to climate change, where populations are growing (Roser & Ortiz-Ospina, 2017) and food demand is increasing rapidly (Godfray et al., 2010).

ACKNOWLEDGEMENTS

We thank the Agricultural Model Intercomparison and Improvement Project (AgMIP) for support. We thank L. Ziska from USDA, A. Bloom from UC Davis, B. Kimball from USDA and D. Lobell from Stanford University for helpful comments on an earlier draft of our manuscript. We thank R. Richards from CSIRO Australia for discussions on potential wheat traits. We acknowledge the contribution of J. Johnson, University of Georgia, C. Griffey, Virginia Tech, S. Harrison, Louisiana State University, D. Van Sanford, University of Kentucky, R. Sutton, Texas A&M, D. West, University of Tennessee for providing different information on AGS2000, USG3120, VA12W-72, and GA06493-13LE6. S.A., B.K., and B.L. received support from the International Food Policy Research Institute (IFPRI) through the Global Futures and Strategic Foresight project, the CGIAR Research Program on Climate Change, Agriculture and Food Security (CCAFS) and the CGIAR Research Program on Wheat. A.M. received support from the EU Marie Curie FP7 COFUND People Programme, through an AgreenSkills fellowship under grant agreement no. PCOFUND-GA-2010-267196. PM, A.M., D.R., and D.W. acknowledge support from the FACCE JPI MACSUR project (031A103B) through the metaprogram Adaptation of Agriculture and Forests to Climate Change (AAFCC) of the French National Institute for Agricultural Research (INRA). L.X. and Y.Z. were supported by the National High-Tech Research and Development Program of China (2013AA100404), the National Natural Science Foundation of China (31271616), the National Research Foundation for the Doctoral Program of Higher Education of China (20120097110042), and the Priority Academic Program Development of Jiangsu Higher Education Institutions (PAPD). F.T. and Z.Z. were supported by the National Natural Science Foundation of China (41571088, 41571493 and 31561143003). R.R. received support from the German Ministry for Research and Education (BMBF) through project SPACES-LLL. Rothamsted Research receives support from the Biotechnology and Biological Sciences Research Council (BBSRC) Designing Future Wheat programme [BB/P016855/1]. M.J. and J.E.O. were supported by Innovation Fund Denmark through the MACSUR project. L.X. and Y.G. acknowledge support from the China Scholarship Council. M.B. and R.F. were funded by JPI FACCE MACSUR2 through the Italian Ministry for Agricultural, Food and Forestry Policies and thank A. Soltani from Gorgan Univ. of Agric. Sci. & Natur. Resour. for his support. R.P.R., T.P., and F.T. received financial support from the FACCE MACSUR project funded through the Finnish Ministry of Agriculture and Forestry (MMM) and from the Academy of Finland through the projects NORFASYS (decision nos. 268277 and 292944) and PLUMES (decision nos. 277403 and 292836). K.C.K. and C.N. received support from the German Ministry for Research and Education (BMBF) within the FACCE JPI MACSUR project. S.M. and C.M. acknowledge financial support from the MACMIT project (01LN1317A) funded through BMBF. G.J.O. and G.J.F. acknowledge support from the Victorian Department of Economic Development, Jobs, Transport and Resources, the Australian Department of Agriculture and Water Resources, The University of Melbourne and the

Grains Research Development Corporation, Australia. P.K.A.'s work was implemented as part of the CGIAR Research Program on Climate Change, Agriculture and Food Security (CCAFS), which is carried out with support from the CGIAR Trust Fund and through bilateral funding agreements. For details please visit <https://ccafs.cgiar.org/donors>. The views expressed in this document cannot be taken to reflect the official opinions of these organizations. B.B. received financial support from USDA NIFA-Water Cap Award 2015-68007-23133. F.E. acknowledges support from the FACCE JPI MACSUR project through the German Federal Ministry of Food and Agriculture (2815ERA01J) and from the German Science Foundation (project EW 119/5-1).

ORCID

SentholdAsseng  <https://orcid.org/0000-0002-7583-3811>
 KatharinaWaha  <https://orcid.org/0000-0002-8631-8639>
 JurajBalkovič  <https://orcid.org/0000-0003-2955-4931>
 BrunoBasso  <https://orcid.org/0000-0003-2090-4616>
 DavideCammarano  <https://orcid.org/0000-0003-0918-550X>
 GiacomoDe Sanctis  <https://orcid.org/0000-0002-3527-8091>
 Curtis D.Jones  <https://orcid.org/0000-0002-4008-5964>
 FuluTao  <https://orcid.org/0000-0001-8342-077X>
 HeidiWebber  <https://orcid.org/0000-0001-8301-5424>
 YanZhu  <https://orcid.org/0000-0002-1884-2404>

REFERENCES

- Ainsworth, E. A., & Long, S. P. (2005). What have we learned from 15 years of free-air CO₂ enrichment (FACE)? A meta-analytic review of the responses of photosynthesis, canopy. *New Phytologist*, 165, 351–371. <https://doi.org/10.1111/j.1469-8137.2004.01224.x>
- Allen, M. R., & Ingram, W. J. (2002). Constraints on future changes in climate and the hydrologic cycle. *Nature*, 419, 224–232. <https://doi.org/10.1038/nature01092>
- Anderson, W., You, L., Wood, S., Wood-Sichra, U., & Wu, W. B. (2015). An analysis of methodological and spatial differences in global cropping systems models and maps. *Global Ecology and Biogeography*, 24, 180–191. <https://doi.org/10.1111/geb.12243>
- Asseng, S., Ewert, F., Martre, P., Rötter, R. P., Lobell, D. B., Cammarano, D., ... Zhu, Y. (2015). Rising temperatures reduce global wheat production. *Nature Climate Change*, 5, 143–147. <https://doi.org/10.1038/nclimate2470>
- Asseng, S., Ewert, F., Rosenzweig, C., Jones, J. W., Hatfield, J. W., Ruane, A. C., ... Wolf, J. (2013). Uncertainty in simulating wheat yields under climate change. *Nature Climate Change*, 3, 827–832. <https://doi.org/10.1038/nclimate1916>
- Asseng, S., Foster, I., & Turner, N. C. (2011). The impact of temperature variability on wheat yields. *Global Change Biology*, 17, 997–1012. <https://doi.org/10.1111/j.1365-2486.2010.02262.x>
- Asseng, S., & Milroy, S. P. (2006). Simulation of environmental and genetic effects on grain protein concentration in wheat. *European Journal of Agronomy*, 25, 119–128. <https://doi.org/10.1016/j.eja.2006.04.005>
- Asseng, S., Van Keulen, H., & Stol, W. (2000). Performance and application of the APSIM Nwheat model in the Netherlands. *European Journal of Agronomy*, 12, 37–54. [https://doi.org/10.1016/S1161-0301\(99\)00044-1](https://doi.org/10.1016/S1161-0301(99)00044-1)

- Avni, R., Zhao, R., Pearce, S., Jun, Y., Uauy, C., Tabbita, F., ... Distelfeld, A. (2014). Functional characterization of GPC-1 genes in hexaploid wheat. *Planta*, 239, 313–324. <https://doi.org/10.1007/s00425-013-1977-y>
- Bajželj, B., Richards, K. S., Allwood, J. M., Smith, P., Dennis, J. S., Curmi, E., & Gilligan, C. A. (2014). Importance of food-demand management for climate mitigation. *Nature Climate Change*, 4, 924–929. <https://doi.org/10.1038/nclimate2353>
- Bassu, S., Brisson, N., Durand, J.-L., Boote, K., Lizaso, J., Jones, J. W., ... Waha, K. (2014). How do various maize crop models vary in their responses to climate change factors? *Global Change Biology*, 20, 2301–2320. <https://doi.org/10.1111/gcb.12520>
- Bloom, A. J., Burger, M., Rubio-Asensio, J. S., & Cousins, A. B. (2010). Carbon dioxide enrichment inhibits nitrate assimilation in wheat and *Arabidopsis*. *Science*, 328, 899–903. <https://doi.org/10.1126/science.1186440>
- Bogard, M., Jourdan, M., Allard, V., Martre, P., Perretant, M. R., Ravel, C., ... Le Gouis, J. (2011). Anthesis date mainly explained correlations between post-anthesis leaf senescence, grain yield, and grain protein concentration in a winter wheat population segregating for flowering time QTLs. *Journal of Experimental Botany*, 62, 3621–3636. <https://doi.org/10.1093/jxb/err061>
- Brisson, N., Gate, P., Gouache, D., Charmet, G., Oury, F.-X., & Huard, F. (2010). Why are wheat yields stagnating in Europe? A comprehensive data analysis for France. *Field Crops Research*, 119, 201–212. <https://doi.org/10.1016/j.fcr.2010.07.012>
- Broberg, M. C., Högy, P., & Pleijel, H. (2017). CO₂-Induced changes in wheat grain composition: Meta-analysis and response functions. *Agronomy*, 7, 32. <https://doi.org/10.3390/agronomy7020032>
- Charmet, G., Robert, N., Branlard, G., Linossier, L., Martre, P., & Triboi, E. (2005). Genetic analysis of dry matter and nitrogen accumulation and protein composition in wheat kernels. *Theoretical and Applied Genetics*, 111, 540–550. <https://doi.org/10.1007/s00122-005-2045-1>
- Chenu, K., Porter, J. R., Martre, P., Basso, B., Chapman, S. C., Ewert, F., ... Asseng, S. (2017). Contribution of crop models to adaptation in wheat. *Trends in Plant Science*. <https://doi.org/10.1016/j.tplants.2017.02.003>
- Ewert, F., Van Ittersum, M., Heckelee, T., Therond, O., Bezlepkin, I., & Andersen, E. (2011). Scale changes and model linking methods for integrated assessment of agri-environmental systems. *Agriculture, Ecosystems & Environment*, 142, 6–17. <https://doi.org/10.1016/j.agee.2011.05.016>
- Ewert, F., vanBussel, L. G. J., Zhao, G., Hoffmann, H., Gaiser, T., Specka, X., ... Moriondo, M. (2015). Uncertainties in Scaling up Crop Models for Large Area Climate Change Impact Assessments. In C. Rosenzweig, & D. Hillel (Eds.), *Handbook of Climate Change and Agroecosystems: The Agricultural Model Intercomparison and Improvement Project (AgMIP)* (pp 261–277). Singapore, Singapore: World Scientific Publishing.
- FAO. (2016). Food and Agriculture Organization of the United Nations. Retrieved from <https://fao.org>. (Accessed 15 June 2016).
- FAO. (2018). Food and Agriculture Organization of the United Nations. Retrieved from <https://fao.org>. (Accessed, 10 September, 2018).
- Fitzgerald, G. J., Tausz, M., O'Leary, G., Mollah, M. R., Tausz-Pösch, S., Seneweera, S., ... Norton, R. M. (2016). Elevated atmospheric [CO₂] can dramatically increase wheat yields in semi-arid environments and buffer against heat waves. *Global Change Biology*, 22, 2269–2284.
- Gbegbelegbe, S., Cammarano, D., Asseng, S., Robertson, R., Chung, U., Adam, M., ... Nelson, G. (2017). Baseline simulation for global wheat production with CIMMYT mega-environment specific cultivars. *Field Crops Research*, 202, 122–135. <https://doi.org/10.1016/j.fcr.2016.06.010>
- Godfray, H. C. J., Beddington, J. R., Crute, I. R., Haddad, L., Lawrence, D., Muir, J. F., ... Toulmin, C. (2010). Food Security: The Challenge of Feeding 9 Billion People. *Science*, 327, 812–818. <https://doi.org/10.1126/science.1185383>
- Griffiths, S., Simmonds, J., Leverington, M., Wang, Y., Fish, L., Sayers, L., ... Snape, J. (2009). Meta-QTL analysis of the genetic control of ear emergence in elite European winter wheat germplasm. *Theoretical and Applied Genetics*, 119, 383–395. <https://doi.org/10.1007/s00122-009-1046-x>
- Haddad, L., Hawkes, C., Webb, P., Thomas, S., Beddington, J., Waage, J., & Flynn, D. (2016). A new global research agenda for food. *Nature*, 540, 30–32. <https://doi.org/10.1038/540030a>
- Kimball, B. A. (2016). Crop responses to elevated CO₂ and interactions with H₂O, N, and temperature. *Current Opinion in Plant Biology*, 31, 36–43. <https://doi.org/10.1016/j.pbi.2016.03.006>
- Kimball, B. A., Lamorte, R. L., Pinter, P. J. Jr, et al. (1999). Free-air CO₂ enrichment and soil nitrogen effects on energy balance and evapotranspiration of wheat. *Water Resources Research*, 35, 1179–1190.
- LeGouis, J., Bordes, J., Ravel, C., Heumez, E., Faure, S., Praud, S., ... Rousset, M. (2012). Genome-wide association analysis to identify chromosomal regions determining components of earliness in wheat. *Theoretical and Applied Genetics*, 124, 597–611. <https://doi.org/10.1007/s00122-011-1732-3>
- Li, T., Hasegawa, T., Yin, X., Zhu, Y., Boote, K., Adam, M., ... Bouman, B. (2015). Uncertainties in predicting rice yield by current crop models under a wide range of climatic conditions. *Global Change Biology*, 21, 1328–1341. <https://doi.org/10.1111/gcb.12758>
- Liu, B., Asseng, S., Muller, C., Ewert, F., Elliott, J., Lobell, D. B., ... Zhu, Y. (2016). Similar estimates of temperature impacts on global wheat yield by three independent methods. *Nature. Climate Change*, 6, 1130+.
- Majoul-Haddad, T., Bancel, E., Martre, P., Triboi, E., & Branlard, G. (2013). Effect of short heat shocks applied during grain development on wheat (*Triticum aestivum* L.) grain proteome. *Journal of Cereal Science*, 57, 486–495. <https://doi.org/10.1016/j.jcs.2013.02.003>
- Martre, P., Wallach, D., Asseng, S., Ewert, F., Jones, J. W., Rötter, R. P., ... Wolf, J. (2015). Multimodel ensembles of wheat growth: Many models are better than one. *Global Change Biology*, 21, 911–925. <https://doi.org/10.1111/gcb.12768>
- Mcsweeney, C. F., & Jones, R. G. (2016). How representative is the spread of climate projections from the 5 CMIP5 GCMs used in ISI-MIP? *Climate Services*, 1, 24–29. <https://doi.org/10.1016/j.cliser.2016.02.001>
- Mollah, M., Norton, R., & Huzzey, J. (2009). Australian Grains Free Air Carbon dioxide Enrichment (AGFACE) facility: Design and performance. *Crop and Pasture Science*, 60, 697–707. <https://doi.org/10.1071/CP08354>
- Monfreda, C., Ramankutty, N., & Foley, J. A. (2008) Farming the planet: 2. Geographic distribution of crop areas, yields, physiological types, and net primary production in the year 2000. *Global Biogeochemical Cycles*, 22, GB1022.
- Myers, S. S., Zanobetti, A., Kloog, I., Huybers, P., Leakey, A. D. B., Bloom, A. J., ... Usui, Y. (2014). Increasing CO₂ threatens human nutrition. *Nature*, 510, 139–142. <https://doi.org/10.1038/nature13179>
- O'Leary, G. J., Christy, B., Nuttall, J., Huth, N., Cammarano, D., Stöckle, C., ... Asseng, S. (2015). Response of wheat growth, grain yield and water use to elevated CO₂ under a Free-Air CO₂ Enrichment (FACE) experiment and modelling in a semi-arid environment. *Global Change Biology*, 21, 2670–2686.
- Olesen, J. E., Trnka, M., Kersebaum, K. C., Skjelvåg, A. O., Seguin, B., Peltonen-Sainio, P., ... Micale, F. (2011). Impacts and adaptation of European crop production systems to climate change. *European Journal of Agronomy*, 34, 96–112. <https://doi.org/10.1016/j.eja.2010.11.003>
- Peltonen-Sainio, P., Salo, T., Jauhiainen, L., Lehtonen, H., & Sieviläinen, E. (2015). Static yields and quality issues: Is the agri-environment

- program the primary driver? *Ambio*, 44, 544–556. <https://doi.org/10.1007/s13280-015-0637-9>
- Pleijel, H., & Uddling, J. (2012). Yield vs. Quality trade-offs for wheat in response to carbon dioxide and ozone. *Global Change Biology*, 18, 596–605. <https://doi.org/10.1111/j.1365-2486.2011.2489.x>
- Porter, J. R., Xie, L., Challinor, A. J., Cochrane, K., Howden, S. M., Iqbal, M. M., ... Travasso, M. I. (2014). Food security and food production systems. In V. R. Barros, C. B. Field, D. J. Dokken, M. D. Mastrandrea, K. J. Mach, T. E. Bilir, M. Chatterjee, K. I. Ebi, R. C. Yo Estrada, B. G. Genova, E. S. Kissel, A. N. Levy, S. MacCracken, P. R. Mastrandrea, & L. I. White (Eds.), *Impacts, Adaptation, and Vulnerability. Part A: Global and Sectoral Aspects. Contribution of Working Group II to the Fifth Assessment Report of the Intergovernmental Panel on Climate Change* (pp. 485–533). Cambridge, UK; New York, NY: Cambridge University Press.
- Porwollik, V., Müller, C., Elliott, J., Chryssanthacopoulos, J., Iizumi, T., Ray, D. K., ... Wu, X. (2017). Spatial and temporal uncertainty of crop yield aggregations. *European Journal of Agronomy*, 88, 10–21. <https://doi.org/10.1016/j.eja.2016.08.006>
- Reynolds, M. P., Balota, M., Delgado, M. I. B., Amani, I., & Fischer, R. A. (1994). Physiological and morphological traits associated with spring wheat yield under hot, irrigated conditions. *Australian Journal of Plant Physiology*, 21, 717–730. <https://doi.org/10.1071/PP9940717>
- Reynolds, M., & Braun, H. (2013). In M. Reynolds, & H. Braun (Eds.), *Archiving yield gains in Wheat: Overview. CENEB, CIMMYT*. In: *Proceedings of the 3rd International Workshop of Wheat Yield Consortium*. Obregon, Sonora, Mexico: CIMMYT.
- Rosenzweig, C., Elliott, J., Deryng, D., Ruane, A. C., Müller, C., Arneth, A., ... Jones, J. W. (2014). Assessing agricultural risks of climate change in the 21st century in a global gridded crop model intercomparison. *Proceedings of the National Academy of Sciences of the United States of America*, 111, 3268–3273. <https://doi.org/10.1073/pnas.1222463110>
- Rosenzweig, C., Jones, J. W., Hatfield, J. I., Ruane, A. C., Boote, K. J., Thorburn, P., ... Winter, J. M. (2013). The Agricultural Model Intercomparison and Improvement Project (AgMIP): Protocols and pilot studies. *Agricultural and Forest Meteorology*, 170, 166–182. <https://doi.org/10.1016/j.agrformet.2012.09.011>
- Roser, M., & Ortiz-Ospina, E. (2017). OurWorldInData.org. Retrieved from <https://ourworldindata.org/world-population-growth/>
- Ruane, A. C., Goldberg, R., & Chryssanthacopoulos, J. (2015). Climate forcing datasets for agricultural modeling: Merged products for gap-filling and historical climate series estimation. *Agricultural and Forest Meteorology*, 200, 233–248.
- Ruane, A. C., & Mcdermid, S. P. (2017). Selection of a representative subset of global climate models that captures the profile of regional changes for integrated climate impacts assessment. *Earth Perspectives*, 4, 1. <https://doi.org/10.1186/s40322-017-0036-4>
- Ruane, A. C., Winter, J. M., Mcdermid, S. P., & Hudson, N. I. (2015). AgMIP climate data and scenarios for integrated assessment. In C. Rosenzweig, & D. Hillel, (Eds.), *Handbook of Climate Change and Agroecosystems: The Agricultural Model Intercomparison and Improvement Project* (pp. 45–78). London, UK: Imperial College Press.
- Ruiz-Ramos, M., Ferrise, R., Rodríguez, A., Lorite, I. J., Bindi, M., Carter, T. C., ... Rotter, R. P. (2017). Adaptation response surfaces for managing wheat under perturbed climate and CO₂ in a Mediterranean environment. *Agricultural Systems*, 159, 260–274.
- Semenov, M. A., & Stratonovitch, P. (2015). Adapting wheat ideotypes for climate change: Accounting for uncertainties in CMIP5 climate projections. *Climate Research*, 65, 123–139. <https://doi.org/10.3354/cr01297>
- Shewry, P. R., & Halford, N. G. (2002). Cereal seed storage proteins: Structures, properties and role in grain utilization. *Journal of Experimental Botany*, 53, 947–958. <https://doi.org/10.1093/jexbot/53.370.947>
- Shewry, P. R., & Hey, S. J. (2015). The contribution of wheat to human diet and health. *Food and Energy Security*, 4, 178–202. <https://doi.org/10.1002/fes3.64>
- Tao, F., Feng, Z., Tang, H., Chen, Y., & Kobayashi, K. (2017). Effects of climate change, CO₂ and O₃ on wheat productivity in Eastern China, singly and in combination. *Atmospheric Environment*, 153, 182–193.
- Tao, F., Rotter, R. P., Palosuo, T., Diaz-Ambrona, C. G. H., Minguez, M. I., Semenov, M. A., ... Schulma, A. H. (2017). Designing future barley ideotypes using a crop model ensemble. *European Journal of Agronomy*, 82, 144–162.
- Tilman, D., Balzer, C., Hill, J., & Befort, B. L. (2011). Global food demand and the sustainable intensification of agriculture. *Proceedings of the National Academy of Sciences of the United States of America*, 108, 20260–20264. <https://doi.org/10.1073/pnas.1116437108>
- Triboi, E., Martre, P., Girousse, C., Ravel, C., & Triboi-Blondel, A. (2006). Unravelling environmental and genetic relationships between grain yield and nitrogen concentration for wheat. *European Journal of Agronomy*, 25, 108–118. <https://doi.org/10.1016/j.eja.2006.04.004>
- Triboi, E., & Triboi-Blondel, A.-M. (2002). Productivity and grain or seed composition: A new approach to an old problem—invited paper. *European Journal of Agronomy*, 16, 163–186. [https://doi.org/10.1016/S1161-0301\(01\)00146-0](https://doi.org/10.1016/S1161-0301(01)00146-0)
- Uauy, C., Distelfeld, A., Fahima, T., Blechl, A., & Dubcovsky, J. (2006). A NAC gene regulating senescence improves grain protein, zinc, and iron content in wheat. *Science*, 314, 1298–1301. <https://doi.org/10.1126/science.1133649>
- Underdahl, J. L., Mergoum, M., Schatz, B., & Ransom, J. K. (2008). Quality trait variation in major hard red spring wheat cultivars released in North Dakota since 1968. *Cereal Chemistry*, 85, 509–516. <https://doi.org/10.1094/CCHEM-85-4-0507>
- Van Bussel, L. G. J., Grassini, P., Wart, V., Justin, W., Joost, C., Lieven, Y., ... Van Ittersum, M. K. (2015). From field to atlas: Upscaling of location-specific yield gap estimates. *Field Crops Research*, 177, 98–108. <https://doi.org/10.1016/j.fcr.2015.03.005>
- Van Bussel, V., Lenny, G. J., Ewert, F., Zhao, G., Hoffmann, H., Enders, A., ... Tao, F. (2016). Spatial sampling of weather data for regional crop yield simulations. *Agricultural and Forest Meteorology*, 220, 101–115. <https://doi.org/10.1016/j.agrformet.2016.01.014>
- Vogel, K. P., Johnson, V. A., & Mattern, P. J. (1976). Protein and lysine content of grain, endosperm, and bran of wheats from USDA World wheat collection. *Crop Science*, 16, 655–660.
- Waha, K., Muller, C., Bondeau, A., Dietrich, J. P., Kurukulasuriya, P., Heinke, J., & Lotze-Campen, H. (2013). Adaptation to climate change through the choice of cropping system and sowing date in sub-Saharan Africa. *Global Environmental Change-Human and Policy Dimensions*, 23, 130–143. <https://doi.org/10.1016/j.gloenvcha.2012.11.001>
- Wang, R., Hai, L., Zhang, X., You, G., Yan, C., & Xiao, S. (2009). QTL mapping for grain filling rate and yield-related traits in RILs of the Chinese winter wheat population Heshangmaix Yu8679. *Theoretical and Applied Genetics*, 118, 313–325.
- Wheeler, T. R., Batts, G. R., Ellis, R. H., Hadley, P., & Morison, J. I. L. (1996). Growth and yield of winter wheat (*Triticum aestivum*) crops in response to CO₂ and temperature. *Journal of Agricultural Science*, 127, 37–48. <https://doi.org/10.1017/S0021859600077352>
- Wheeler, T., & Von Braun, J. (2013). Climate change impacts on global food security. *Science*, 341, 508–513. <https://doi.org/10.1126/science.1239402>
- Wieser, H., Manderscheid, R., Erbs, M., & Weigel, H. J. (2008). Effects of elevated atmospheric CO₂ concentrations on the quantitative protein composition of wheat grain. *Journal of Agricultural and Food Chemistry*, 56, 6531–6535.
- Yang, X., Wu, L., Zhu, Z., Ren, G., & Liu, S. (2014). Variation and trends in dough rheological properties and flour quality in 330 Chinese wheat varieties. *The Crop Journal*, 2, 195–200.
- Zhao, G., Hoffmann, H., Yeluripati, J., Xenia, S., Nendel, C., Coucheney, E., ... Ewert, F. (2016). Evaluating the precision of eight spatial

sampling schemes in estimating regional mean of simulated yields for two crops. *Environmental Modelling and Software*, 80, 100–112.

SUPPORTING INFORMATION

Additional supporting information may be found online in the Supporting Information section at the end of the article.

How to cite this article: Asseng S, Martre P, Maiorano A, et al. Climate change impact and adaptation for wheat protein. *Glob Change Biol.* 2019;25:155–173. <https://doi.org/10.1111/gcb.14481>

24 Sept 2018

Supplementary Materials for

Climate change impact and adaptation for wheat protein

S. Asseng, P. Martre, A. Maiorano, R.P. Rötter, G.J. O’Leary, G.J. Fitzgerald, C. Girousse, R. Motzo, F. Giunta, M.A. Babar, M.P. Reynolds, A.M.S. Kheir, P.J. Thorburn, K. Waha, A.C. Ruane, P.K. Aggarwal, M. Ahmed, J. Balkovic, B. Basso, C. Biernath, M. Bindi, D. Cammarano, A.J. Challinor, G. De Sanctis, B. Dumont, E. Eyshi Rezaei, E. Fereres, R. Ferrise, M. Garcia-Vila, S. Gayler, Y. Gao, H. Horan, G. Hoogenboom, R.C. Izaurralde, M. Jabloun, C.D. Jones, B.T. Kassie, K.C. Kersebaum, C. Klein, A.-K. Koehler, B. Liu, S. Minoli, M. Montesino San Martin, C. Müller, S. Naresh Kumar, C. Nendel, J.E. Olesen, T. Palosuo, J.R. Porter, E. Priesack, D. Ripoche, M.A. Semenov, C. Stöckle, P. Stratonovitch, T. Streck, I. Supit, F. Tao, M. Van der Velde, D. Wallach, E. Wang, H. Webber, J. Wolf, L. Xiao, Z. Zhang, Z. Zhao, Y. Zhu, and F. Ewert

1 Supplementary Materials and Methods

2

3 **Table S1.** List of the 32 wheat crop models used in the AgMIP Wheat study.

Code	Name (version)	Reference	Documentation
AE	APSIM-E*	(Chen <i>et al.</i> , 2010a, Keating <i>et al.</i> , 2003, Wang <i>et al.</i> , 2002)	http://www.apsim.info/Wiki
AF	AFRCWHEAT2*	(Porter, 1984, Porter, 1993, Weir <i>et al.</i> , 1984)	Request from John Porter: jrp@plen.ku.dk
AQ	AQUACROP (V.4.0)	(Steduto <i>et al.</i> , 2009)	http://www.fao.org/nr/water/aquacrop.html
AW	APSIM-Wheat (V.7.3)*	(Keating <i>et al.</i> , 2003)	http://www.apsim.info/Wiki
CS	CropSyst (V.3.04.08)	(Stockle <i>et al.</i> , 2003)	http://modeling.bsyse.wsu.edu/CS_Suite_4/CropSyst/index.html
DC	DSSAT-CERES-Wheat (V.4.0.1.0)*	(Hoogenboom & White, 2003, Jones <i>et al.</i> , 2003, Ritchie <i>et al.</i> , 1985)	http://dssat.net/
DN	DSSAT-Nwheat*	(Asseng, 2004, Kassie <i>et al.</i> , 2016)	http://dssat.net/
DR	DSSAT-CROPSIM (V4.5.1.013)*	(Hunt & Pararajasingham, 1995, Jones <i>et al.</i> , 2003)	http://dssat.net/
DS	DAISY (V.5.24)*	(Hansen <i>et al.</i> , 2012, Hansen <i>et al.</i> , 1991)	http://daisy.ku.dk
EI	EPIC-I (V0810)	(Balkovič <i>et al.</i> , 2013, Balkovič <i>et al.</i> , 2014, Kiniry <i>et al.</i> , 1995, Williams, 1995, Williams <i>et al.</i> , 1989)	http://epicapex.tamu.edu/epic
EW	EPIC-Wheat(V1102)	(Izaurrealde <i>et al.</i> , 2006, Izaurrealde <i>et al.</i> , 2012, Kiniry <i>et al.</i> , 1995,	http://epicapex.brc.tamus.edu

		Williams, 1995, Williams <i>et al.</i> , 1989)	
GL	GLAM (V.2 updated)	(Challinor <i>et al.</i> , 2004, Li <i>et al.</i> , 2010)	https://www.see.leeds.ac.uk/research/icas/research-themes/climate-change-and-impacts/climate-impacts/glam
HE	HERMES (V.4.26)*	(Kersebaum, 2007, Kersebaum, 2011)	http://www.zalf.de/en/forschung/institute/lsa/forschung/oekomod/hermes
IC	INFOCROP (V.1)	(Aggarwal <i>et al.</i> , 2006)	http://infocrop.iari.res.in/wheatmodel/UserInterface/HomeModule/Default.aspx
LI	LINTUL4 (V.1)	(Shibu <i>et al.</i> , 2010, Spitters & Schapendonk, 1990)	http://models.pps.wur.nl/node/950
L5	SIMPLACE<Lintul-5* SlimWater3,FAO-56, CanopyT,HeatStressHourly	(Gaiser <i>et al.</i> , 2013, Shibu <i>et al.</i> , 2010, Spitters & Schapendonk, 1990, Webber <i>et al.</i> , 2016)	http://www.simplace.net/Joomla/
LP	LPJmL (V3.2)	(Beringer <i>et al.</i> , 2011, Bondeau <i>et al.</i> , 2007, Fader <i>et al.</i> , 2010, Gerten <i>et al.</i> , 2004, Müller <i>et al.</i> , 2007, Rost <i>et al.</i> , 2008)	http://www.pik-potsdam.de/research/projects/lpjweb
MC	MCWLA-Wheat (V.2.0)	(Tao <i>et al.</i> , 2009a, Tao & Zhang, 2010, Tao & Zhang, 2013, Tao <i>et al.</i> , 2009b)	Request from taofl@igsnr.ac.cn
MO	MONICA (V.1.0)*	(Nendel <i>et al.</i> , 2011)	http://monica.agrosystem-models.com
NC	Expert-N (V3.0.10) – CERES (V2.0)*	(Biernath <i>et al.</i> , 2011, Priesack <i>et al.</i> , 2006, Ritchie <i>et al.</i> , 1987, Stenger <i>et al.</i> , 1999)	http://www.helmholtz-muenchen.de/en/iboe/expertn
NG	Expert-N (V3.0.10) – GECROS (V1.0)*	(Biernath <i>et al.</i> , 2011, Stenger <i>et al.</i> , 1999)	http://www.helmholtz-muenchen.de/en/iboe/expertn
NP	Expert-N (V3.0.10) – SPASS (2.0)*	(Biernath <i>et al.</i> , 2011, Priesack <i>et al.</i> , 2006, Stenger <i>et al.</i> , 1999,	http://www.helmholtz-muenchen.de/en/iboe/expertn

		Wang & Engel, 2000, Yin & van Laar, 2005)	
NS	Expert-N (V3.0.10) – SUCROS (V2)	(Biernath <i>et al.</i> , 2011, Goudriaan & Van Laar, 1994, Priesack <i>et al.</i> , 2006, Stenger <i>et al.</i> , 1999)	http://www.helmholtz-muenchen.de/en/iboe/expertn
OL	OLEARY (V.8)*	(Latta & O'Leary, 2003, O'Leary & Connor, 1996a, O'Leary & Connor, 1996b, O'Leary <i>et al.</i> , 1985)	Request from gjoleary@yahoo.com
S2	Sirius (V2014)*	(Jamieson & Semenov, 2000, Jamieson <i>et al.</i> , 1998, Lawless <i>et al.</i> , 2005, Semenov & Shewry, 2011)	http://www.rothamsted.ac.uk/mas-models/sirius.php
SA	SALUS (V.1.0)*	(Basso <i>et al.</i> , 2010, Senthilkumar <i>et al.</i> , 2009)	http://salusmodel.glg.msu.edu
SP	SIMPLACE<Lintul-2 CC,Heat,CanopyT,Re-Translocation	(Angulo <i>et al.</i> , 2013)	http://www.simplace.net/Joomla/
SQ	SiriusQuality (V3.0)*	(Ferrise <i>et al.</i> , 2010, He <i>et al.</i> , 2010, Maiorano <i>et al.</i> , 2017, Martre <i>et al.</i> , 2006)	http://www1.clermont.inra.fr/siriusquality
SS	SSM-Wheat	(Soltani <i>et al.</i> , 2013)	Request from afshin.soltani@gmail.com
ST	STICS (V.1.1)*	(Brisson <i>et al.</i> , 2003, Brisson <i>et al.</i> , 1998)	http://www6.paca.inra.fr/stics_eng
WG	WheatGrow (V3.1)	(Cao <i>et al.</i> , 2002, Cao & Moss, 1997, Hu <i>et al.</i> , 2004, Li <i>et al.</i> , 2002, Pan <i>et al.</i> , 2007, Pan <i>et al.</i> , 2006, Yan <i>et al.</i> , 2001)	Request from yanzhu@njau.edu.cn
WO	WOFOST (V.7.1)	(Boogaard & Kroes, 1998)	http://www.wofost.wur.nl

*Models that have routines to simulate crop and grain nitrogen dynamics leading to grain protein and have been tested with field measurements before. These 18 models have been used in the grain protein analysis.

1 *Field experiments for model testing*

2 *INRA temperature experiment*

3 In all INRA experiments, crops were grown outside in 2 m² containers with 0.5 m depth, filled with a 2:1 (v:v) mixture of black soil
4 and peat. Seeds were sown on 10 November 1999, 08 November 2000, and 07 November 2006 at 2.5 cm from the soil surface with a
5 density of 578 seeds m⁻² and a row spacing of 6.25 cm, resulting in 554 to 666 fertile tillers m⁻² at anthesis, mimicking field density
6 and plant competition. The high plant density inhibited the development of axillary tillers, which coordinated the development of the
7 crops within and between the containers. In 1999 and 2000, ammonium phosphate (N: P, 18:46; 20 g m⁻²) and potassium sulphate
8 (K₂SO₄; 20 g m⁻²) were hand-dressed at sowing. The preceding crops were sunflower and wheat, and three years fallow in 1999, 2000,
9 and 2006. During the wheat growth period, crops were fertilized with ammonium-nitrate or ammonium-phosphate and received a total
10 of 15 to 20 g N m⁻² in two to three applications between one week after the beginning of tillering and male meiosis. From sowing to
11 anthesis the crops received the following amounts of rainfall: 199 mm (1999-2000), 247 mm (2000-2001), and 145 mm (2006-2007).
12 In addition, during that period the crops received the following irrigation amounts to maintain the soil water content above 80% of
13 field capacity: 208 mm (1999-2000), 90 mm (2000-2001), and 143 mm (2006-2007). At anthesis, all the containers were irrigated to
14 field capacity by applying 90 mm of water, they then received 6 to 50 mm of water every 2 to 7 days until maturity to replace
15 measured crop evapotranspiration. Spikes were tagged at anthesis to allow accurate determination of the developmental stage when
16 harvesting. All other crop inputs, including disease and pest control, were applied at levels to prevent diseases and pests from limiting
17 plant growth and grain yield.

18 Between 1 and 5 d after anthesis the containers were transferred under transparent enclosures under natural light in the Crop Climate
19 Control and Gas Exchange Measurement (C3-GEM) experimental platform. The C3-GEM platform allows monitoring and controlling
20 air temperature, air CO₂ concentration, water supply, and gas exchange of up to four 2 m² containers (Triboï *et al.*, 1996). Air CO₂
21 concentration was maintained at 378 ± 5 ppm. Different temperature regimes were applied under the enclosures. In 2000, day/night air

temperatures were controlled at 18 °C/10 °C (control treatment) or at 28 °C/15 °C (chronic high temperature treatment). Heat shocks consisting of two consecutive days with air temperature of 38 °C for 3 h between 11:30 and 14:30 solar time during the first day and 6 h between 10:15 and 16:15 solar time during the second day were applied starting 30 days after anthesis (i.e., during the linear grain filling period) on one container maintained at the cooler temperature regime the rest of the time. In 2001, all containers were maintained at 18 °C/10 °C (day/night) and heat shocks consisting of 4 h a day at 38 °C (air temperature), between 10:00 and 14:00 solar time and 20 °C (air temperature) the rest of the day were applied for four consecutive days starting 7 days after anthesis (i.e., during the endosperm cell division period) or 18 days after anthesis (i.e., during the linear grain filling period). In 2007, all containers were maintained at 21°C/14°C (day/night) and heat shocks consisting of 4 h a day at 38 °C (air temperature), between 10:00 and 14:00 solar time and 21 °C (air temperature) the rest of the day were applied for four consecutive days during either the endosperm cell division period (starting 8 days after anthesis), the linear grain filling period (starting 23 days after anthesis), or during both phases. The rate of heating or cooling before and after the heat shocks was 8.5°C h⁻¹. Air relative humidity was maintained between 65% and 80%, corresponding to a vapor pressure deficit (VPD) of 0.5/0.3 kPa (day/night) in 2000 and 2001, and 0.6/0.4 kPa (day/night) in 2007. During the 4 h of heat shock, the air relative humidity ranged from 40% to 50% and the air VPD from 3.0 to 3.7 kPa.

To study the dynamic accumulation of dry mass and total N in leaves, stems, chaffs, and grains, three replicates of 20 plants were collected in each container every 2 to 9 days from anthesis to grain maturity. At maturity 0.4 to 1.25 m² were harvested. Samples were collected starting from the south. Stems, leaves, chaffs, and grains were separated, and their dry mass was determined after oven drying at 80 °C to a constant mass. Total N content of oven-dried samples was determined by the Kjeldhal method using a Kjeltac 2300 analyser (Foss Tecator AB, Hoeganaes, Sweden) in 2000 and 2001, and by the Dumas combustion method using a FlashEA 1112 N/Protein analyser (Thermo Electron Corp., Waltham, MA, USA) in 2007. Grain protein concentration was calculated from the percentage of total N by multiplying by a conversion factor of 5.62 for grains of wheat (Mossé *et al.*, 1985).

1 **Table S2.** Layout of the experiment treatments of the INRA Clermont-Ferrand temperature experiments. Grain yield and protein data are medians and the 25th
2 and 75th quantiles between squared brackets.

Treatment name	Sowing date	Post-anthesis day/night air temperature (°C)	Treatment description	Grain yield (t DM ha ⁻¹)	Grain protein (% of yield)
HSE01_CTRL	10-Nov-99	18/10	Control	7.94 [7.87-8.02]	10.28 [10.28-10.29]
HSE02_HS1	10-Nov-99	18/10	Heat shock during the grain filling lag period (2 days at T_{\max} 38°C during 4 hours)	7.98 [7.87-8.07]	12.23 [12.06-12.17]
HSE03_HT	10-Nov-99	28/15	Chronic high temperature during grain filling	6.22 [6.05-6.38]	12.29 [12.25-12.45]
HSE04_CTRL	08-Nov-00	18/10	Control	8.45 [8.45-8.45]	10.28 [10.27-10.34]
HSE05_HS1	08-Nov-00	18/10	Heat shock during the grain filling lag period (4 days at T_{\max} 38°C during 4 hours)	6.67 [6.67-6.67]	12.13 [12.13-12.28]
HSE06_HS2	08-Nov-00	18/10	Heat shock during the linear grain filling period (4 days at T_{\max} 38°C during 4 hours)	7.45 [7.45-7.45]	12.59 [12.52-12.77]
HSE07_CTRL	07-Nov-06	21/14	Control	6.93 [6.75-7.32]	11.52 [11.27-11.66]
HSE08_HS1	07-Nov-06	21/14	Heat shock during the grain filling lag period (4 days at T_{\max} 38°C during 4h)	7.01 [6.28-7.32]	11.66 [11.52-12.13]
HSE09_HS12	07-Nov-06	21/14	Heat shock during both the grain filling lag period and the linear grain filling	5.6 [5.37-5.83]	13.46 [13.57-13.32]

			period (2 x 4 days at T_{\max} 38°C during 4h)		
HSE10_HS2	07-Nov-06	21/14	Heat shock during the linear grain filling period (4 days at T_{\max} 38°C during 4h)	6.31 [5.44-6.63]	12.69 [13.14-12.73]

AGFACE Australia experiment ($CO_2 \times temperature \times water$)

The agronomic design of the AGFACE Australia experiment with the two times of sowing over three years (2007-2009) comprised a complete randomized block experimental design of four replicates. Sowing time altered biomass partitioning including yield because crops are forced to develop into warmer, less efficient conditions as summer approaches.

Gravimetric soil water content was measured at sowing and harvest using a hydraulically operated soil sampler. Sampling was done for layers 0-0.1m and 0.1-0.2m and for 0.2 m increments thereafter to 2 m from one core per plot (42 mm diameter cores). Soil mineral nitrogen (NO_3 and NH_4) was also measured from an additional core taken close to the sampling time of the soil water measurements. Soil bulk density was measured from 70 mm diameter \times 75 mm deep sampling rings from each octagonal area. Large soil mineral nitrogen content (~ 300 kg N ha^{-1}) at the site precluded any significant effects of applied N, so soil analyses were pooled across the N treatments.

Biomass samples taken at stem elongation (DC31), anthesis (DC65), and maturity (DC90) were oven dried at 70°C and leaf and stem area measurements were made from using an electronic planimeter from subsamples comprising approximately 25% of the collected fresh biomass. Mean sowing plant density measured by plant counts approximately three weeks after emergence was 120 plants m^{-2} and ranged from 60 to 175 plants m^{-2} . Grain yield was measured at maturity including its component grain number per m^2 and grain

dry mass and nitrogen content. Agronomic management at both sites was according to local practices, including spraying fungicides and herbicides, as needed. Granular phosphorus and Sulphur (i.e., ‘superphosphate’) were incorporated into the soil at sowing at rates between 7 and 9 kg P ha⁻¹ and 8 and 11 kg S ha⁻¹ depending on the year. Because of large variability across the experimental site, the initial soil water content at sowing across the ambient and elevated CO₂ treatments were pooled to be consistent with single soil type parameters for the site (O’Leary *et al.*, 2015).

Table S3. Summary of 18 selected treatments used to compare the simulated and observed grain yield and grain protein concentration from the Horsham FACE experiment (AGFACE). Grain yield and protein data are medians and the 25th and 75th quantiles between squared brackets.

Treatment name	Sowing date	CO ₂ (ppm)	Sowing	Irrigation (mm)	Applied N (kg N ha ⁻¹)	Grain yield (t DM ha ⁻¹)	Grain protein (% of yield)
A7T1 + N+I	18-Jun-07	365	Early	96	138	3.15 [3.06-3.23]	15.28 [15.45-15.17]
E7T1+N+I	18-Jun-07	550	Early	96	138	4.17 [3.73-4.66]	14.76 [14.79-14.67]
A7T2 +N+I	23-Aug-07	365	Late	96	138	2.04 [1.34-2.81]	15.37 [15.79-15.07]
E7T2+N+I	23-Aug-07	550	Late	96	138	3.25 [2.92-3.8]	14.65 [15.11-14.4]
A7T2+N-I	23-Aug-07	365	Late	48	138	2.09 [1.81-2.39]	15.49 [15.67-15.29]
E7T2+N-I	23-Aug-07	550	Late	48	138	2.15 [1.86-2.4]	15.47 [15.7-15.2]
A8T1+N+I	04-Jun-08	365	Early	40	53	2.86 [2.41-3.48]	18.47 [19.35-17.75]
E8T1+N+I	04-Jun-08	550	Early	40	53	3.88 [3.5-4.46]	17.06 [17.75-15.79]
A8T2+N+I	05-Aug-08	365	Late	80	53	1.83 [1.7-1.92]	17.74 [18.41-17.28]
E8T2+N+I	05-Aug-08	550	Late	80	53	2.09 [1.67-2.48]	16.17 [16.6-16.2]
A8T2+N-I	05-Aug-08	365	Late	25	53	1.43 [1.33-1.48]	16.81 [16.77-16.91]
E8T2+N-I	05-Aug-08	550	Late	25	53	0.89 [0.68-1.24]	18.39 [18.99-17.71]
23-Jun-09	23-Jun-09	365	Early	70	53	2.56 [2.18-2.89]	17.16 [17.57-17.13]

23-Jun-09	23-Jun-09	550	Early	70	53	3.04 [2.72-3.3]	15.03 [14.91-15.94]
19-Aug-09	19-Aug-09	365	Late	60	53	1.24 [1.14-1.38]	18.93 [19.22-18.72]
19-Aug-09	19-Aug-09	550	Late	60	53	1.79 [1.32-2.34]	18.86 [18.71-18.25]
19-Aug-09	19-Aug-09	365	Late	0	53	0.98 [0.84-1.17]	21.51 [21.9-19.9]
19-Aug-09	19-Aug-09	550	Late	0	53	1.61 [1.43-1.93]	18.72 [18.96-17.41]

5

6 ***Field experiments for adaptation***

7 *Egypt experiment*

8 Experimental data from Egypt were collected from four field experimental sites along the river Nile over three growing seasons
9 (2011/2012, 2012/2013 and 2013/2014). These locations were based on the variability of agro-climatic zones in Egypt from North to
10 South (Khalil *et al.*, 2011). The locations from North (moderate temperature) to South (high temperature) were as follows: Sakha
11 (North delta, lower Egypt, 31.0° N, 30.9° E, 5 m elevation); Menofya (Middle delta, 30.7° N, 31.0° E, 10 m elevation); Benisuef
12 (Middle Egypt, 29.1° N, 31.0° E, 30 m elevation); and Aswan (upper Egypt, 23.9 N°, 32.9° E, 180 m elevation). Daily measured
13 weather data were collected at the four field experiments by the Central Laboratory of Agricultural Climate (CLAC) in Egypt
14 (www.clac.edu.eg) and used for specifying the range of wheat growing season mean temperature in each location. Based on the World
15 Reference Base for Soil Resources, the main soil group along the river Nile is Fluvisols, and main texture is clay and loamy clay
16 (FAO, 1998, Taha, 2000).

17 The field experiments were conducted using two of the most common modern cultivars (Misr2 and Misr1) and a standard cultivar
18 (Sakha93) under full irrigation and high fertilization (180 kg N ha⁻¹). Cultivars were sown on two planting dates, 20 November, which
19 was the date recommended by (MALR, 2003), and 30 November (late sowing), which provided a contrasting temperature regime at
20 the same location.

1 Field experiment measurements included 50% anthesis date, physiological maturity date, grain yield, for all cultivars under both
2 recommended and late planting dates. Determination of nitrogen content in oven dry samples was carried out using Kjeldahl method
3 and the percentage of total nitrogen was converted to protein concentration by multiplying by a conversion factor of 5.7 for grains of
4 wheat (Mossé *et al.*, 1985).

5

6 *Italy experiment*

7 Experiments were carried out in 2003/2004 and 2004/2005 at the experimental station in Ottava, Sardinia, Italy (41°N, 8°E, 80 m
8 elevation). The soil at the site is a sandy-clay-loam of depth about 0.6 m overlaid on limestone (Xerochrepts), with an average
9 nitrogen content of 0.76%, and a C:N (w:w) ratio of 12. The soil water content was 22.4% (w:w) at field capacity (-0.02 MPa), and
10 11.9% at -1.5 MPa. The climate is typically Mediterranean, with a long-term average annual rainfall of 538 mm. In 2003/2004, the
11 first sowing was made on 20 November and the second on 16 February. In 2004/2005, the first sowing was made on 5 January and the
12 second on 17 March. Nitrogen fertilizer was applied at sowing at 60 kg N ha⁻¹ or 100 kg N ha⁻¹ as urea and ammonium bi-phosphate,
13 respectively. The cv. Claudio and cv. Creso analyzed in this study were part of a wider set of 20 cultivars. In both seasons, two
14 adjacent fields were assigned to the two sowing dates and divided into three blocks. Within each block, nitrogen rate represented the
15 main plots, and cultivars represented the sub-plots. Plots were 10 m². Sprinkler irrigation was used to ensure optimal growing
16 conditions. Weeds, pests, and diseases were chemically controlled.

17 Anthesis (anthers exerted from the spikelets) and maturity ('yellow peduncle stage') (Chen *et al.*, 2010b) were timed when 50% of the
18 ears in a plot reached the stage. At maturity, two 1 linear meter samples per plot from different rows were cut at the ground level, and
19 then air-dried and weighed. Ears were separated from the rest of the sample, and then counted and threshed. Grain yield was
20 calculated on a whole plot basis, following mechanical harvesting. Grain nitrogen concentrations were determined by the Kjeldhal

1 method and the percentage of total nitrogen was converted to protein concentration by multiplying by a conversion factor of 5.7 for
2 grains of wheat (Mossé *et al.*, 1985). More details about the experiments can be found in (Giunta *et al.*, 2007).

3

4 *USA experiment*

5 Two soft wheat advanced breeding lines, VA12W-72 developed by university of Virginia and GA06493-13LE6 developed by
6 university of Georgia, and three standard cultivars, AGS2000, Jamestown, and USG3120, were planted at the plant science research
7 and education unit in Citra (29.4° N, 82.2° W, 24 m elevation), FL on 15 December 2014. The experiment was laid out in a
8 randomized complete block design with three replications at 6.9 m² plots (1.5 m × 4.6 m). The soil of the location is mostly sandy
9 loam. Round-up® herbicide was applied 15 days before planting to control different narrow leaf weeds. Buctril® and Harmony® Extra
10 were applied at 4 and 6 weeks after planting to control broad-leaf weeds. Prosaro® fungicide was applied three times (at 10, 13, and 15
11 weeks) to control foliar diseases such as leaf and stripe rust and Septoria leaf and glume blotch. NPK were applied at the rate of 5-10-
12 15 kg ha⁻¹ plus sulphur and micronutrients at the day of planting. Additionally, 36 kg N ha⁻¹ was applied as top dress two times
13 through irrigation during January and February. Irrigation was applied throughout the cropping cycle by using a central pivot
14 irrigation system to avoid water stress. The experiment was machine harvested in the first week of June 2015. Days to anthesis were
15 recorded as days from emergence at which 50% of plants in a plot flowered. Days to maturity were calculated as emergence at which
16 50% of peduncles turned yellow. A machine harvested sample from freshly harvested grains was collected and oven dried for 48 h,
17 and dry weights were measured. The fresh and dry weight samples were used to adjust moisture percent and final yield. Grain filling
18 rate was calculated as yield divided by the difference of days to maturity to days to anthesis.

19 The data on the same genotypes were collected from ten other locations, including Griffin (33.3° N, 84.3° W, 298 m elevation) and
20 Plains (32.1° N, 84.4° W, 755 m elevation) in Georgia; Quincy (30.6° N, 84.6° W, 63 m elevation) in Florida; Warsaw (38.0° N, 76.8°
21 W, 40 m elevation) and Blacksburg (37.2° N, 80.4° W, 633 m elevation) in Virginia; Winnsboro (32.1° N, 91.7° W, 22 m elevation) in

Louisiana; Knoxville (36.0° N, 84.2° W, 270 m elevation) in Tennessee; Farmersville (33.1° N, 96.2° W, 199 m elevation) in Texas; and Lexington (38.0° N, 84.5° W, 298 m elevation) in Kentucky. In general, soils of these locations were heavier (more clay) than Citra, Florida. Fertilizers were applied based on soil testing in those locations. Fall and spring applications of fertilizers were practiced. Chemicals were applied to control narrow and broad leaf weeds. The plots were machine harvested at maturity.

CIMMYT experiment

The fourth data set was the International Heat Stress Genotype Experiment (IHSGE) carried out by CIMMYT that included six temperature environments (Reynolds *et al.*, 1994). The IHSGE was a 4-year collaboration between CIMMYT and key national agricultural research system partners to identify important physiological traits that have value as predictors of yield at high temperatures (Reynolds *et al.*, 1994). Experimental locations were selected based on a classification of temperature and humidity during the wheat growing cycle. “Hot” and “very hot” locations were defined as having mean temperatures above 17.5 and 22.5°C, respectively, during the coolest month. “Dry” and “humid” locations were defined as having mean VPD above and below 1.0 kPa, respectively. The present study used data from four of the original 12 locations (i.e., two growing seasons in two Mexico locations, and one growing season in two locations in Egypt and Sudan) to represent a range of temperatures. Of the sixteen genotypes originally included in the experiment, two were selected for the present study (cv. Bacanora 88 as the modern cultivar and cv. Debeira as the standard cultivar). Variables measured in the experiment included days to 50% anthesis, days to physiological maturity, final grain yield. All experiments were well watered and fertilized with temperature being the most important variable.

1 *Statistical analysis of model performance*

2 Measured (y_i) and simulated (\hat{y}_i) grain yield, grain protein yield, and grain protein concentration were compared using the mean squared
3 error (MSE):

4
$$RMSE = \sqrt{\frac{1}{n} \sum_{i=1}^n (y_i - \hat{y}_i)^2} \quad (1)$$

5 The root mean squared relative error (RMSRE) was also calculated as an error metric scaled to the unit of the measurement as:

6
$$RMSRE = 100 \times \sqrt{\frac{1}{n} \sum_{i=1}^n \left(\frac{y_i - \hat{y}_i}{y_i} \right)^2} \quad (2)$$

7 To assess the model skill the Nash–Sutcliffe modeling efficiency (EF; (Nash & Sutcliffe, 1970)) was calculated:

8
$$EF = 1 - \frac{\sum_{i=1}^N (y_i - \hat{y}_i)^2}{\sum_{i=1}^N (y_i - \bar{y})^2} = 1 - \frac{MSE}{MSE_{\bar{y}}} \quad (3)$$

9 where \bar{y} is the average over the y_i and $MSE_{\bar{y}}$ is the MSE for the model that uses \bar{y} as an estimator. EF is a skill measure that compares
10 model MSE with the MSE of using the average of measured values as an estimator.

11 Results are given in Table S4.

12

Table S4. Model error and skill for grain yield, grain protein yield, and grain protein concentration for the INRA and the Australian FACE experiments for the median of the 32 (grain yield) or 18 (grain protein) wheat model ensembles. RMSE, root mean squared error; RMSRE, root mean squared relative error; EF, modeling efficiency. The values in parenthesis were calculated when also including the treatments used for model calibration.

Experiment	Grain dry mass yield			Grain N yield			Grain protein concentration		
	RMSE	RMSRE	EF	RMSE	RMSRE	EF	RMSE	RMSRE	EF
	(t ha ⁻¹)	(%)	(-)	(kg N ha ⁻¹)	(%)	(-)	(% of grain yield)	(%)	(-)
INRA	0.37	5.36	0.82	12.43	8.04	-0.08	0.82	7.73	0.55
	(0.42)	(6.09)	(0.70)	(14.52)	(9.36)	(-0.08)	(0.91)	(8.61)	(0.41)
AGFACE	1.88	44.04	0.51	7.18	25.59	0.51	3.23	17.77	-3.05
	(0.66)	(44.04)	(0.51)	(16.80)	(25.59)	(0.51)	(3.23)	(17.77)	(-3.05)

Global impact assessment

Model inputs for global simulations

To carry out the global impact assessment and exclusively focus on climate change, region-specific cultivars were used in all 60 locations. The cultivars for locations 31 to 60 were partly based on the cultivars for locations 1 to 30. Observed local mean sowing, anthesis, and maturity dates were supplied to modelers with qualitative information on vernalization requirements and photoperiod sensitivity for each cultivar (Supplementary Fig. S5-6). Modelers were asked to sow at the supplied sowing dates and calibrate their cultivar parameters against the observed anthesis and maturity dates by considering the qualitative information on vernalization requirements and photoperiod sensitivity.

1 For locations 1 to 30 sowing dates were fixed at a specific date. For locations 31 to 60, sowing windows were defined and a sowing
 2 rule was used. The sowing window was based on sowing dates reported in literature. For locations 41, 43, 46, 53, 54, and 59, sowing
 3 dates were not reported in literature and estimates from a global cropping calendar were used (Portmann *et al.*, 2010). The cropping
 4 calendar provided a month (the 15th of the month was used) in which wheat is usually sown in the region of the location. The start of
 5 the sowing window was the reported sowing date and the end of the sowing window was set two months later. Sowing was triggered
 6 in the simulations on the day after cumulative rainfall reached or exceeds 10 mm over a 5-day period during the predefined sowing
 7 window. Rainfall from up to 5 days before the start of the sowing window was considered. If these criteria were not met by the end of
 8 the sowing window, wheat was sown on the last day of the sowing window. Sowing dates were left unchanged for future scenarios.

9 For locations 35, 39, 47, 49, and 55 to 57 (Supplementary Table S5), anthesis dates were reported in the literature. For the remaining
 10 sites, anthesis dates were estimated with the APSIM-Wheat model. Maturity dates were estimated from a cropping calendar for sites
 11 31 to 32, 37 to 38, 41 to 46, 49 to 54, and 58 to 59 (Supplementary Table S5) where no information from literature was available. For
 12 locations 31 to 60, observed grain yields from the literature (Supplementary Table S5) were provided to modelers with the aim to set
 13 up wheat models to have similar yield levels, as well as similar anthesis and maturity dates. No yields were reported for sites 49 and
 14 56 (Supplementary Table S5), so APSIM-Wheat yields were estimated and used as a guide.

15 Locations 1 to 30 (no water or N limitations; Supplementary Table S5) were simulated using the same soil information from
 16 Maricopa, USA. Soil information for locations 31 to 60 (Supplementary Table S5) were obtained from a global soil database (Romero
 17 *et al.*, 2012). The soil closest to a location was used, but for locations 39 and 59 (Supplementary Table S5), soil carbon was decreased
 18 after consulting local experts.

19 Initial soil nitrogen was set to 25 kg N ha⁻¹ NO₃-N and 5 kg N ha⁻¹ NH₄-N per 100 cm soil depth and reset each year for locations 31
 20 to 60. Initial soil water for spring wheat sown after winter at locations 31 to 60 was set to 100 mm PAW, starting from 10 cm depth
 21 until 100 mm was filled in between LL and DUL. The first 10 cm were kept at LL (see soil profiles) and reset each year. If wheat was

1 sown after summer, initial soil water was set to 50 mm PAW, starting from 10 cm depth until 50 mm was filled in between LL and
2 DUL. The first 10 cm were kept at LL (see soil profiles) and reset each year.

3 For locations 31 to 60, fertilizer rates were determined from (Gbegbelegbe *et al.*, 2017) except for site 59 (Ethiopia) where N fertilizer
4 was set to 60 kg N ha⁻¹. Fertilizer rates were set low (20 to 50 kg N ha⁻¹) at locations 31 to 32, 48, 51, 53, 60; medium (60 kg N ha⁻¹) at
5 locations 33 to 43, 45 to 47, 49 to 50, 52, 54, 57 to 59; and relatively high (100 to 120 kg N ha⁻¹) at locations 44, 55 to 56. All fertilizer
6 was applied at sowing.

7

Table S5. Location, name and characteristics of the cultivars, sowing date (locations 1-30) or sowing window (locations (31-60)), and mean anthesis and physiological maturity date for the 30 locations (1-30) from high rainfall or irrigated wheat regions and thirty locations from low rainfall (low input) regions (31-60) of the world used in this study.

Cultivar													
Location number	Country	Location	Latitude / longitude (decimal)	Elevation (m a.s.l)	Irrigation (Y/N)	Name	Growth habit ^a			Sowing date or window	Mean 50%-anthesis date	Mean maturity date	Reference used for choosing anthesis date
							Vernalization requirement ^b	Photoperiod sensitivity ^b					
01	USA, NE	Maricopa	33.06 / -112.05	358	Y	Yecora Rojo	S	2	1	25 Dec.	5 Apr.	15 May	-
02	Mexico	Obregon	27.33 / -109.9	41	Y	Tacupeto C2001	S	2	2	1 Dec.	15 Feb.	30 Apr.	-
03	Mexico	Toluca	19.40 / -99.68	2,667	Y	Tacupeto C2001	S	2	2	10 May	5 Aug.	20 Sep.	-
04	Brazil	Londrina	-23.31 / -51.13	610	Y	Atilla	S	3	3	20 Apr.	10 Jul.	1 Sep.	-
05	Egypt	Aswan	24.10 / 32.90	193	Y	Seri M 82	S	3	2	20 Nov.	20 Mar.	30 Apr.	-
06	The Sudan	Wad Medani	14.40 / 33.50	413	Y	Debeira	S	3	2	20 Nov.	25 Jan.	25 Feb.	-
07	India	Dharwar	15.43 / 75.12	751	Y	Debeira	S	3	2	25 Oct.	15 Jan.	25 Feb.	-
08	Bangladesh	Dinajpur	25.65 / 88.68	40	Y	Kanchan	S	2	2	1 Dec.	15 Feb.	15 Mar.	-
09	The Netherland	Wageningen	51.97 / 5.63	12	N	Aminda	W	6	6	5 Nov.	25 Jun.	5 Aug.	-
10	Argentina	Balcarce	-37.75 / -58.3	122	N	Oasis	W	5	5	5 Aug.	25 Nov.	25 Dec.	-
11	India	Ludhiana	30.90 / 75.85	244	Y	HD 2687	S	1	1	15 Nov.	5 Feb.	5 Apr.	-

12	India	Indore	22.72 / 75.86	58	Y	HI 1544	S	0	1	25 Oct.	25 Jan.	25 Mar.	-
13	USA, WI	Madison	43.03 / -89.4	267	N	Brigadier	W	6	6	15 Sep.	15 Jun.	30 Jul.	-
14	USA, KS	Manhattan	39.14 / -96.63	316	N	Fuller	W	4	4	1 Oct.	15 May	01 Jul.	-
15	UK	Rothamsted	51.82 / -0.37	128	N	Avalon	W	3	3	15 Oct.	10 Jun.	20 Aug.	-
16	France	Estrées-Mons	49.88 / 3.00	87	N	Bermude	W	6	6	5 Oct.	31 May	15 Jul.	-
17	France	Orleans	47.83 / 1.91	116	N	Apache	W	5	4	20 Oct.	25 May	7 Jul.	-
18	Germany	Schleswig	54.53 / 9.55	13	N	Dekan	W	5	2	25 Sep.	15 Jun.	25 Jul.	-
19	China	Nanjing	32.03 / 118.48	13	N	NM13	W	4	4	5 Oct.	5 May	5 Jun.	-
20	China	Luancheng	37.53 / 114.41	54	Y	SM15	W	6	4	5 Oct.	5 May	5 Jun.	-
21	China	Harbin	45.45 / 126.46	118	Y	LM26	S	1	5	5 Apr.	15 Jun.	25 Jul.	-
22	Australia	Kojonup	-33.84 / 117.15	324	N	Wyallkatchem	S	2	4	15 May	5 Oct.	25 Nov.	-
23	Australia	Griffith	-34.17 / 146.03	193	Y	Avocet	S	2	4	15 Jun.	15 Oct.	25 Nov.	-
24	Iran	Karaj	35.92 / 50.90	1,312	Y	Pishtaz	S	2	2	1 Nov.	1 May	20 Jun.	-
25	Pakistan	Faisalabad	31.42 / 73.12	192	Y	Faisalabad-2008	S	0	2	15 Nov.	5 Mar.	5 Apr.	-
26	Kazakhstan	Karagandy	50.17 / 72.74	356	Y	Steklov-24	S	2	4	20 May	1 Aug.	15 Sep.	-
27	Russia	Krasnodar	45.02 / 38.95	30	Y	Brigadier	W	6	6	15 Sep.	20 May	10 Jul.	-
28	Ukraine	Poltava	49.37 / 33.17	161	Y	Brigadier	W	6	6	15 Sep.	20 May	15 Jul.	-
29	Turkey	Izmir	38.60 / 27.06	14	Y	Basri Bey	S	4	4	15 Nov.	1 May	1 Jun.	-
30	Canada	Lethbridge	49.70 / -112.83	904	Y	AC Radiant	W	6	6	10 Sept.	10 Jun.	25 July.	-
31	Paraguay	Itapúa	-27.33 / -55.88	216	N	Based on Atilla	S	3	3	25 May – 25 Jul.	- ^d	15 Oct. ^e	(Ramirez-Rodrigues <i>et al.</i> , 2014)
32	Argentina	Santa Rosa	-36.37 / -64.17	177	N	Based on Avocet	S	2	4	5 Jun. – 5 Aug.	- ^d	15 Dec. ^e	(Asseng <i>et al.</i> , 2013)
33	USA, GA	Watkinsville	34.03 / -83.41	220	N	Based on Brigadier	W	6	6	25 Nov. – 25 Jan.	- ^d	22 Jun.	(Franzlu bbers & Stuedema nn, 2014)
34	USA, WA	Lind	47.00 / -118.56	522	N	Based on AC Radiant	W	4	4	28 Aug. – 28 Oct.	- ^d	31 Jul.	(Al-Mulla <i>et al.</i> , 2009, Donaldso n <i>et al.</i> , 2001, Schillinge r <i>et al.</i> , 2008)
35	Canada	Swift Current	50.28 / -107.78	10	N	Based on Steklov-24	S	2	4	18 May. – 18 Jul.	16 Jul.	28 Aug.	(Hu <i>et al.</i> , 2015)

36	Canada	Josephburg	53.7 / -113.06	631	N	Based on Steklov-24	S	2	4	15 May. – 15 Jul.	- ^d	28 Aug.	(Izaurreald e <i>et al.</i> , 1998)
37	Spain	Ventas Huelma	37.16 / -3.83	848	N	Based on Basri Bey	S	4	4	18 Dec. – 18 Feb.	- ^d	15 Jun. ^e	(Royo <i>et al.</i> , 2006)
38	Italy	Policoro	40.2 / 16.66	14	N	Based on Basri Bey	S	4	4	17 Nov. – 17 Jan.	- ^d	15 May ^e	(Steduto <i>et al.</i> , 1995)
39	Italy	Libertinia	37.5 / 14.58	267	N	Based on Basri Bey	S	4	4	26 Nov. – 26 Jan.	4 May	30 May	(Pecetti & Hollington, 1997)
40	Greece	Thessaloniki	41.08 / 22.15	36	N	Based on Basri Bey	S	4	4	15 Nov. – 15 Jan.	- ^d	22 Jun.	(Lithourgi dis <i>et al.</i> , 2006)
41	Hungary	Martonvásár	47.35 / 18.81	113	N	Based on Apache	S	5	4	15 Nov. – 15 Jan. ^c	- ^d	15 Jun. ^e	(Berzseny i <i>et al.</i> , 2000)
42	Romania	Alexandria	43.98 / 25.35	73	N	Based on Brigadier	W	6	6	7 Oct. – 7 Dec.	- ^d	15 Aug. ^e	(Cuculeanu u <i>et al.</i> , 1999)
43	Bulgaria	Sadovo	42.13 / 24.93	154	N	Based on Brigadier	W	6	6	15 Oct. – 15 Dec. ^c	- ^d	15 Jul. ^e	(Islam, 1991)
44	Finland	Jokioinen	60.80 / 23.48	107	N	Based on Steklov-24	S	2	2	1 May – 1 Jul.	- ^d	15 Aug. ^e	(Rötter <i>et al.</i> , 2012)
45	Russia	Yershov	51.36 / 48.26	102	N	Based on Steklov-24	S	2	4	6 May – 6 Jul.	- ^d	15 Sep. ^e	(Pavlova <i>et al.</i> , 2014)
46	Kazakhstan	Altbasar	52.33 / 68.58	289	N	Based on Steklov-24	S	2	4	15 Mar. – 15 May ^c	- ^d	15 Sep. ^e	(Pavlova <i>et al.</i> , 2014)
47	Uzbekistan	Samarkand	39.70 / 66.98	742	N	Based on SM15	W	6	4	5 Nov. – 5 Jan.	7 May	5 Jul.	(FAO, 2010)
48	Morocco	Sidi El Aydi / Jemaa Riah	33.07 / -7.00	648	N	Based on Yecora	S	1	1	5 Nov. – 5 Jan.	- ^d	1 Jun.	(Heng <i>et al.</i> , 2007)
49	Tunisia	Nabeul / Tunis	36.75 / 10.75	167	N	Based on Pishtaz	S	2	2	1 Dec. – 1 Feb.	29 Mar.	15 Jun. ^e	(Latiri <i>et al.</i> , 2010)
50	Syria	Tel Hadya / Aleppo	36.01 / 36.56	263	N	Based on Pishtaz	S	2	2	20 Nov. – 20 Jan.	- ^d	15 Jun. ^e	(Sommer <i>et al.</i> , 2012)
51	Iran	Maragheh	37.38 / 46.23	1,472	N	Based on SM15	W	6	4	13 Oct. – 13 Dec.	- ^d	15 Jun. ^e	(Tavakkoli & Oweis, 2004)

52	Turkey	Ankara	39.92 / 32.85	895	N	Based on Fuller	W	4	4	1 Sep. – 1 Nov	- ^d	15 Jul. ^e	(Ilbeyi <i>et al.</i> , 2006)
53	Iran	Ghoochan / Quchan	37.66 / 58.50	1,555	N	Based on Pishtaz	S	2	2	15 Oct. – 15 Dec. ^c	- ^d	15 Jun. ^e	(Bannayan <i>et al.</i> , 2010)
54	Pakistan	Urmur	34.00 / 71.55	340	N	Based on Yecora	S	1	1	15 Nov. – 15 Jan. ^c	- ^d	15 May	(Iqbal <i>et al.</i> , 2005)
55	China	Dingxi	35.46 / 104.73	2,009	N	Based on Pishtaz	S	2	2	15 Mar. – 15 May.	15 Jun.	2 Aug.	(Huang <i>et al.</i> , 2008) ^f
56	China	Xuchang	34.01 / 113.51	110	N	Based on Wenmai	W	4	4	10 Oct. – 10 Dec.	25 Apr.	1 Jun.	
57	Australia	Merredin	-31.50 / 118.2	3000	N	Based on Wyalkatchem	S	2	4	15 May – 25 Jul.	5 Oct.	25 Nov.	(Asseng <i>et al.</i> , 1998)
58	Australia	Rupanyup / Wimmera	-37.00 / 143.00	219	N	Based on Avocet	S	2	4	1 May – 1 Jul.	- ^d	15 Nov. ^e	(van Rees <i>et al.</i> , 2014)
59	Ethiopia	Adi Gudom	13.25 / 39.51	2,090	N	Based on Debeira	S	2	4	15 Jun. – 15 Aug. ^c	- ^d	15 Dec. ^e	(Araya <i>et al.</i> , 2015)
60	South Africa	Glen / Bloemfontein	-28.95 / 26.33	1,290	N	Based on Wyalkatchem	S	2	4	15 May – 15 Jul.	- ^d	15 Nov.	(Singels & De Jager, 1991)

^a S, spring type; W, winter type.

^b Vernalization requirement and photoperiod sensitivity of the cultivars range from nil (0) to high (6).

^c Sowing date estimated using global cropping calendar.

^d See Figure S8.

^e Maturity date estimated using global cropping calendar.

^f Yan Zhu, personal communication, August 4, 2015.

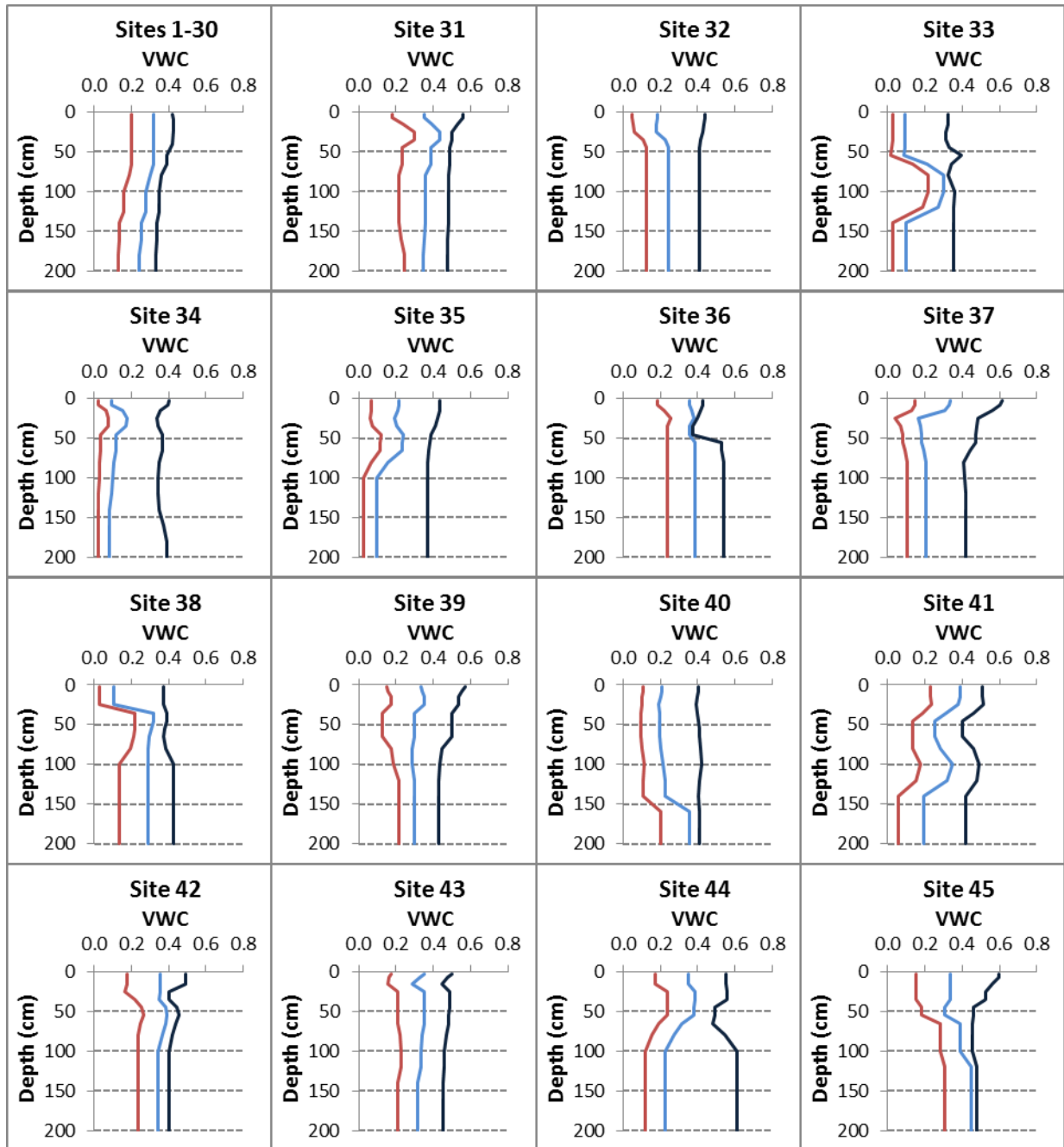


Fig. S1. Soil profile hydrological parameters used for locations 1 to 45. Changes in volumetric water content (VWC in v/v) with soil depth for characteristics water contents. The red line is the drained lower limit (-15 bar); the blue line is drained upper limit (field capacity); and the black line is saturated water content. The lower limit of crop water extraction was assumed to be the same as -15 bar lower limit.

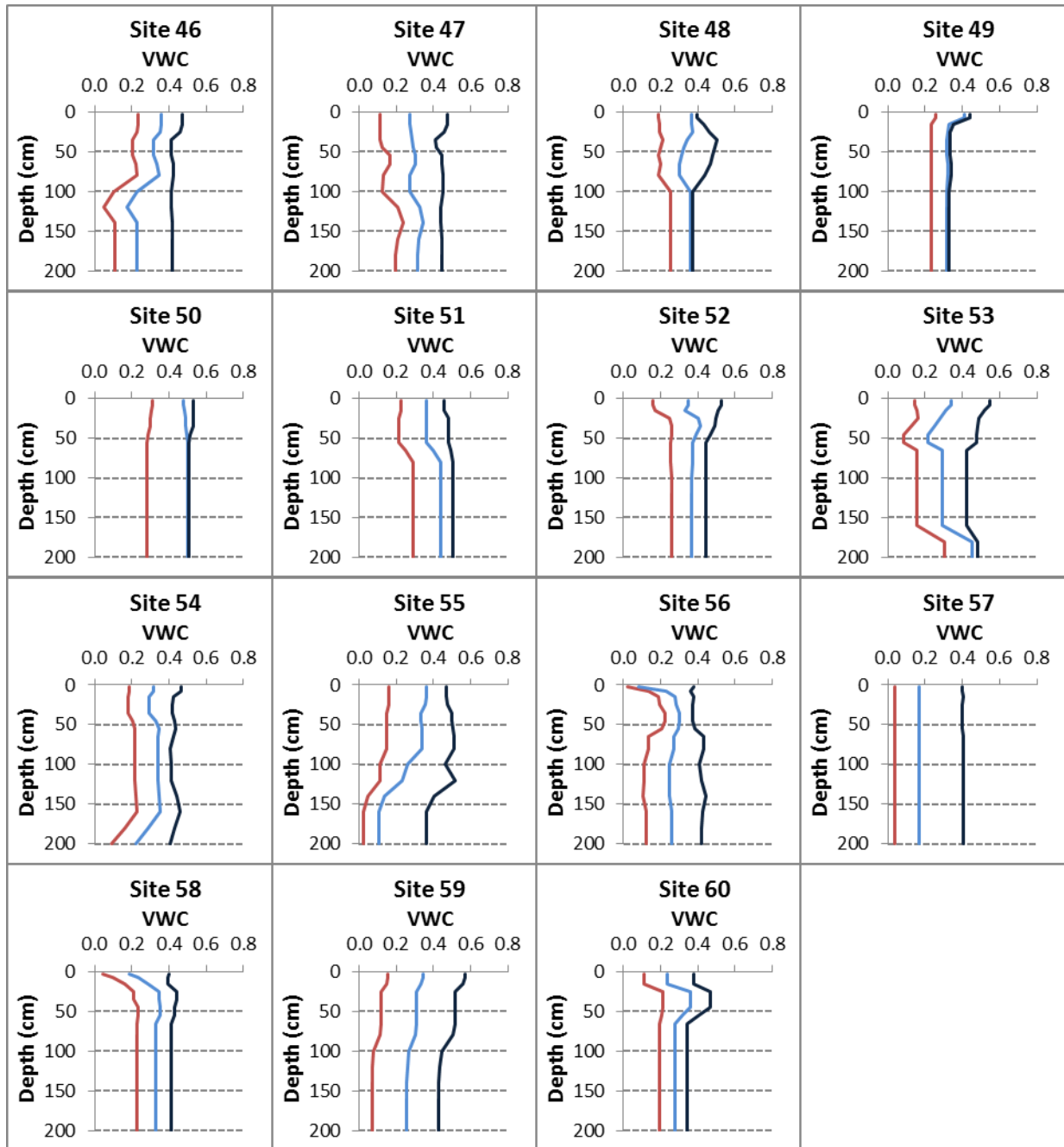
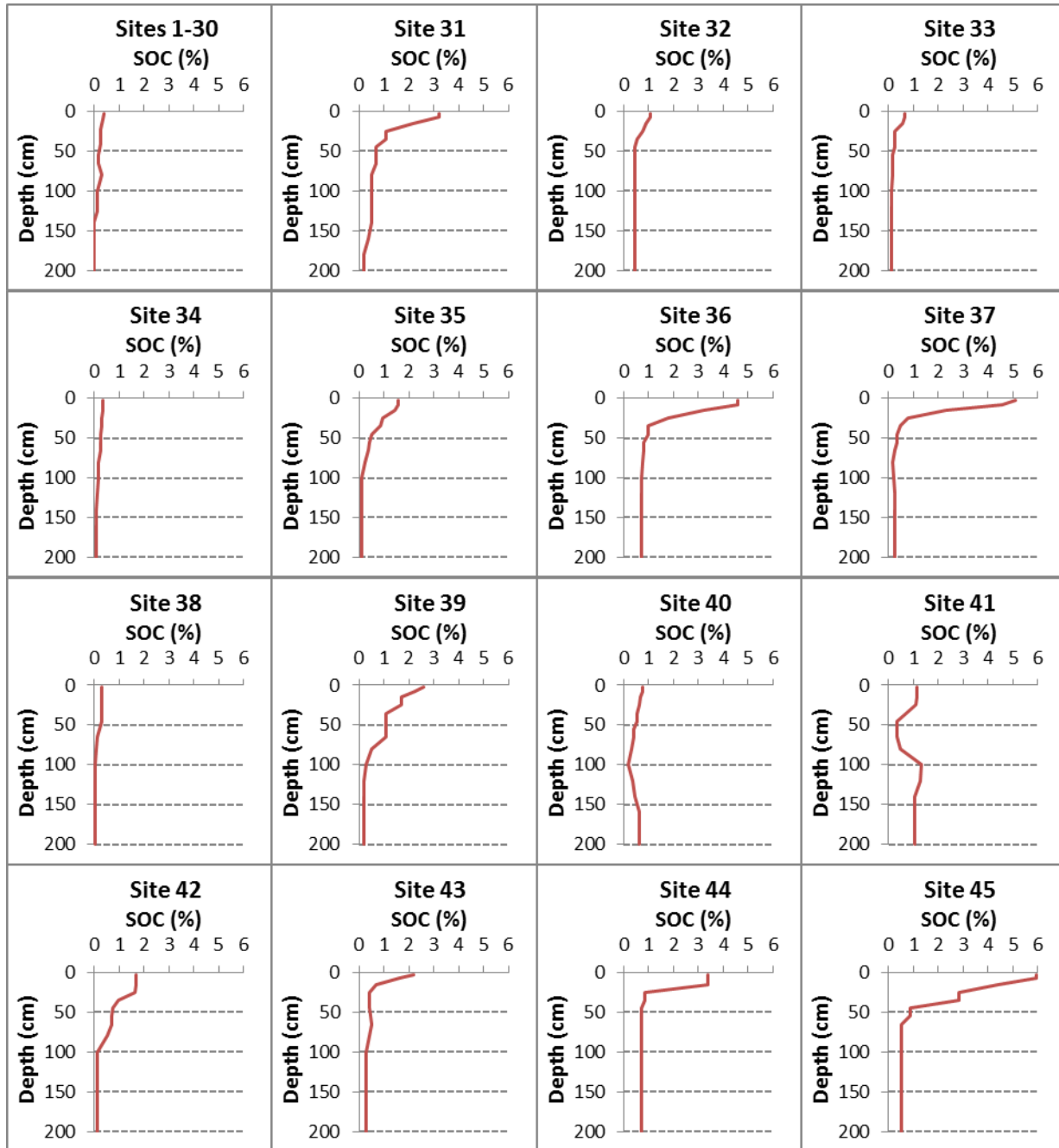


Fig. S2. Soil profile hydrological parameters used for locations 46 to 60. Changes in volumetric water content (VWC in v/v) with soil depth for characteristics water contents. The red line is drained lower limit (-15 bar); the blue line is drained upper limit; and the black line is saturated water content. The lower limit of crop water extraction was assumed to be the same as -15 bar lower limit.

1



2
3

4 **Fig. S3.** Soil Organic Carbon (SOC) in different soil layers for locations 1 to 45.

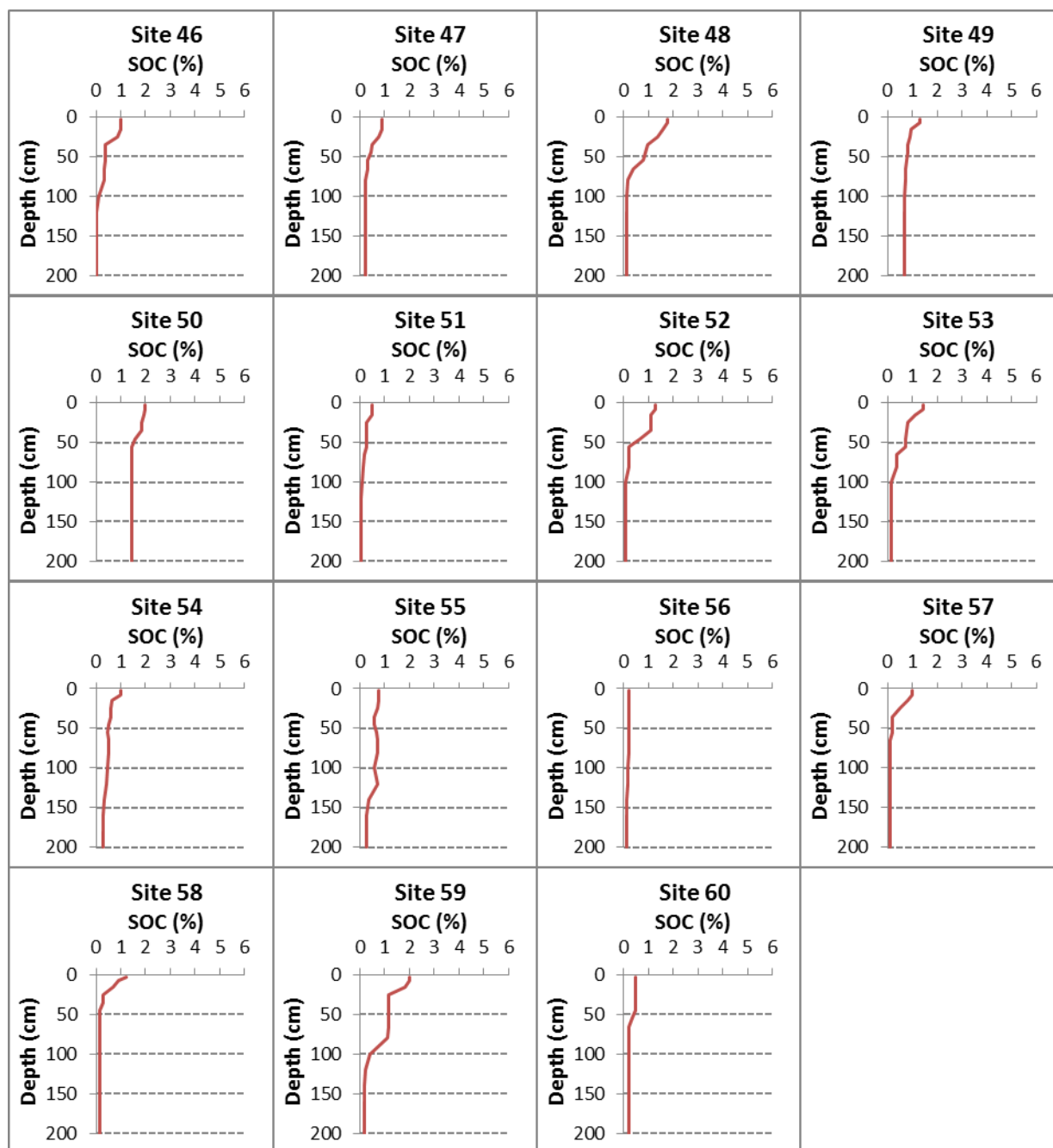


Fig. S4. Soil Organic Carbon (SOC) in different soil layers for locations 56 to 60.

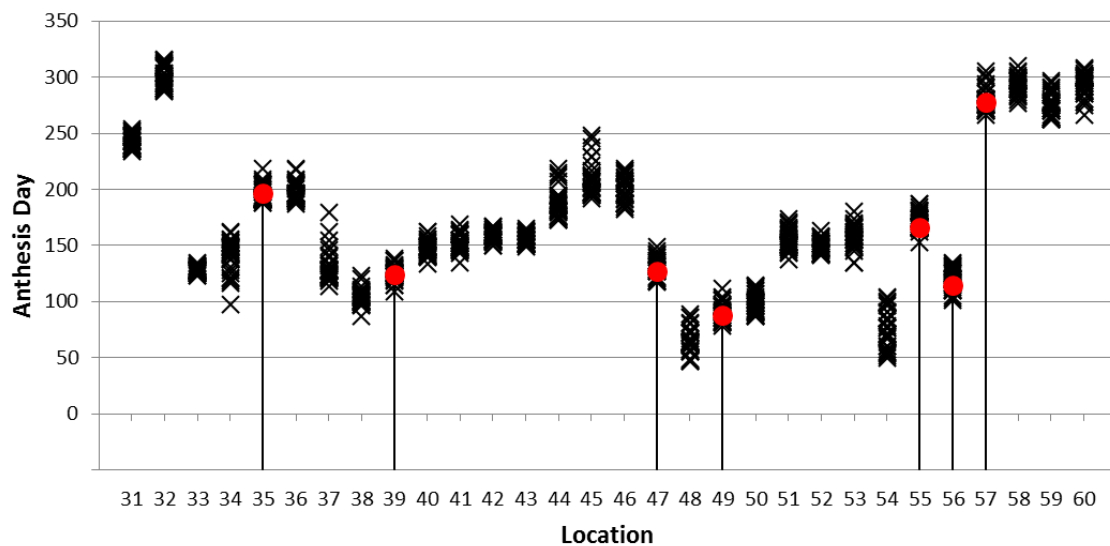


Fig. S5. Observed and simulated anthesis dates for location 31 to 60. Red dots are reported dates and black crosses are dates estimated by APSIM-Wheat model for years 1981-2010.

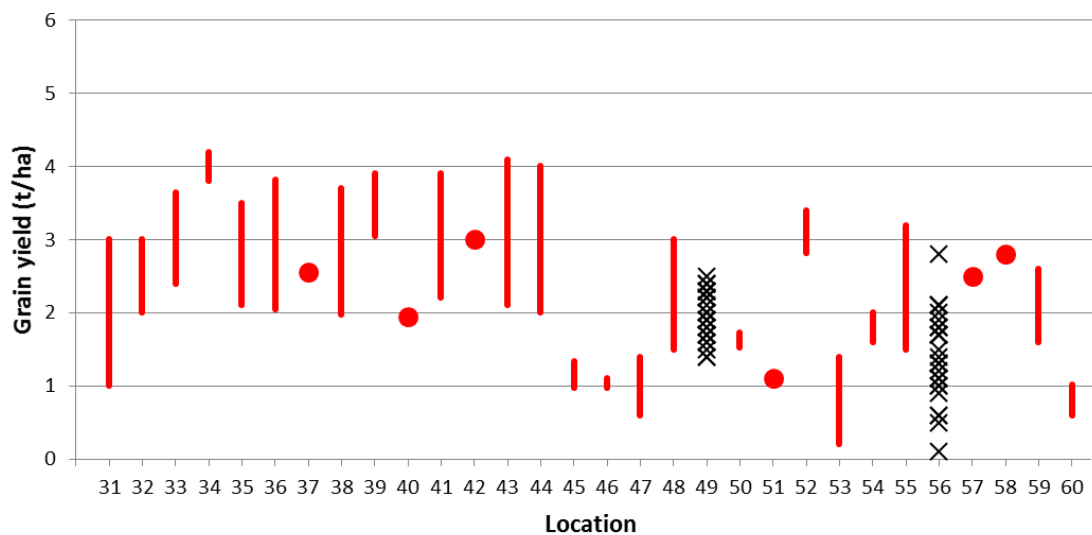
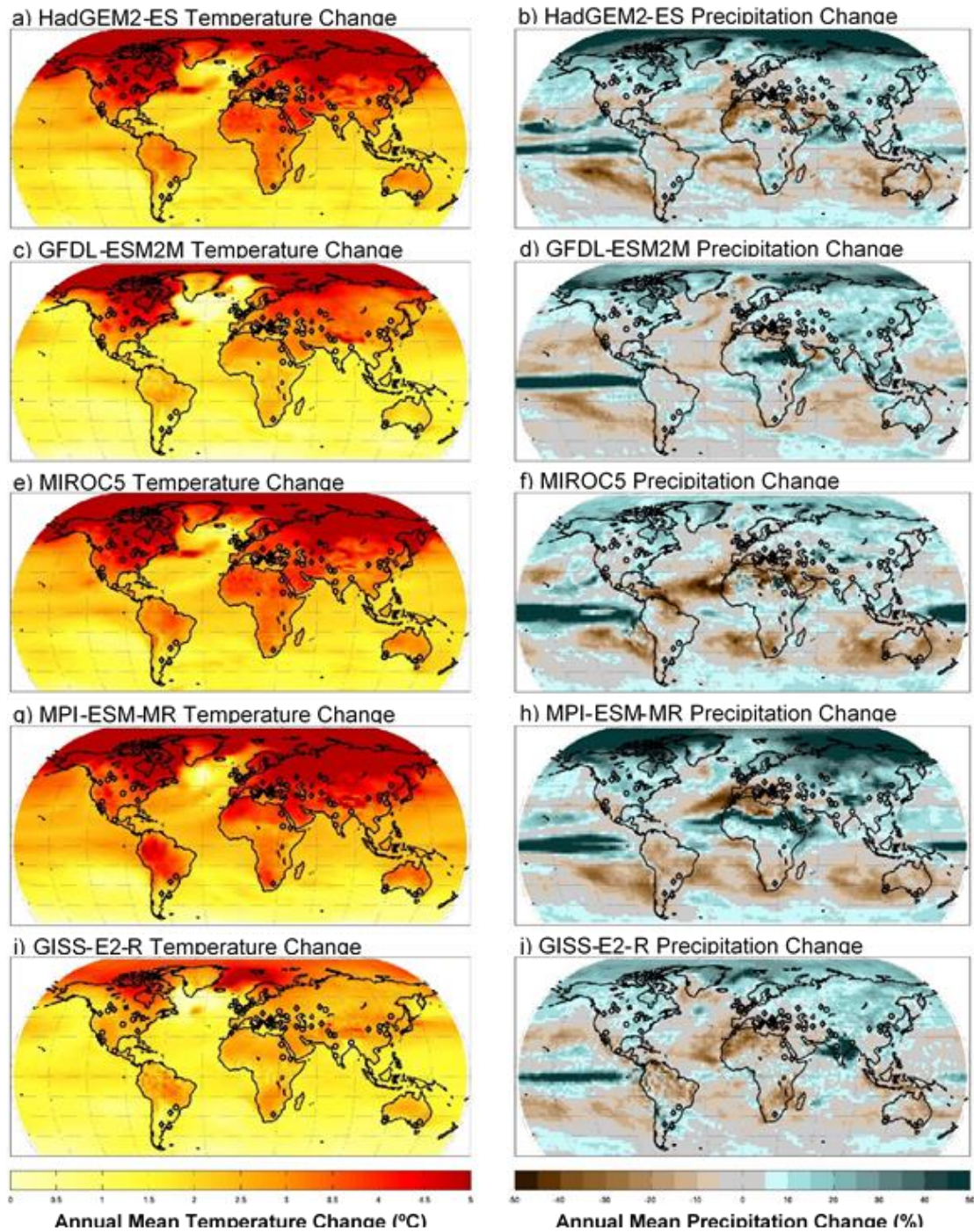


Fig. S6. Observed and simulated grain yields for locations 31 to 60. Red dots and lines show reported yield and yield ranges over several years, when available. Black crosses show grain yields simulated with the APSIM-Wheat model for locations 49 and 56 (1981-2010) where no observed yields were reported.

1 *Future climate projections*

2



3

4 **Fig. S7.** Mean temperature and precipitation changes for the five GCMs used in this study. Mean annual RCP8.5
5 mid-century (2040-2069) temperature (left) and precipitation (right) changes compared to historical baseline (1980-
6 2009) for the five selected GCMs. The locations of the 30 well-watered and 30 water-limited sites are noted as
7 circles and diamonds, respectively.

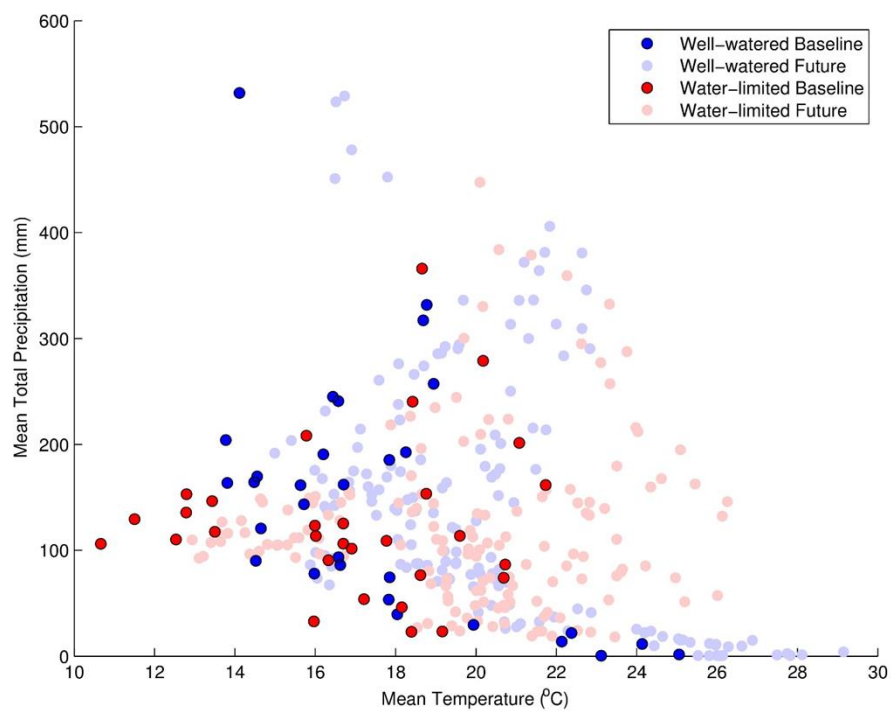


Fig. S8. Critical growing season climate for 60 wheat locations. Mean total precipitation versus mean temperature during the growing season for each the 30 high-rainfall or irrigated locations (well-watered) and 30 low rainfall (water-limited) for 1980-2010 (Baseline) and 2040-2069 (Future). Data for the future are for five GCM scenarios for RCP8.5.

1 ***Simulated adaptation***

2 In 30 of the 32 models, anthesis date was delayed by increasing the thermal time requirement
3 between emergence and anthesis, and for six models (AE, AF, DC, DN, OL, and WG) also by
4 increasing the cold requirement and/or the photoperiod sensitivity. In two models (AE and DN)
5 anthesis date was delayed without changing the thermal time requirement.

6

7 For the adaptation of grain filling trait, the 32 models were divided into five group according to
8 how models incorporated the adaptation to increase grain filling rate.

9 Group 1: 17 models increased rate of grain filling (or HI change): AE, AF, AW, DN, EW, GL,
10 IC, LI, MC, NC, NP, NS, OL, SA, MC, SS, ST, and WG.

11 Group 2: Five models with increased potential grain size (or final HI): CS, DC, DR, EI, and LP.

12 Group 3: Two models with increased fraction of vegetative biomass remobilization: L5 and SP.

13 Group 4: One model with decreased grain filling duration: AQ.

14 Group 5: Seven models with no parameter change to increase the rate of grain filling: DS, HE,
15 MO, NG, S2, SQ, and WO.

16 The distributions of simulated grain yield with and without genetic adaptation under climate
17 change the climate change scenarios for all 32 crop models and for the five groups were similar
18 (Supplementary Fig. S9).

Table S6. Crop model parameters changed for adaptation to climate change. For each model the name, unit, definition, value of the parameters modified to delay anthesis date by 2 weeks and increase the rate of grain filling by 20% to adapt to climate change.

Model name	Trait	Parameter			Value ^a	
		Name	Unit	Definition	Without adaptation	With adaptation
APSIM-E	anthesis	Vern_sens	-	Vernalization sensitivity	1.61 [0.01-4.2]	2.81 [0.2-5]
	anthesis	photo_sens	-	Photoperiod sensitivity	1.62 [0.01-4.5]	2.98 [0.2-5]
	grain filling	potential_grain_filling_rate	mg/grain/d	Potential rate of grain filling	1.94 [1.5-3.0]	2.33 [1.8-3.6]
AFRCWHEAT2 ^b	anthesis	TT-EmAn	°Cd	Thermal time between emergence and anthesis	864 [531-1239]	1049 [794-1239]
	anthesis	Psat	h	Saturation photoperiod	14.4 [6-20]	15.2 [6-20]
	grain filling	GMAXGR	mg/grain/°Cd	Potential grain filling rate	0.074	0.089
AQUACROP	anthesis	GDDays: from sowing to anthesis	°Cd	Thermal time between sowing and anthesis	1428 [610-2100]	1673 [820-2400]
	grain filling	GDDays: building-up of Harvest Index during yield formation	°Cd	Thermal time for the building-up of harvest index during yield formation	929 [508-1478]	689 [280-1200]
APSIM-Wheat	anthesis	tt_end_juv	°Cd	Thermal time between end juvenile and floral initiation	380 [150-400]	462 [218-512]
	anthesis	tt_flor_init	°Cd	Thermal time between floral initiation and anthesis	534 [250-555]	651 [363-710]
	grain filling	potential_grain_filling_rate	mg/grain/d	Potential rate of grain filling	2.03	2.43
CropSyst	anthesis	Tteman	°Cd	Thermal time between crop emergence and anthesis	1581 [671-3318]	1327 [455-3020]
	grain filling	HI	-	Potential harvest Index	0.48	0.58
DSSAT-CERES-Wheat	anthesis	P1	°Cd	Thermal time between end juvenile and floral initiation	277 [140-460]	392 [250-500]
	anthesis	P1V	Vday	Optimum number of vernalizing days	30.3 [10-60]	31.5 [10-60]
	anthesis	P1D	%/10h	Photoperiod response	90 [10-200]	91 [10-200]
	grain filling	G2	mg/grain	Standard grain size under optimum conditions	40.3 [12-80]	48.3 [14-96]
DSSAT-Nwheat	anthesis	VSEN	°Cd	Vernalisation sensitivity	2.33 [1-5]	2.66 [1-5]
	anthesis	PPSEN	°Cd	Photoperiod sensitivity	2.45 [1-5]	4.11 [3-5]
	grain filling	MXFIL	mg/grain/d	Potential rate of grain filling	1.81 [1.4-2.5]	2.17 [1.68-3]

DSSAT-CROPSIM	anthesis	P1	°Cd	Thermal time from end juvenile to floral initiation	434 [350-500]	626 [450-750]
	grain filling	GWTS	mg/grain	Standard grain size under optimum conditions	37 [15-49]	44.4 [18-59]
DAISY	anthesis	DSRate1	DS/d	Development rate in the vegetative stage	0.029 [0.012-0.053]	0.023 [0.01-0.038]
	anthesis	DSeff	-	Development stage factor for assimilate production	1	1.2
EPIC-I	anthesis	PHU	°C	Thermal time between sowing and maturity	1688 [1000-2600]	2004 [1200-2800]
	grain filling	HI	-	Potential harvest index	0.45	0.54
EPIC-Wheat	anthesis	DLAI	-	Fraction of growing season when LAI declines	0.60	0.74 [0.69-0.84]
	grain filling	SCR3	-	Development of harvest index relative to growing season	50.1	58.1
GLAM	anthesis	GCWSPLFL	°Cd	Thermal time between sowing and anthesis	1168 [755-2080]	1419 [987-2412]
	grain filling	DHDT	-	Rate of change in harvest index	0.00797 [0.0035-0.01]	0.00957 [0.0042-0.012]
HERMES	anthesis	Tsum3	°Cd	Thermal time between double ridge and heading	715 [170-1100]	775 [200-1155]
	anthesis	Tsum4	°Cd	Thermal time between heading and anthesis	187 [120-270]	348 [230-400]
INFOCROP	anthesis	TTVG	°Cd	Thermal time between emergence and anthesis	822 [450-1780]	1012 [625-1780]
	grain filling	GFRVAR	mg/grain/d	Potential rate of grain filling	1.32 [0.9-2.4]	1.58 [1.08-2.4]
LINTUL4	anthesis	TSUM1	°Cd	Thermal time between emergence and anthesis	1195 [490-2170]	1455 [710-2510]
	grain filling	PGRIG	mg/grain/d	Potential rate of grain filling	2.0	2.4
SIMPLACE<Lintul-5, SlimWater3,FAO-56, CanopyT,HeatStressHourly>	anthesis	vTSUM1	°Cd	Thermal time between emergence and anthesis	915 [460-1802]	1119 [633-2079]
	grain filling	vFRTDM	-	Proportion of vegetative biomass translocated to grains under optimum conditions	0.074 [0.05-0.09]	0.089 [0.06-0.108]
LPJmL	anthesis	phu	°Cd	Thermal time between emergence and maturity	1876 [1250-2920]	2151 [1395-3300]
	grain filling	hiopt	-	Potential harvest index	0.5	0.6

MCWLA-Wheat	anthesis	rmaxv2	-	Maximum development rate between terminal spikelet initiation and anthesis	0.0435 [0.022-0.0964]	0.0298 [0.0172-0.0554]
	anthesis	rmaxr	-	Maximum development rate between anthesis and maturity	0.0334 [0.0143-0.1182]	0.0401 [0.0172-0.1418]
	grain filling	Hidt	-	Rate of change in harvest index	0.4007 [0.3-0.5]	0.4808 [0.36-0.6]
MONICA	anthesis	Tsum3	°Cd	Thermal time between double ridge and begin anthesis	481 [210-900]	538 [220-1020]
	anthesis	Tsum4	°Cd	Thermal time between begin anthesis and begin grain filling	172 [120-200]	386 [320-400]
Expert-N-CERES	anthesis	PHINT	°Cd	Phyllochron	112 [71-140]	122 [81-150]
	anthesis	P1	°Cd	Thermal time between emergence and terminal spikelet	228 [100-430]	314 [190-525]
	grain filling	G2	mg/grain/d	Potential rate of grain filling	3 [2.9-3.5]	3.6 [3.4-4.2]
Expert-N-GECROS ^c	anthesis	MTDV	d	Minimum thermal days for vegetative phase	54 [22-98]	64 [29-99]
Expert-N-SPASS	anthesis	PDD1	d	Phenological development days between emergence and anthesis	39 [31-51]	48 [38-61]
	grain filling	G2	mg/grain/d	Potential rate of grain filling	2.5 [2.5-3.5]	3.1 [3-4.2]
Expert-N-SUCROS	anthesis	Tsum_1	°Cd	Thermal time between emergence and anthesis	1206 [700-2100]	1428 [900-2420]
	grain filling	G2	mg/grain/d	Potential rate of grain filling	2.5 [2.5-3.5]	3.1 [3-4.2]
OLEARY	anthesis	ANTHDL	°Cdh	Photothermal time between sowing and anthesis	11700 [2500-22278]	14446 [3625-25620]
	anthesis	BOOTDL	°Cdh	Photothermal time between stem extension and booting	5087 [2500-6500]	5173 [2500-6500]
	grain filling	GRMAX	mg/grain/d	Potential rate of grain filling	2.56 [2-2.9]	3.07 [2.4-3.48]
Sirius	anthesis	PHYLL	°Cd/leaf	Phyllochron	83 [70-126]	105 [70-149]
SALUS	anthesis	Phase 3	Phyllochrone	Phyllochronic duration of phase 3	4.5	6.5
	grain filling	krPGR	mg/grain/d	Potential rate of grain filling	2	2.4
SIMPLACE<Lintul-2,CC,Heat,CanopyT,Re-Translocation>	anthesis	AirTemperatureSumAnthesis	°Cd	Thermal time between emergence and anthesis	692 [400-2000]	781 [423-2302]
	grain filling	FRTDM	-	Proportion of vegetative biomass translocated to grains under optimum conditions	0.15	0.18
<i>SiriusQuality</i>	anthesis	P	°Cd/leaf	Phyllochron	113 [80-160]	143 [95-190]

SSM-Wheat	anthesis	bdSELBOT	d	Biological days between stem elongation and booting	10.9 [10.9-10.9]	24.2 [12.1-36.7]
	grain filling	PDHI	1/d	Rate of change in harvest index	0.014 [0.014-0.014]	0.0168 [0.0168-0.0168]
STICS	anthesis	STLEVDRP	°Cd	Thermal time between emergence and anthesis	906 [505-1745]	1125 [715-2050]
	grain filling	VITIRCARB	1/d	Rate of change in harvest index	0.0081	0.00972
WHEATGROW ^d	anthesis	TS	-	Thermal sensitivity	0.85 [0.58-1.81]	0.79 [0.5-1.81]
	anthesis	PS	-	Photoperiod sensitivity	0.000263 [0.0001-0.00054]	0.000268 [0.0001-0.00075]
	anthesis	IE	-	Intrinsic earliness	0.96 [0.58-1.2]	1.38 [0.2-1.95]
	grain filling	BFF	-	Basic filling factor	0.78 [0.45-1.2]	1.11 [0.65-1.75]
WOFOST	anthesis	TSUM1	°Cd	Thermal time between emergence and anthesis	1393 [520-2120]	1643 [740-2500]

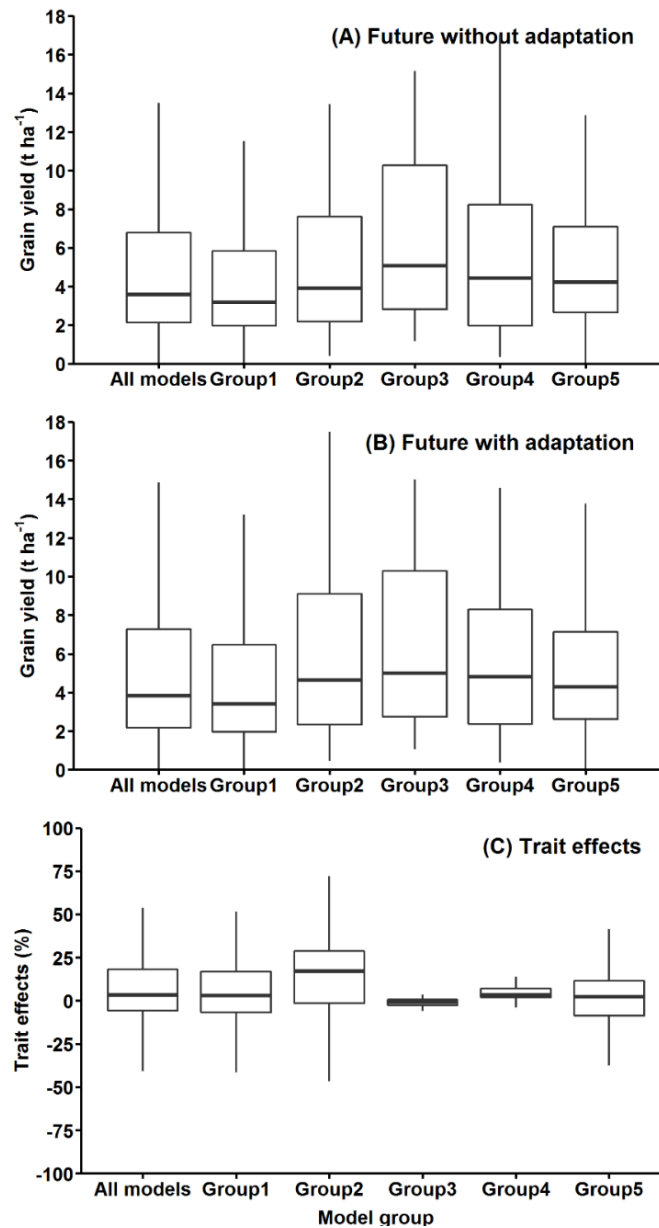
^a For genotypic parameters the mean, minimum and maximum values (between squared brackets) for the 60 locations are given.

^b In order to reach maturity thermal time between anthesis and maturity was increased by 33% at one site (#44).

^c In order to delay the anthesis date by two weeks the base temperatures and/or the curvature of the temperature response function for phenology were also changed at three sites (#5, 22 and 25).

^d In order to reach maturity the grain filling heat tolerance sensitivity parameter (HTS) was also increased by 17 to 80% at three sites (#10, 26, and 45).

1



2

3 **Fig. S9.** Comparison of simulated absolute grain yield and genetic adaptation of grain yield for groups of crop
 4 models with different trait to increase grain filling rate. **(A)** Simulated yield distributions without adaptation, **(B)**
 5 simulated yield distributions with adaptation, and **(C)** distributions of simulated trait effects across the 60 global
 6 locations. All simulations are for 2040-2069 (RCP8.5, five GCMs). In each box plot, end of vertical lines represent
 7 from top to bottom, the 10th, and 90th percentiles, horizontal lines represent from top to bottom, the 25th, 50th, and
 8 75th percentiles of the simulations.

9

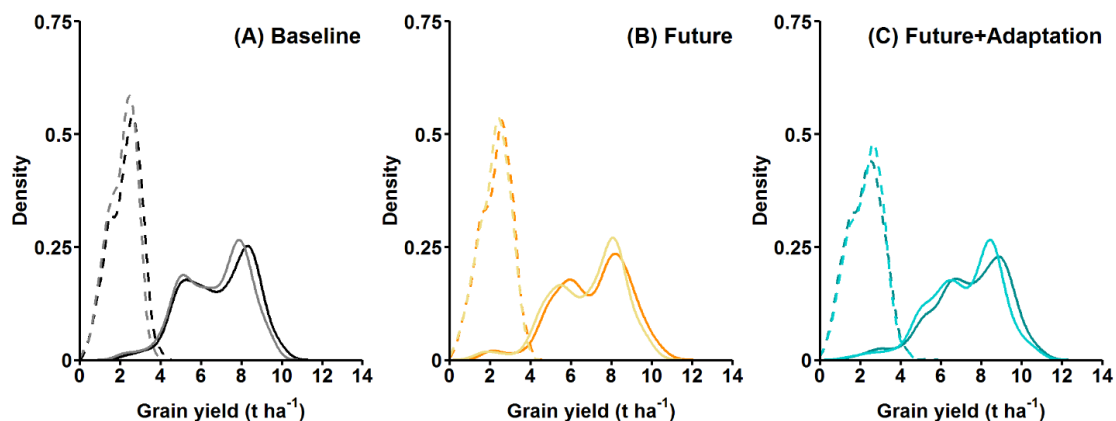


Fig. S10. Comparison of the distributions of simulated annual wheat grain yields from the 32-crop model ensemble median and the 18-crop model ensemble median used in grain protein simulations. **(A)** Baseline (grey: 18 models, black: 32 models); **(B)** climate change scenarios (light orange: 18 models, dark orange: 32 models); and **(C)** climate change scenario with genetic adaptation (light cyan: 18 models, dark cyan: 32 models) at rainfed (dash lines) and high rainfall or irrigated (solid lines) locations.

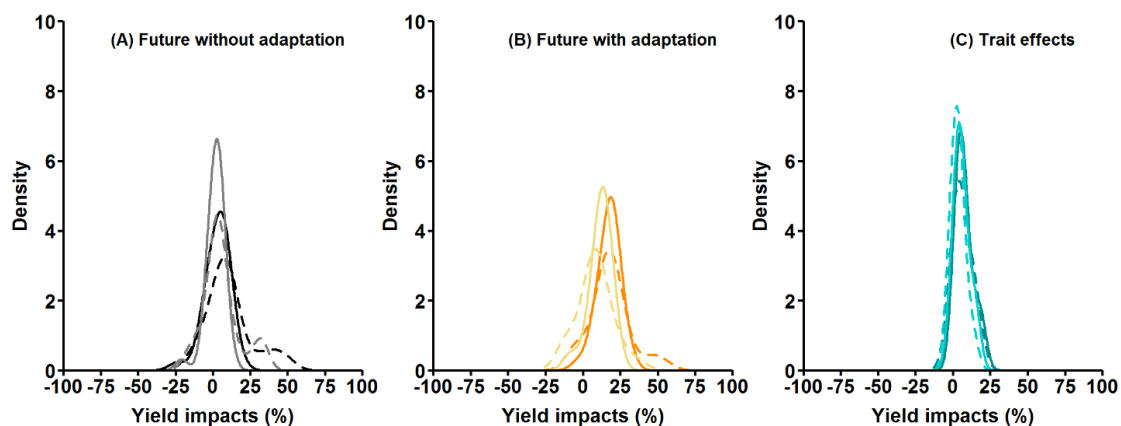


Fig. S11. Comparison of the distributions of simulated 30-year mean wheat yield impacts from the 32-crop model ensemble median and the 18-crop model ensemble median used in grain protein simulations. **(A)** Baseline (grey: 18 models, black: 32 models); **(B)** Future (light orange: 18 models, dark orange: 32 models); and **(C)** climate change scenario with genetic adaptation (light cyan: 18 models, dark cyan: 32 models) at rainfed (dash lines) and high rainfall or irrigated (solid lines) locations.

1

Table S7. Comparison of the distributions of simulated yield impacts of climate change without (Climate impacts) and with (Climate impacts + traits) genetic adaptation, and of genetic adaptation (Trait effects) for the 32 multi-model ensemble and the subset of 18 models used in the protein analysis. Impacts were calculated for 2040-2069 (RCP85, five GCMs) at the 30 low-rainfall or irrigated locations (Locations 1 to 30) and at the 30 low rainfall/input locations (Locations 31 to 60). Data are *P*-value from a Kolmogorov–Smirnov test.

Impacts	<i>P</i>-value ^a	
	High rainfall or irrigated locations	Low rainfall locations
Climate impacts	0.07	0.07
Climate impacts + traits	< 0.01	< 0.01
Trait effects	0.81	0.24

^a *P* < 0.01 indicates that the two distributions were significantly different.

2

3

Supplementary additional supporting results

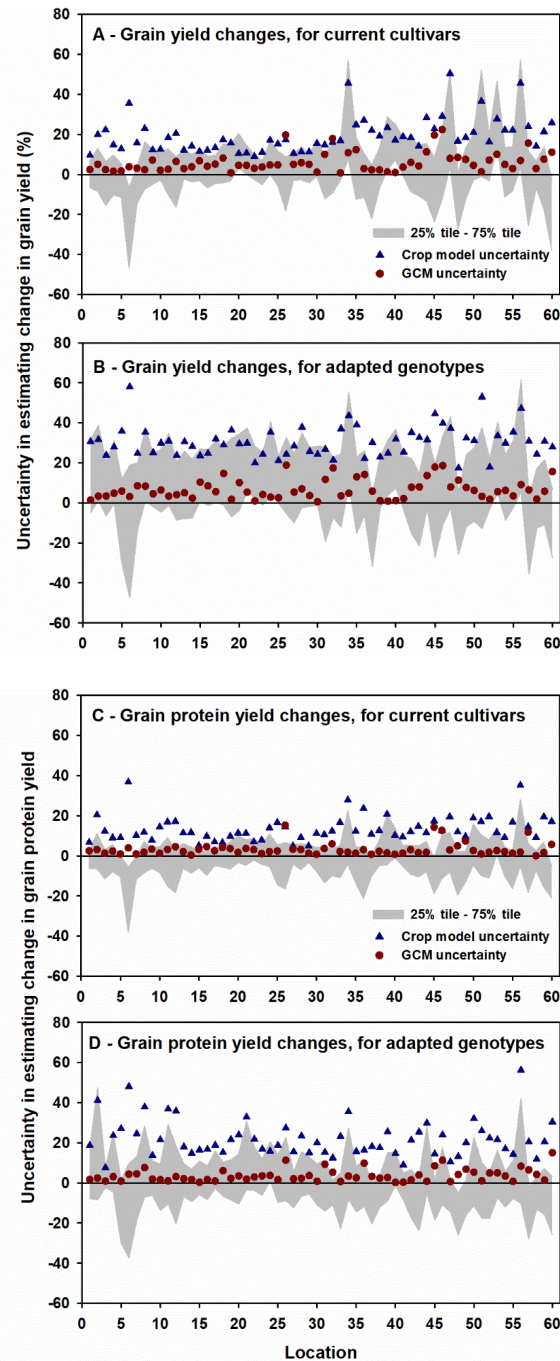


Fig. S12. Relative uncertainty (25th to 75th percentile) in estimating change in (A and B) grain yield and (C and D) grain protein yield, (A and C) with currently grown cultivars and (B and D) with adapted genotypes for crop models (triangle), GCMs (circles) and 25th to 75th percentile uncertainty range (grey shaded area) for crop models and GCM combined, based on a simulated multi-model ensemble projection under climate change of global wheat grain and protein yield for 2036-2065 under RCP8.5 compared with the 1981-2010 baseline across 32 models (or 18 for protein yield estimates) and five GCMs and the average over 30 years of yields using region-specific soils, cultivars and crop management. Locations are connected by line for uncertainty range (gray) to improve readability of this figure.

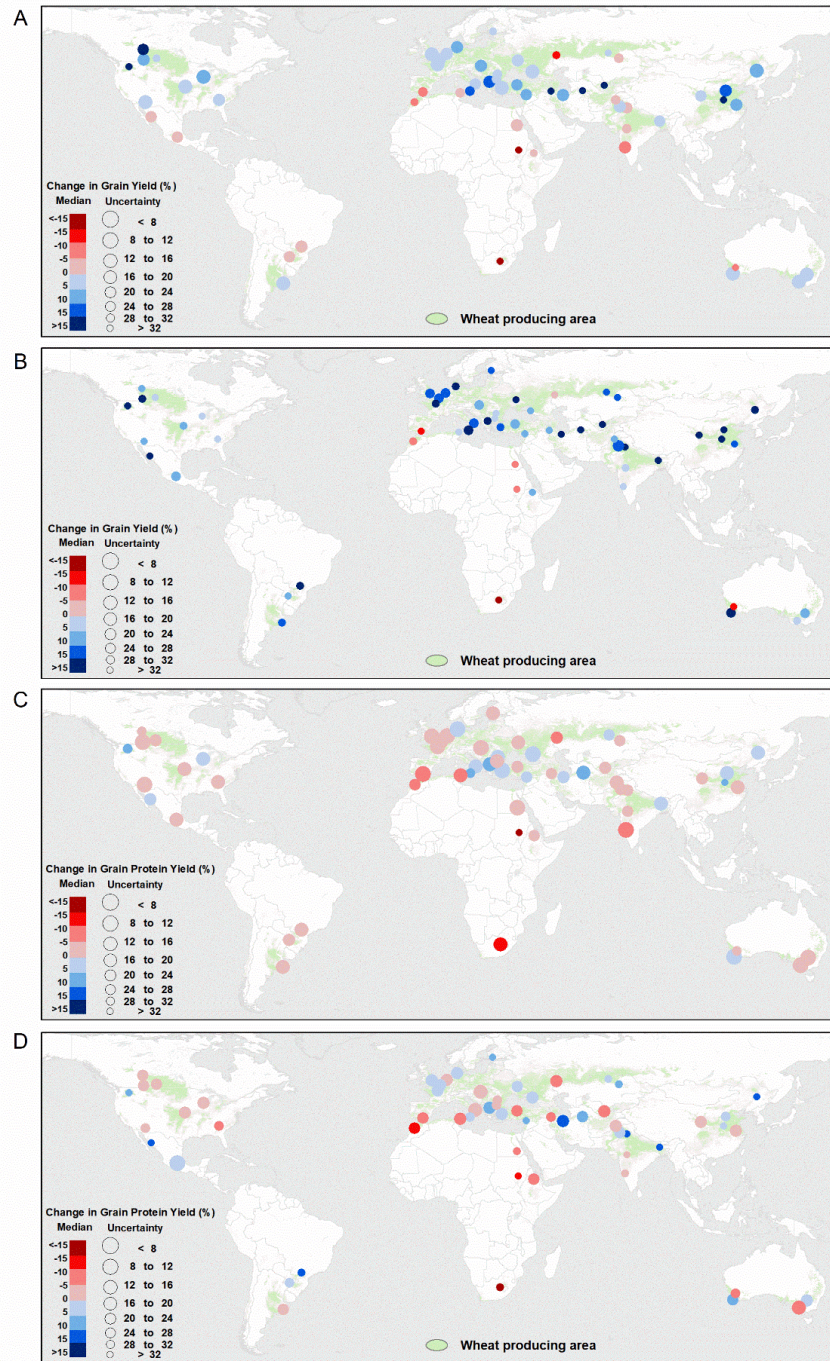


Fig. S13. Simulated global wheat grain and protein yield impacts from climate change with genotypic adaptation. Relative (A and B) grain yield and (C and D) grain protein yield impacts from climate change (A and C) without genetic adaptation and (B and D) with genetic adaptation for 2040-2069 (RCP8.5). Median across 32 crop models (18 for protein) and five GCMs and mean of 30 years using region-specific soils, cultivars, and crop management. Estimate of uncertainty (circle size) given as range between 25th and 75th percentiles for crop models and GCMs together. The larger the symbol, the higher the certainty.

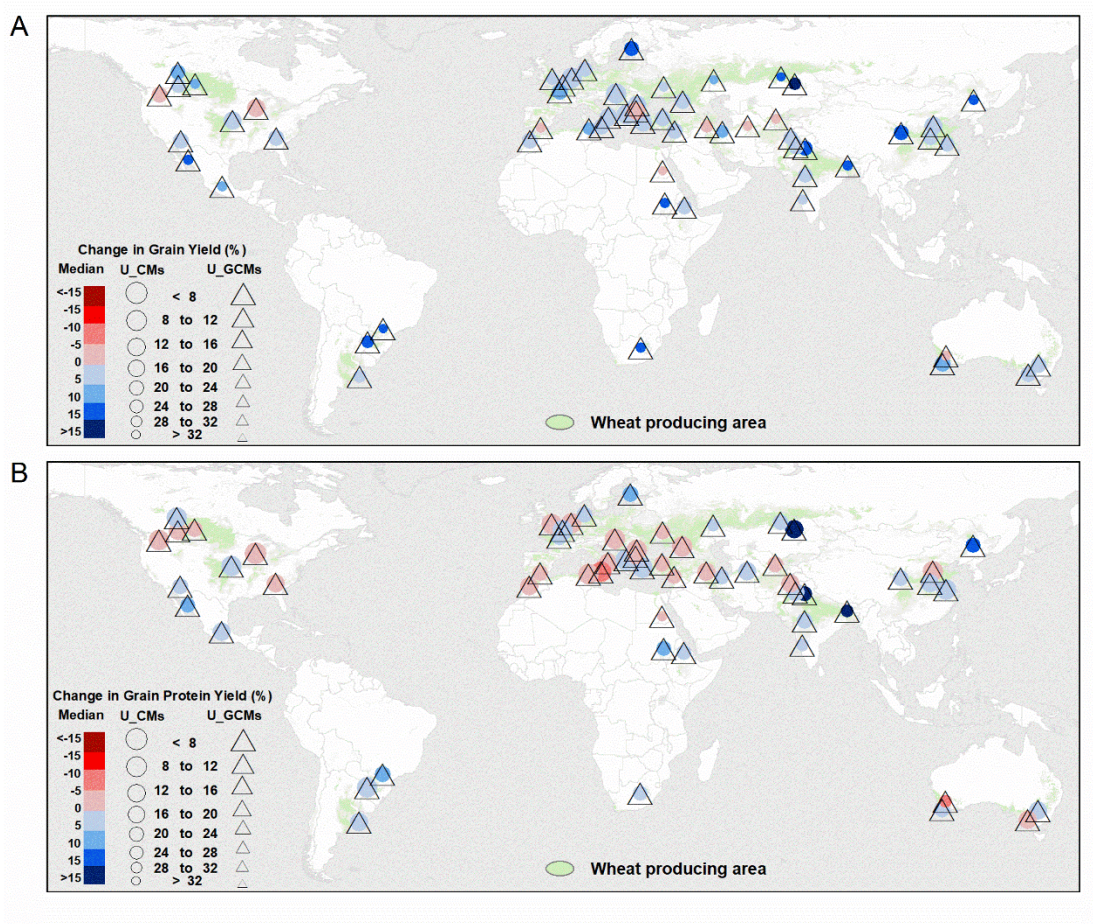


Fig. S14. Simulated trait effect for global wheat grain and protein yield. Relative effect of genetic adaptation on (A) grain yield and (B) grain protein yield for 2040-2069 (RCP8.5). Median across 32 crop models (18 for protein) and five GCMs and mean of 30 years using region-specific soils, cultivars, and crop management. Estimate of uncertainty given as range between 25th and 75th percentiles for crop models (circle size) and GCMs (triangle size). The larger the symbol, the less the uncertainty.

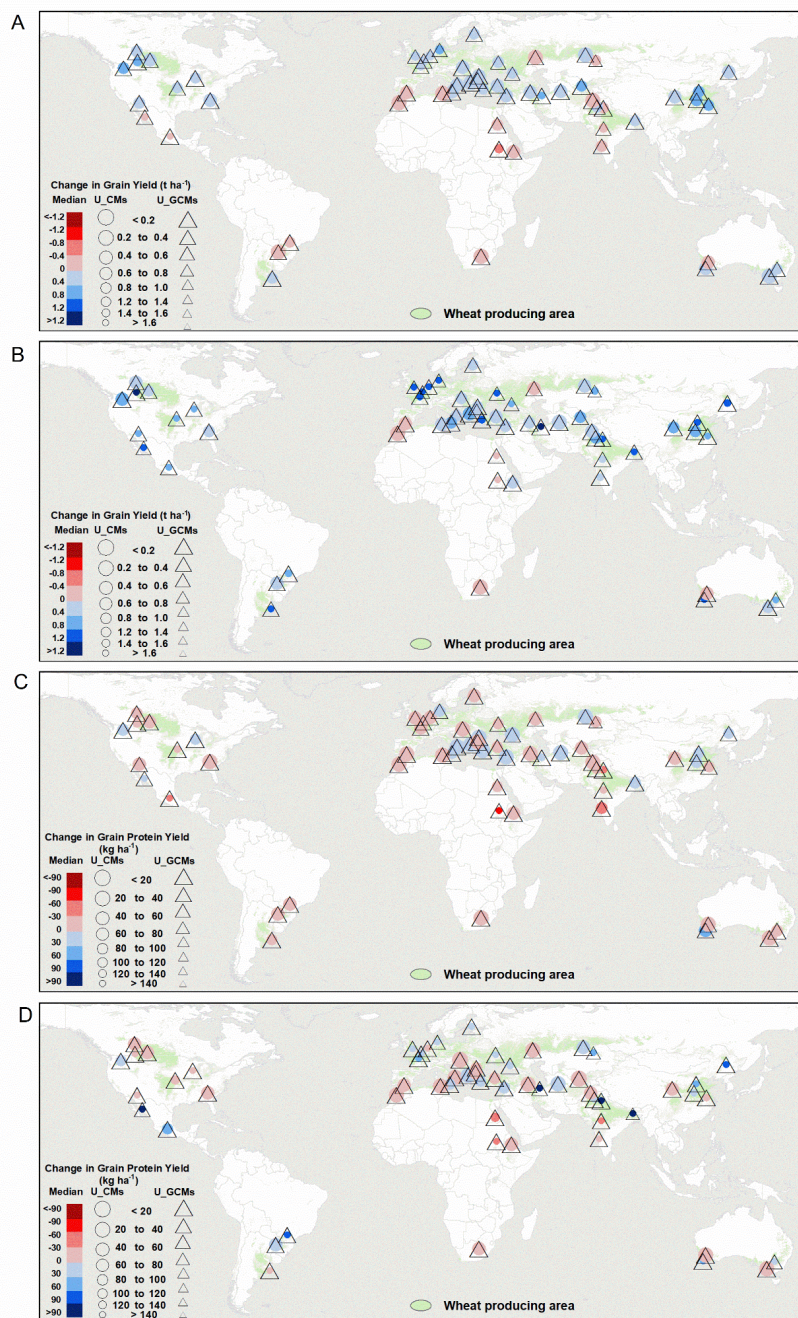


Fig. S15. Simulated global wheat grain and protein yield impacts from climate change with genotypic adaptation. Absolute (**A** and **B**) grain yield and (**C** and **D**) grain protein yield impacts from climate change (**A** and **C**) without genetic adaptation and (**B** and **D**) with genetic adaptation for 2030-2069 (RCP8.5). Median across 32 crop models (18 for protein) and five GCMs and mean of 30 years using region-specific soils, cultivars and crop management. Estimate of uncertainty given as range between 25th and 75th percentiles for crop models (circle size) and GCMs (triangle size). The larger the symbol, the higher the certainty.

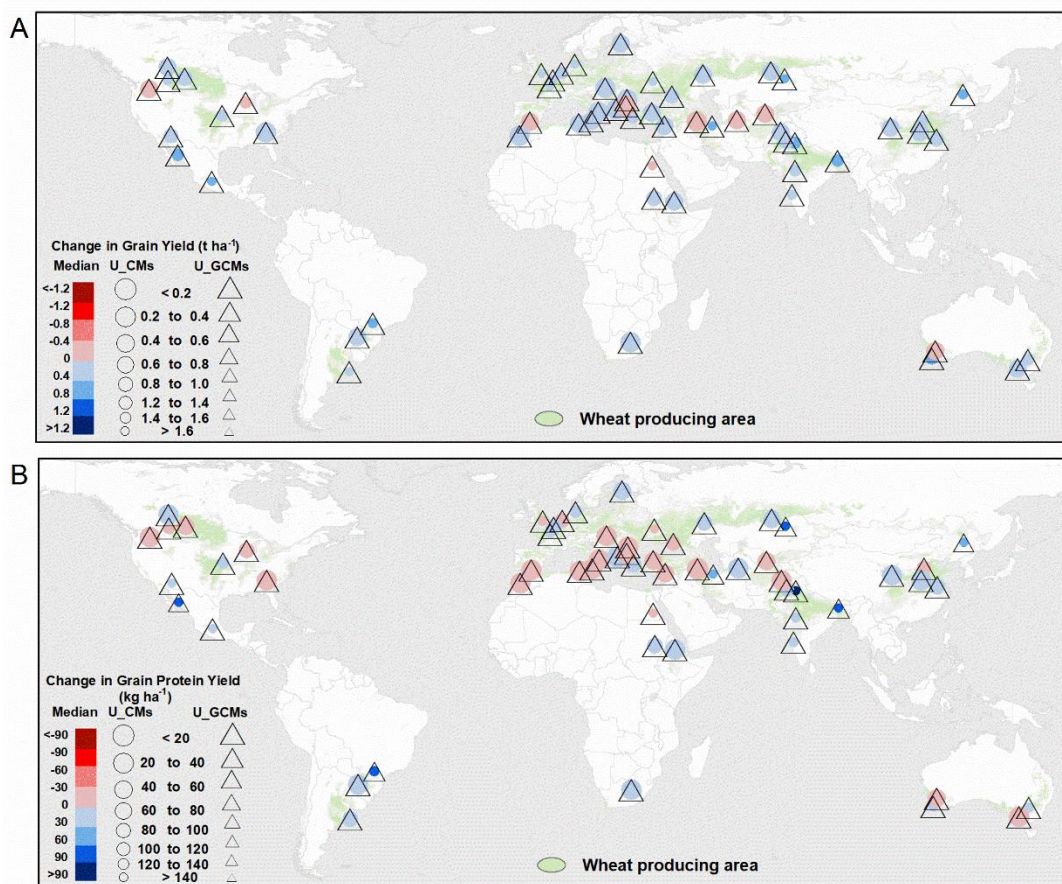
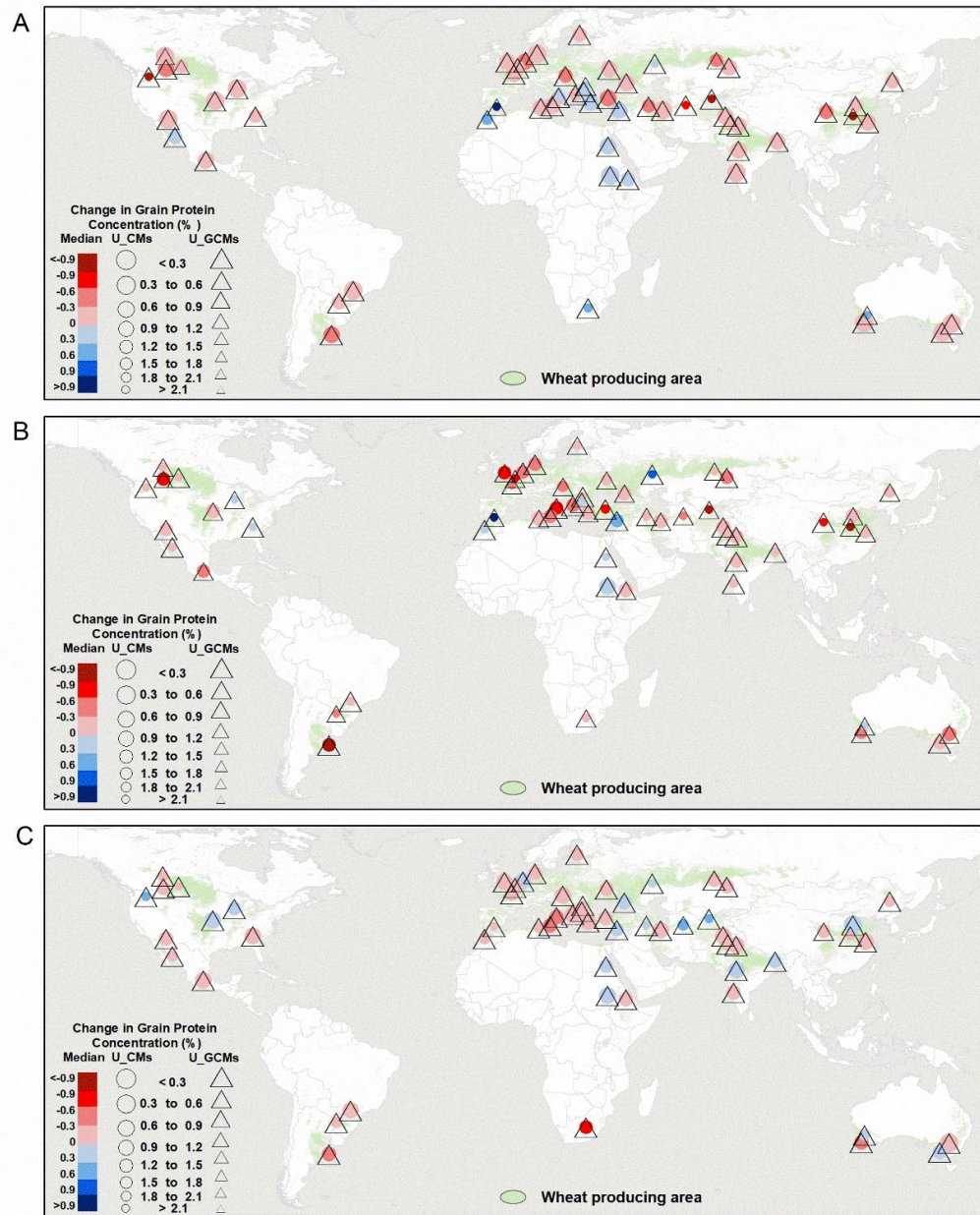


Fig. S16. Simulated trait effect for global wheat grain and protein yield. Absolute (A) grain yield and (B) grain protein trait effect for 2040-2069 (RCP8.5). Median across 32 crop models (18 for protein) and five GCMs and mean of 30 years using region-specific soils, cultivars, and crop management. Estimate of uncertainty given as range between 25th and 75th percentiles for crop models (circle size) and GCMs (triangle size). The larger the symbol, the less the uncertainty.



1

2 **Fig. S17.** Simulated global wheat grain protein concentration impacts from climate change with genotypic
3 adaptation. Absolute grain protein concentration impacts from climate change (A) without genetic adaptation and
4 (B) with genetic adaptation and (C) absolute traits effects for 2040-2069 (RCP8.5). Median across 18 crop models
5 and five GCMs and mean of 30 years using region-specific soils, cultivars, and crop management. Estimate of
6 uncertainty given as range between 25th and 75th percentiles for crop models (circle size) and GCMs (triangle size).
7 The larger the symbol, the higher the certainty.

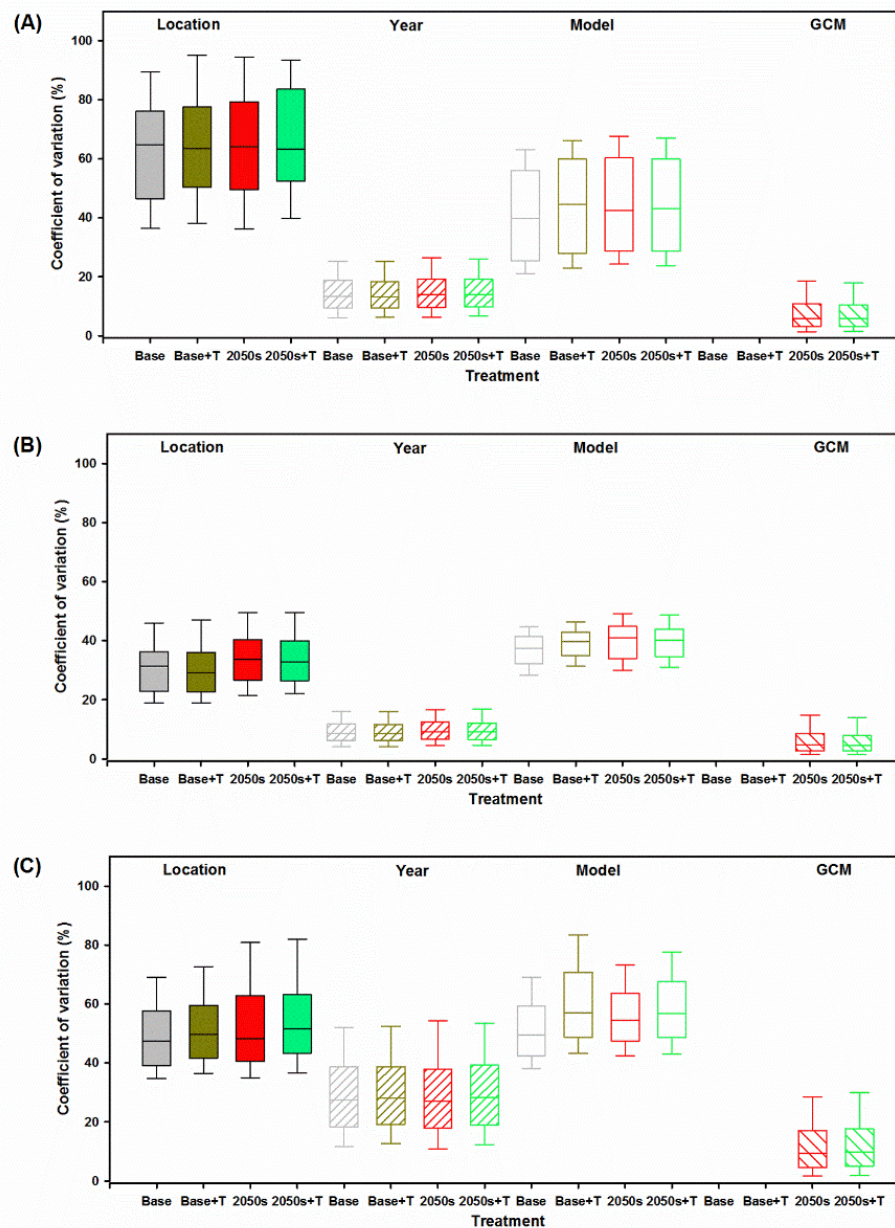
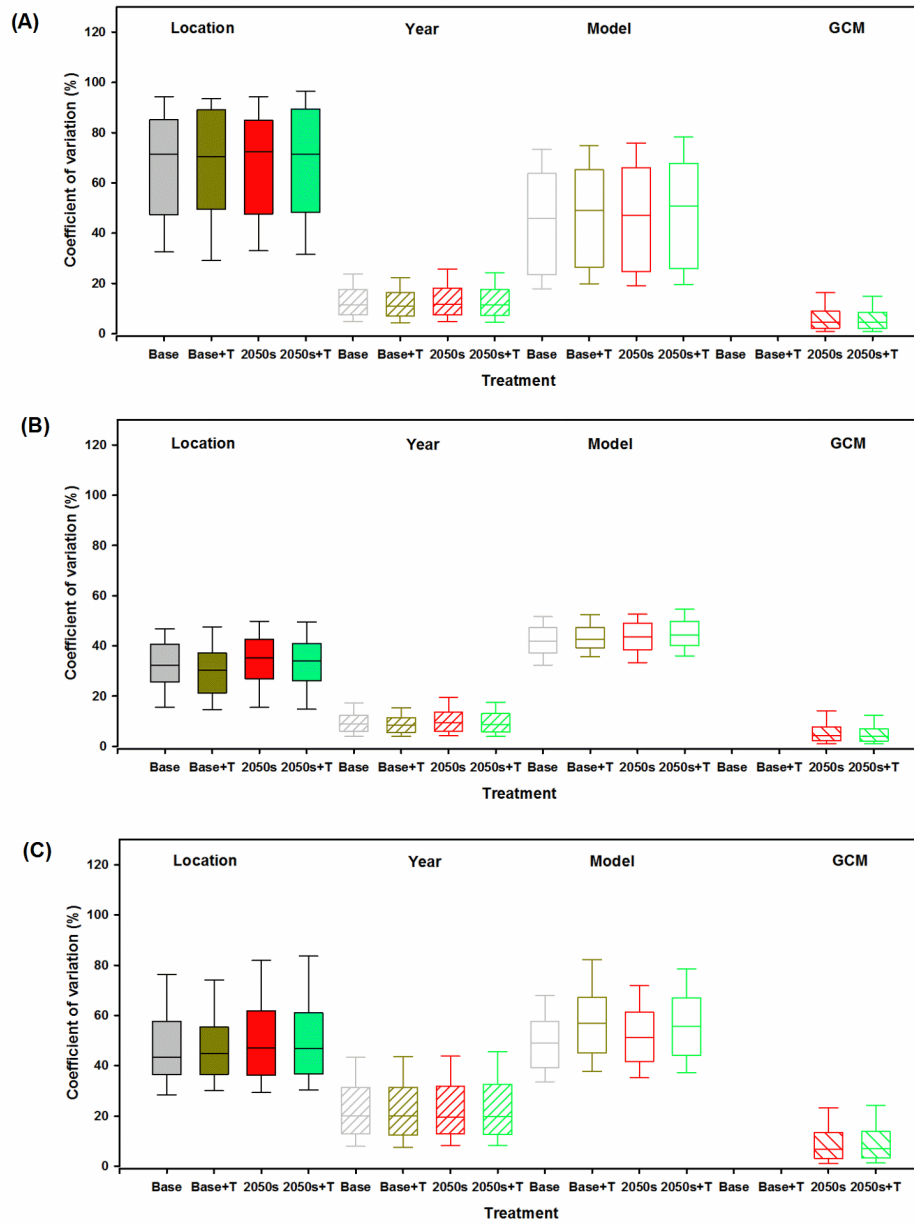


Fig. S18. Coefficient of variability of simulated wheat grain yields. (A) all 60 locations, (B) the 30 high rainfall or irrigated locations, and (C) the 30 low rainfall locations based on 32 crop models, five GCMs, and 30 years for baseline (Base), baseline with genetic adaptation (Base+T), climate change scenarios from 5 GCMs for 2040-2069 (RCP8.5) without genetic adaptation (2050s) and with genetic adaptation (2050s+T). In each box plot, horizontal lines represent from top to bottom, the 10th, 25th, 50th, 75th, and 90th percentiles of the simulations.



1

2 **Fig. S19.** Coefficient of variability of simulated wheat grain protein yields for (A) 60 locations, (B) for the high
3 rainfall and irrigated locations, and (C) for low rainfall locations, based on 18 crop models, 5 global climate models
4 (GCMs), 30 years. (A) 60 locations and (B) 30 high rainfall/irrigated locations and (C) 30 low rainfall locations for
5 baseline (Base), baseline plus traits (Base+T), climate change scenario for 2050s (RCP8.5) without traits (2050s)
6 and with traits (2050s+T). In each box plot, horizontal lines represent from top to bottom, the 10th, 25th, 50th, 75th,
7 and 90th percentiles of the simulations.

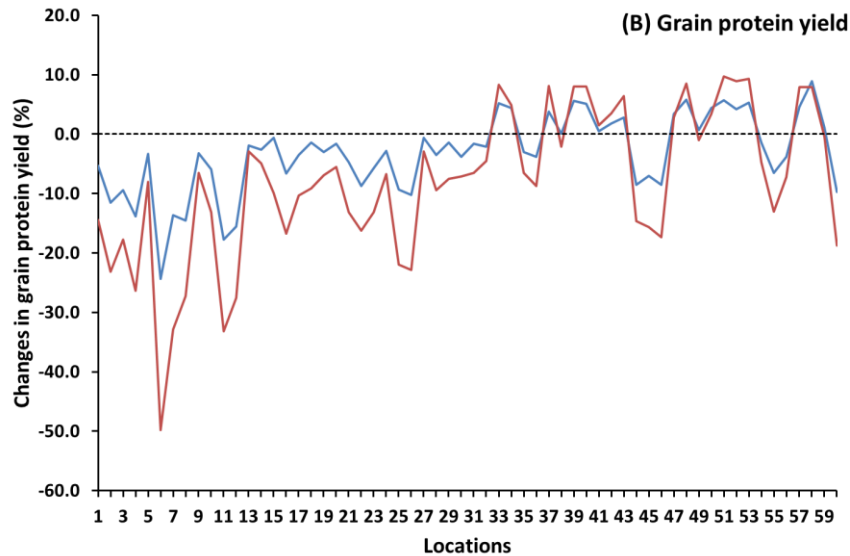
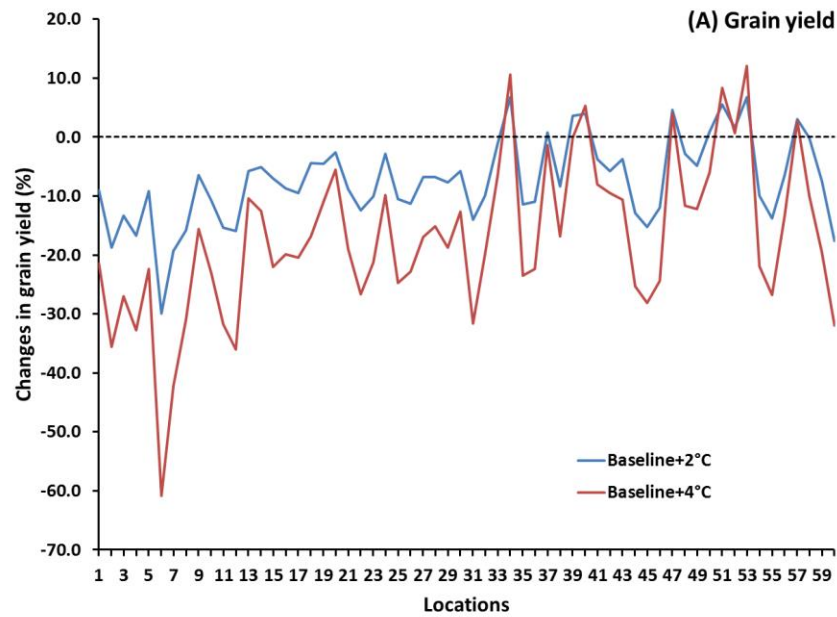


Fig. S20. Simulated wheat grain and protein yield impacts from increasing temperatures. Relative change in (A) grain yield and (B) for grain protein yield in response to a temperature increase of 2°C (Baseline+2°C) or 4°C (Baseline+4°C) for the baseline period (1981-2010) under historical CO₂ concentration (360 ppm) at the 60 global locations (locations 1 to 30 are irrigated or high rainfall and locations 31 to 60 are rainfed/low input; see Table S5 for details of the locations). Data are ensemble median for 32 crop models (18 for protein) and mean of 30 years using region-specific soils, cultivars, and crop management. Locations are connected by line to improve readability of this figure.

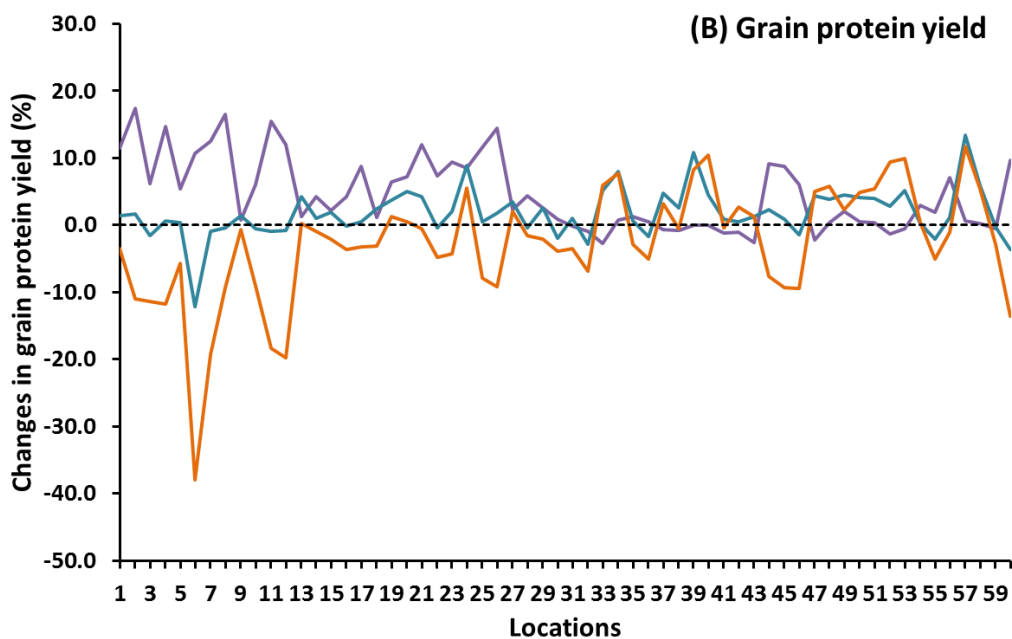
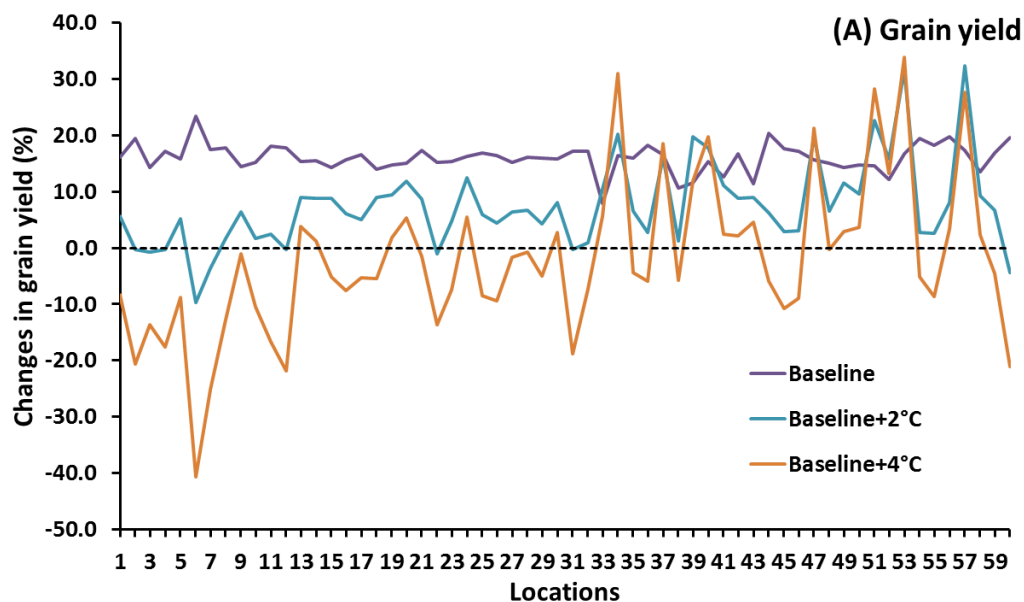


Fig. S21. Simulated wheat grain and protein yield impacts from elevated CO₂. Relative response to CO₂ (360 vs. 550 ppm) for (A) grain yield and (B) for grain protein yield for the baseline period (1981-2010; Baseline) and for the baseline period with a temperature increase of 2°C (Baseline+2°C) or 4°C (Baseline+4°C) at the 60 global locations (locations 1 to 30 are irrigated or high rainfall and locations 31 to 60 are rainfed/low input; see Table S5 for details of locations). Data are ensemble median for 32 crop models (18 for protein) and mean of 30 years using region-specific soils, cultivars, and crop management. Locations are connected by line to improve readability of this figure.

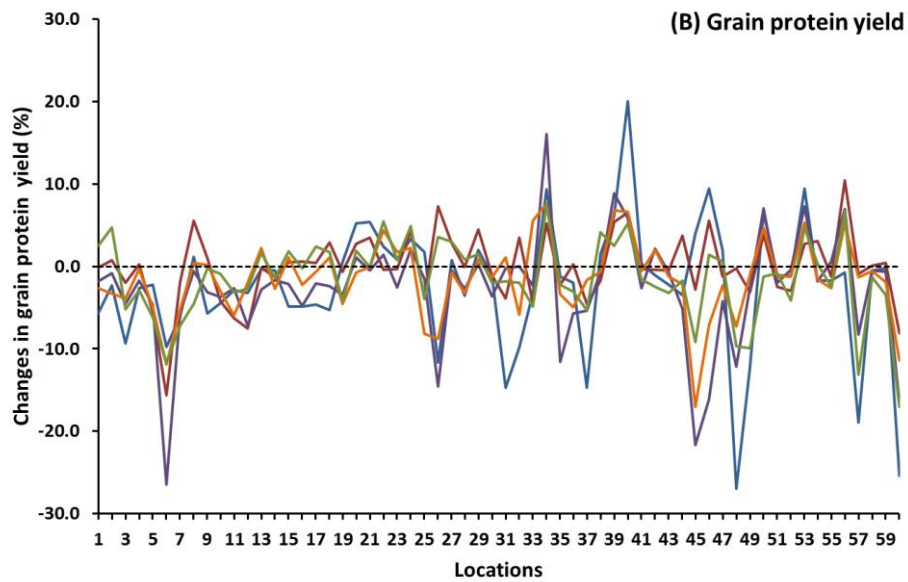
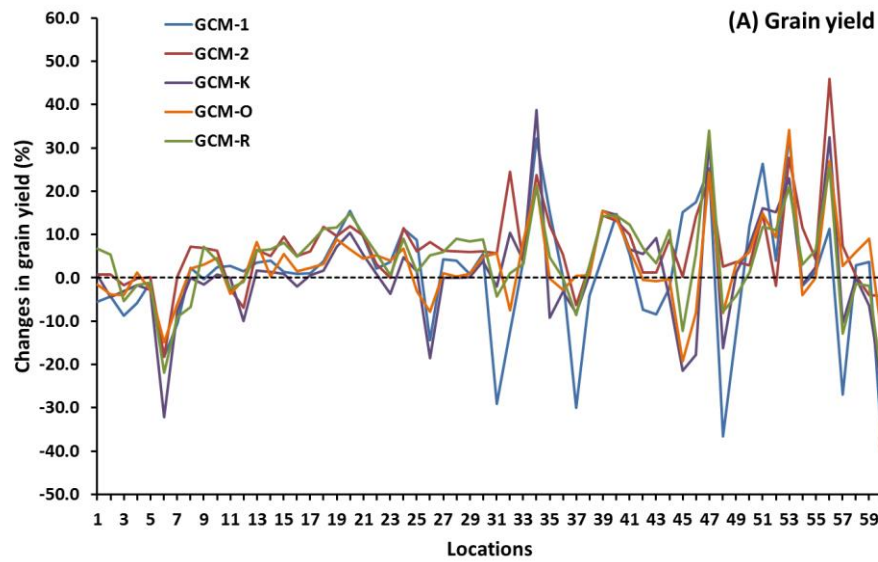


Fig. S22. Simulated wheat grain and protein yield impacts with climate change under five global climate models (GCMs) without genetic adaptation. Relative (A) grain yield and (B) grain protein yield impact for five GCMs for 2040-2069 (RCP8.5) at the 60 global locations (locations 1 to 30 are irrigated or high rainfall; locations 31 to 60 are rainfed/low input; see Table S5 for details of the locations). Data are ensemble median for 32 crop models (18 for protein), and mean of 30 years using region-specific soils, cultivars and crop management. Locations are connected by line to improve readability of this figure.

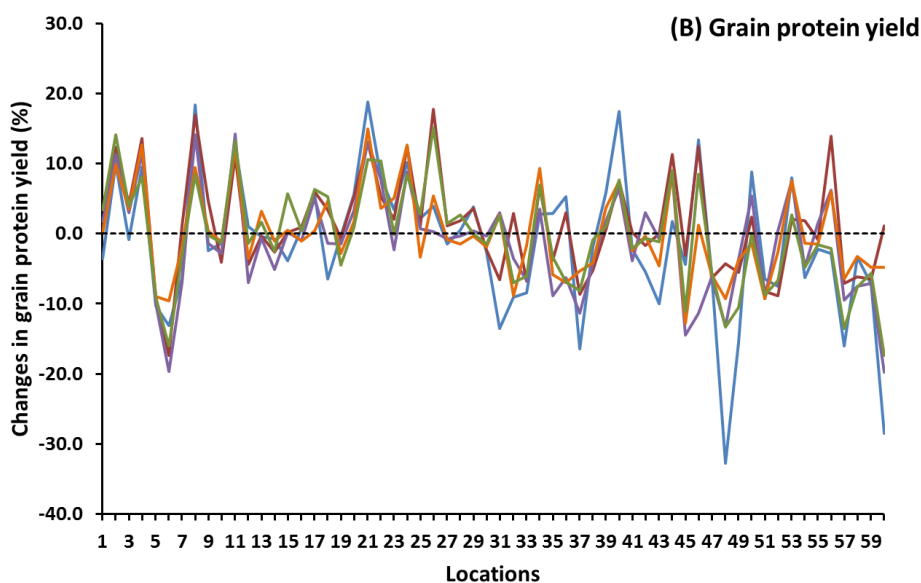
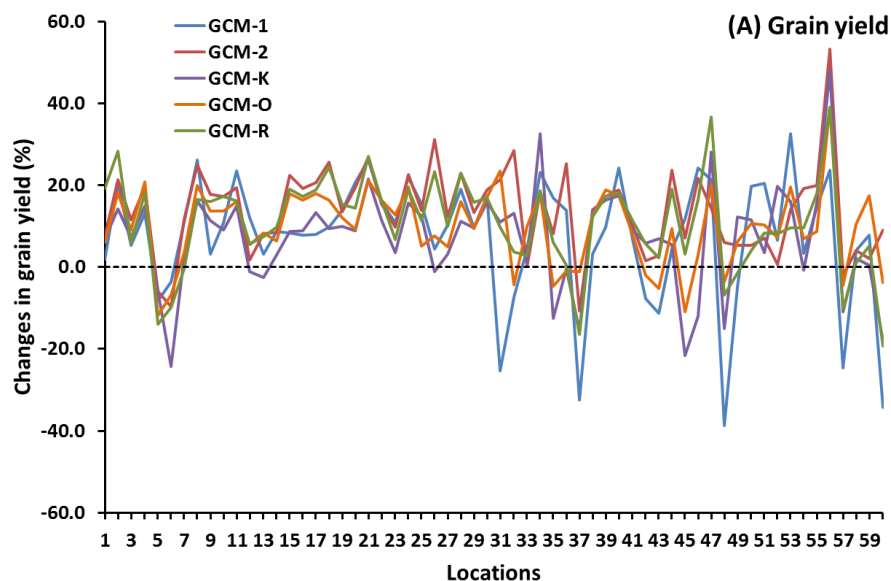


Fig. S23. Simulated wheat grain and protein yield impacts with climate change under five global climate models (GCMs) with genetic adaptation. Relative **(A)** grain yield and **(B)** grain protein yield impact for five GCMs for 2040-2069 (RCP8.5) at the 60 global locations (locations 1 to 30 are irrigated or high rainfall and locations 31 to 60 are rainfed/low input; see Table S5 for details of the locations). Data are ensemble median for 32 crop models (18 for protein), and mean of 30 years using region-specific soils, cultivars, and crop management. Locations are connected by line to improve readability of this figure.

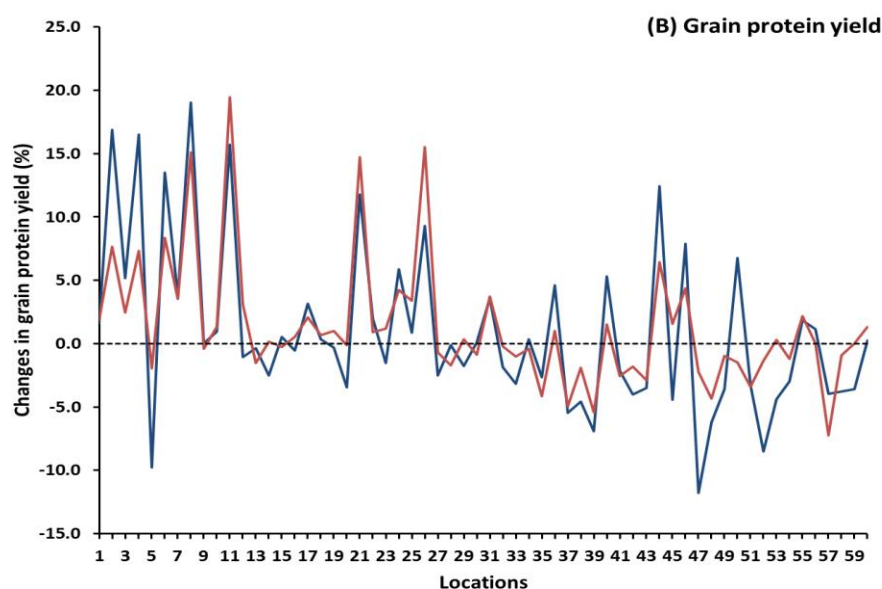
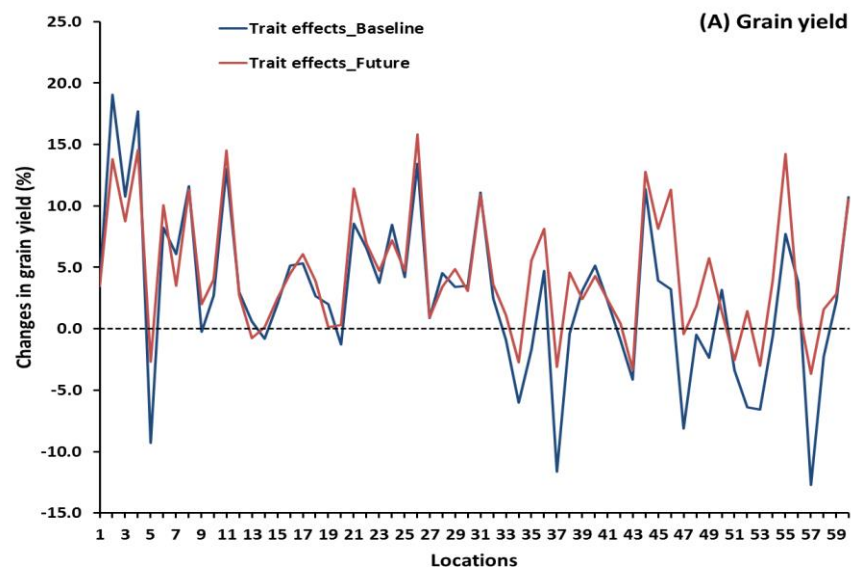


Fig. S24. Simulated effect of genetic adaptation for wheat grain and protein yield under baseline and climate change scenario for 2050s. Relative change in **(A)** grain yield and **(B)** grain protein yield for the baseline (1981-2010) and future climate scenarios for 2040-2069 (RCP8.5, five GCMs) at the 60 global locations (locations 1 to 30 are irrigated or high rainfall and locations 31 to 60 are rainfed/low input; see Table S5 for details of the locations). Data are ensemble median for 32 crop models (18 for protein) and mean of 30 years using region-specific soils, cultivars, and crop management. Locations are connected by line to improve readability of this figure.

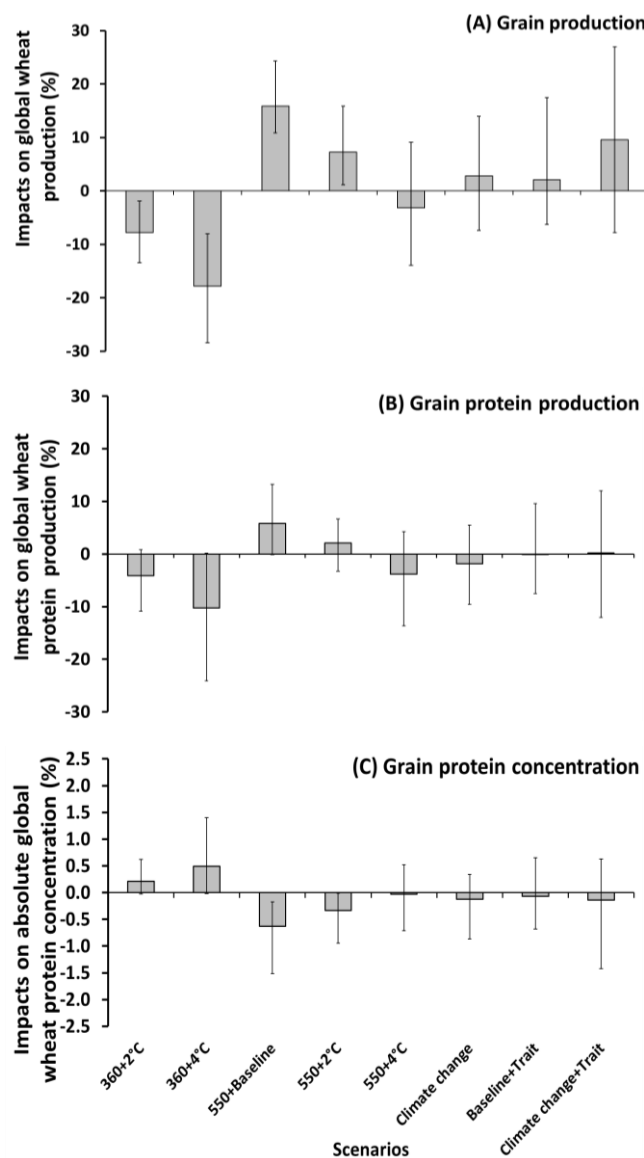


Fig. S25. Simulated global impacts of climate change scenarios on wheat production and protein. Relative impact on (A) grain production and (B) grain protein production, and (C) absolute impact on grain protein concentration for a 2°C (360+2°C) or 4°C (360+4°C) temperature increase for the baseline period with historical atmospheric CO₂ concentration (360 ppm) and for a 2°C (550+2°C) or 4°C (550+4°C) temperature increase for the baseline period with elevated CO₂ (550 ppm), and climate scenarios for 2040-2069 (RCP8.5, 5 GCMs) without (Climate change) and with (Climate change+Trait) genetic adaptation, and for the baseline period with genetic adaptation (Baseline+Trait). Impacts were weighted by production area. Data are ensemble median of 32 crop models (18 for protein) for 360+2°C, 360+4°C, 550+Baseline, 550+2°C, 550+4°C and Baseline+Trait, and ensemble median across 32 crop models and five GCMs for Climate change and Climate change+Trait, and mean of 30 years using region-specific soils, cultivars, and crop management. Error bars for 360+2°C, 360+4°C, 550+Baseline, 550+2°C, 550+4°C, and Baseline+Trait are the 25th and 75th percentiles across 32 crop models (18 for grain protein), and for Climate change and Climate change+Trait the 25th and 75th percentiles across 32 crop models and five GCMs together.

References

- Aggarwal P, Banerjee B, Daryaei M *et al.* (2006) InfoCrop: A dynamic simulation model for the assessment of crop yields, losses due to pests, and environmental impact of agro-ecosystems in tropical environments. II. Performance of the model. *Agricultural Systems*, **89**, 47-67.
- Al-Mulla Y, Wu J, Singh P, Flury M, Schillinger W, Huggins D, Stockle C (2009) Soil water and temperature in chemical versus reduced-tillage fallow in a Mediterranean climate. *Applied Engineering in Agriculture*, **25**, 45.
- Angulo C, Rötter R, Lock R, Enders A, Fronzek S, Ewert F (2013) Implication of crop model calibration strategies for assessing regional impacts of climate change in Europe. *Agricultural and Forest Meteorology*, **170**, 32-46.
- Araya T, Nyssen J, Govaerts B, Deckers J, Cornelis Wm (2015) Impacts of conservation agriculture-based farming systems on optimizing seasonal rainfall partitioning and productivity on vertisols in the Ethiopian drylands. *Soil and Tillage Research*, **148**, 1-13.
- Asseng S (2004) *Wheat Crop Systems: A Simulation Analysis*, Melbourne, Australia, CSIRO Publishing.
- Asseng S, Keating Ba, Fillery Irp *et al.* (1998) Performance of the APSIM-wheat model in Western Australia. *Field Crops Research*, **57**, 163-179.
- Asseng S, Travasso Mi, Ludwig F, Magrin Go (2013) Has climate change opened new opportunities for wheat cropping in Argentina? *Climatic change*, **117**, 181-196.
- Balkovič J, Van Der Velde M, Schmid E *et al.* (2013) Pan-European crop modelling with EPIC: Implementation, up-scaling and regional crop yield validation. *Agricultural Systems*, **120**, 61-75.
- Balkovič J, Van Der Velde M, Skalský R *et al.* (2014) Global wheat production potentials and management flexibility under the representative concentration pathways. *Global and Planetary Change*, **122**, 107-121.
- Bannayan M, Sanjani S, Alizadeh A, Lotfabadi Ss, Mohamadian A (2010) Association between climate indices, aridity index, and rainfed crop yield in northeast of Iran. *Field Crops Research*, **118**, 105-114.
- Basso B, Cammarano D, Troccoli A, Chen D, Ritchie J (2010) Long-term wheat response to nitrogen in a rainfed Mediterranean environment: Field data and simulation analysis. *European Journal of Agronomy*, **33**, 132-138.
- Beringer T, Lucht W, Schaphoff S (2011) Bioenergy production potential of global biomass plantations under environmental and agricultural constraints. *Global Change Biology Bioenergy*, **3**, 299-312.
- Berzsenyi Z, Györfy B, Lap D (2000) Effect of crop rotation and fertilisation on maize and wheat yields and yield stability in a long-term experiment. *European Journal of Agronomy*, **13**, 225-244.
- Biernath C, Gayler S, Bittner S, Klein C, Hogy P, Fangmeier A, Priesack E (2011) Evaluating the ability of four crop models to predict different environmental impacts on spring wheat grown in open-top chambers. *European Journal of Agronomy*, **35**, 71-82.
- Bondeau A, Smith Pc, Zaehle S, Schaphoff S, Lucht W, Cramer W, Gerten D (2007) Modelling the role of agriculture for the 20th century global terrestrial carbon balance. *Global Change Biology*, **13**, 679-706.
- Boogaard H, Kroes J (1998) Leaching of nitrogen and phosphorus from rural areas to surface waters in the Netherlands. *Nutrient Cycling in Agroecosystems*, **50**, 321-324.
- Brisson N, Gary C, Justes E *et al.* (2003) An overview of the crop model STICS. *European Journal of Agronomy*, **18**, 309-332.
- Brisson N, Mary B, Ripoche D *et al.* (1998) STICS: a generic model for the simulation of crops and their water and nitrogen balances. I. Theory and parameterization applied to wheat and corn. *Agronomie*, **18**, 311-346.

- 1 Cao W, Liu T, Luo W, Wang S, Pan J, Guo W (2002) Simulating organic growth in wheat based on the
2 organ-weight fraction concept. *Plant Production Science*, **5**, 248-256.
- 3 Cao W, Moss Dn (1997) Modelling phasic development in wheat: a conceptual integration of
4 physiological components. *Journal of Agricultural Science*, **129**, 163-172.
- 5 Challinor A, Wheeler T, Craufurd P, Slingo J, Grimes D (2004) Design and optimisation of a large-area
6 process-based model for annual crops. *Agricultural and Forest Meteorology*, **124**, 99-120.
- 7 Chen C, Wang E, Yu Q (2010a) Modeling Wheat and Maize Productivity as Affected by Climate Variation
8 and Irrigation Supply in North China Plain. *Agronomy Journal*, **102**, 1037-1049.
- 9 Chen Y, Carver Bf, Wang S, Cao S, Yan L (2010b) Genetic regulation of developmental phases in winter
10 wheat. *Molecular Breeding*, **26**, 573-582.
- 11 Cuculeanu V, Marica A, Simota C (1999) Climate change impact on agricultural crops and adaptation
12 options in Romania. *Climate Research*, **12**, 153-160.
- 13 Donaldson E, Schillinger Wf, Dofing Sm (2001) Straw production and grain yield relationships in winter
14 wheat. *Crop Science*, **41**, 100-106.
- 15 Fader M, Rost S, Muller C, Bondeau A, Gerten D (2010) Virtual water content of temperate cereals and
16 maize: Present and potential future patterns. *Journal of Hydrology*, **384**, 218-231.
- 17 Fao (1998) World Reference Base for Soil Resources. Rep.84. Rome.
- 18 Fao (2010) *Asian wheat producing countries-Uzbekistan-Central Zone*,
19 http://www.fao.org/ag/agp/agpc/doc/field/Wheat/asia/Uzbekistan/agroeco_central.htm (last
20 visited: 09.22.2015).
- 21 Ferrise R, Triossi A, Stratonovitch P, Bindi M, Martre P (2010) Sowing date and nitrogen fertilisation
22 effects on dry matter and nitrogen dynamics for durum wheat: An experimental and simulation
23 study. *Field Crops Research*, **117**, 245-257.
- 24 Franzluebbers Aj, Stuedemann Ja (2014) Crop and cattle production responses to tillage and cover crop
25 management in an integrated crop–livestock system in the southeastern USA. *European Journal*
26 *of Agronomy*, **57**, 62-70.
- 27 Gaiser T, Perkons U, Küpper Pm *et al.* (2013) Modeling biopore effects on root growth and biomass
28 production on soils with pronounced sub-soil clay accumulation. *Ecological Modelling*, **256**, 6-15.
- 29 Gbegbelegbe S, Cammarano D, Asseng S *et al.* (2017) Baseline simulation for global wheat production
30 with CIMMYT mega-environment specific cultivars. *Field Crops Research*, **202**, 122-135.
- 31 Gerten D, Schaphoff S, Haberlandt U, Lucht W, Sitch S (2004) Terrestrial vegetation and water balance -
32 hydrological evaluation of a dynamic global vegetation model. *Journal of Hydrology*, **286**, 249-
33 270.
- 34 Giunta F, Motzo R, Pruneddu G (2007) Trends since 1900 in the yield potential of Italian-bred durum
35 wheat cultivars. *European Journal of Agronomy*, **27**, 12-24.
- 36 Goudriaan J, Van Laar Hh (eds) (1994) *Modelling Potential Crop Growth Processes. Textbook With*
37 *Exercises*, Dordrecht, The Netherlands, Kluwer Academic Publishers.
- 38 Hansen S, Abrahamsen P, Petersen Ct, Styczen M (2012) DAISY: model use, calibration, and validation.
39 *Transaction of the ASABE*, **55**, 1317-1335.
- 40 Hansen S, Jensen H, Nielsen N, Svendsen H (1991) Simulation of nitrogen dynamics and biomass
41 production in winter-wheat using the Danish simulation model DAISY. *Fertilizer Research*, **27**,
42 245-259.
- 43 He J, Stratonovitch P, Allard V, Semenov Ma, Martre P (2010) Global Sensitivity Analysis of the Process-
44 Based Wheat Simulation Model SiriusQuality1 Identifies Key Genotypic Parameters and Unravels
45 Parameters Interactions. *Procedia - Social and Behavioral Sciences*, **2**, 7676-7677.
- 46 Heng Lk, Asseng S, Mejahed K, Rusan M (2007) Optimizing wheat productivity in two rain-fed
47 environments of the West Asia–North Africa region using a simulation model. *European Journal*
48 *of Agronomy*, **26**, 121-129.

- Hoogenboom G, White J (2003) Improving physiological assumptions of simulation models by using gene-based approaches. *Agronomy Journal*, **95**, 82-89.
- Hu J, Cao W, Zhang J, Jiang D, Feng J (2004) Quantifying responses of winter wheat physiological processes to soil water stress for use in growth simulation modeling. *Pedosphere*, **14**, 509-518.
- Hu W, Schoenau Jj, Cutforth Hw, Si Bc (2015) Effects of row-spacing and stubble height on soil water content and water use by canola and wheat in the dry prairie region of Canada. *Agricultural Water Management*, **153**, 77-85.
- Huang G, Zhang R, Li G *et al.* (2008) Productivity and sustainability of a spring wheat–field pea rotation in a semi-arid environment under conventional and conservation tillage systems. *Field Crops Research*, **107**, 43-55.
- Hunt La, Pararajasingham S (1995) CROPSIM-wheat - a model describing the growth and development of wheat. *Canadian Journal of Plant Science*, **75**, 619-632.
- Ilbeyi A, Ustun H, Oweis T, Pala M, Benli B (2006) Wheat water productivity and yield in a cool highland environment: Effect of early sowing with supplemental irrigation. *Agricultural Water Management*, **82**, 399-410.
- Iqbal M, Akhter J, Mohammad W, Shah S, Nawaz H, Mahmood K (2005) Effect of tillage and fertilizer levels on wheat yield, nitrogen uptake and their correlation with carbon isotope discrimination under rainfed conditions in north-west Pakistan. *Soil and Tillage Research*, **80**, 47-57.
- Islam T (1991) Water use of a winter wheat cultivar (*Triticum aestivum*). *Agricultural Water Management*, **19**, 77-84.
- Izaurrealde R, Solberg E, Nyborg M, Malhi S (1998) Immediate effects of topsoil removal on crop productivity loss and its restoration with commercial fertilizers. *Soil and Tillage Research*, **46**, 251-259.
- Izaurrealde R, Williams Jr, McGill Wb, Rosenberg Nj, Jakas Mq (2006) Simulating soil C dynamics with EPIC: Model description and testing against long-term data. *Ecological Modelling*, **192**, 362-384.
- Izaurrealde Rc, McGill Wb, Williams Jr (2012) Development and application of the EPIC model for carbon cycle, greenhouse-gas mitigation, and biofuel studies. In: *Managing agricultural greenhouse gases: Coordinated agricultural research through GRACEnet to address our changing climate*. (eds Liebig Ma, Franzluebbbers Aj, Follett Rf) pp Page. Amsterdam, Elsevier.
- Jamieson P, Semenov M (2000) Modelling nitrogen uptake and redistribution in wheat. *Field Crops Research*, **68**, 21-29.
- Jamieson P, Semenov M, Brooking I, Francis G (1998) Sirius: a mechanistic model of wheat response to environmental variation. *European Journal of Agronomy*, **8**, 161-179.
- Jones J, Hoogenboom G, Porter C *et al.* (2003) The DSSAT cropping system model. *European Journal of Agronomy*, **18**, 235-265.
- Kassie Bt, Asseng A, Porter Ch, Royce F (2016) Performance of DSSAT-Nwheat across a wide range of current and future growing conditions. *Field Crops Research*, **81**, 27-36.
- Keating Ba, Carberry Ps, Hammer Gl *et al.* (2003) An overview of APSIM, a model designed for farming systems simulation. *European Journal of Agronomy*, **18**, 267-288.
- Kersebaum K (2007) Modelling nitrogen dynamics in soil-crop systems with HERMES. *Nutrient Cycling in Agroecosystems*, **77**, 39-52.
- Kersebaum Kc (2011) Special features of the HERMES model and additional procedures for parameterization, calibration, validation, and applications. Ahuja, L.R. and Ma, L. (eds.). *Methods of introducing system models into agricultural research. Advances in Agricultural Systems Modeling Series 2*, Madison (ASA-CSSA-SSSA), 65-94.

- Khalil F, Samiha O, Nemat Allah O, Ghamis A (2011) DETERMINATION OF AGRO-CLIMATIC ZONES IN EGYPT USING A ROBUST STATISTICAL PROCEDURE. Fifteenth International Water Technology Conference, **IWTC - 15**.
- Kiniry Jr, Williams J, Major D *et al.* (1995) EPIC model parameters for cereal, oilseed, and forage crops in the northern Great Plains region. *Canadian Journal of Plant Science*, **75**, 679-688.
- Latiri K, Lhomme J-P, Annabi M, Setter TL (2010) Wheat production in Tunisia: progress, inter-annual variability and relation to rainfall. *European Journal of Agronomy*, **33**, 33-42.
- Latta J, O'leary G (2003) Long-term comparison of rotation and fallow tillage systems of wheat in Australia. *Field Crops Research*, **83**, 173-190.
- Lawless C, Semenov M, Jamieson P (2005) A wheat canopy model linking leaf area and phenology. *European Journal of Agronomy*, **22**, 19-32.
- Li C, Cao W, Zhang Y (2002) Comprehensive Pattern of Primordium Initiation in Shoot Apex of Wheat. *ACTA Botanica Sinica*, 273-278.
- Li S, Wheeler T, Challinor A, Lin E, Xu Y, Ju H (2010) Simulating the Impacts of Global Warming on Wheat in China Using a Large Area Crop Model. *Acta Meteorologica Sinica*, **24**, 123-135.
- Lithourgidis A, Damalas C, Gagianas A (2006) Long-term yield patterns for continuous winter wheat cropping in northern Greece. *European Journal of Agronomy*, **25**, 208-214.
- Maiorano A, Martre P, Asseng S *et al.* (2017) Crop model improvement reduces the uncertainty of the response to temperature of multi-model ensembles. *Field Crops Research*, **202**, 5-20.
- Malr (2003) Bulletin of Agriculture Economics, Central Administration of Agriculture Economics, Ministry of Agriculture and Land Reclamation. Dokki, Egypt.
- Martre P, Jamieson Pd, Semenov Ma, Zyskowski Rf, Porter Jr, Triboi E (2006) Modelling protein content and composition in relation to crop nitrogen dynamics for wheat. *European Journal of Agronomy*, **25**, 138-154.
- Mossé J, Huet J, Baudet J (1985) The amino acid composition of wheat grain as a function of nitrogen content. *Journal of Cereal Science*, **3**, 115-130.
- Müller C, Eickhout B, Zaehle S, Bondeau A, Cramer W, Lucht W (2007) Effects of changes in CO₂, climate, and land use on the carbon balance of the land biosphere during the 21st century. *Journal of Geophysical Research-Biogeosciences*, **112**.
- Nash Je, Sutcliffe Jv (1970) River flow forecasting through conceptual models part I - A discussion of principles. *Journal of Hydrology*, **10**, 282-290.
- Nendel C, Berg M, Kersebaum K *et al.* (2011) The MONICA model: Testing predictability for crop growth, soil moisture and nitrogen dynamics. *Ecological Modelling*, **222**, 1614-1625.
- O'leary G, Christy B, Nuttall J *et al.* (2015) Response of wheat growth, grain yield and water use to elevated CO₂ under a Free-Air CO₂ Enrichment (FACE) experiment and modelling in a semi-arid environment. *Global Change Biology*, **21**, 2670-2686.
- Oleary G, Connor D (1996a) A simulation model of the wheat crop in response to water and nitrogen supply .1. Model construction. *Agricultural Systems*, **52**, 1-29.
- Oleary G, Connor D (1996b) A simulation model of the wheat crop in response to water and nitrogen supply .2. Model validation. *Agricultural Systems*, **52**, 31-55.
- Oleary G, Connor D, White D (1985) A simulation-model of the development, growth and yield of the wheat crop. *Agricultural Systems*, **17**, 1-26.
- Pan J, Zhu Y, Cao W (2007) Modeling plant carbon flow and grain starch accumulation in wheat. *Field Crops Research*, **101**, 276-284.
- Pan J, Zhu Y, Jiang D, Dai Tb, Li Yx, Cao Wx (2006) Modeling plant nitrogen uptake and grain nitrogen accumulation in wheat. *Field Crops Research*, **97**, 322-336.

- Pavlova Vn, Varcheva Se, Bokusheva R, Calanca P (2014) Modelling the effects of climate variability on spring wheat productivity in the steppe zone of Russia and Kazakhstan. *Ecological Modelling*, **277**, 57-67.
- Pecetti L, Hollington P (1997) Application of the CERES-Wheat simulation model to durum wheat in two diverse Mediterranean environments. *European Journal of Agronomy*, **6**, 125-139.
- Porter J (1984) A model of canopy development in winter wheat. *The Journal of Agricultural Science*, **102**, 383-392.
- Porter Jr (1993) AFRCWHEAT2: a model of the growth and development of wheat incorporating responses to water and nitrogen. *European Journal of Agronomy*, **2**, 69-82.
- Portmann Ft, Siebert S, Döll P (2010) MIRCA2000—Global monthly irrigated and rainfed crop areas around the year 2000: A new high - resolution data set for agricultural and hydrological modeling. *Global biogeochemical cycles*, **24**.
- Priesack E, Gayler S, Hartmann H (2006) The impact of crop growth sub-model choice on simulated water and nitrogen balances. *Nutrient Cycling in Agroecosystems*, **75**, 1-13.
- Ramirez-Rodrigues Ma, Asseng S, Fraisse C, Stefanova L, Eisenkolbi A (2014) Tailoring wheat management to ENSO phases for increased wheat production in Paraguay. *Climate Risk Management*, **3**, 24-38.
- Reynolds Mp, Balota M, Delgado Mib, Amani I, Fischer Ra (1994) Physiological and morphological traits associated with spring wheat yield under hot, irrigated conditions. *Australian Journal of Plant Physiology*, **21**, 717-730.
- Ritchie Jt, Godwin Dc, Otter-Nacke S (1985) *CERES-wheat: A user-oriented wheat yield model. Preliminary documentation*.
- Ritchie S, Nguyen H, Holaday A (1987) Genetic diversity in photosynthesis and water-use efficiency of wheat and wheat relatives. *Journal of Cellular Biochemistry*, 43-43.
- Romero Cc, Hoogenboom G, Baigorria Ga, Koo J, Gijsman Aj, Wood S (2012) Reanalysis of a global soil database for crop and environmental modeling. *Environmental Modelling & Software*, **35**, 163-170.
- Rost S, Gerten D, Bondeau A, Lucht W, Rohwer J, Schaphoff S (2008) Agricultural green and blue water consumption and its influence on the global water system. *Water Resources Research*, **44**.
- Royo C, Villegas D, Rharrabti Y, Blanco R, Martos V, García Del Moral L (2006) Grain growth and yield formation of durum wheat grown at contrasting latitudes and water regimes in a Mediterranean environment. *Cereal Research Communications*, **34**, 1021-1028.
- Rötter Rp, Palosuo T, Kersebaum Kc *et al.* (2012) Simulation of spring barley yield in different climatic zones of Northern and Central Europe: a comparison of nine crop models. *Field Crops Research*, **133**, 23-36.
- Schillinger Wf, Schofstoll Se, Alldredge Jr (2008) Available water and wheat grain yield relations in a Mediterranean climate. *Field Crops Research*, **109**, 45-49.
- Semenov M, Shewry P (2011) Modelling predicts that heat stress, not drought, will increase vulnerability of wheat in Europe. *Scientific Reports*, **1**.
- Senthilkumar S, Basso B, Kravchenko An, Robertson Gp (2009) Contemporary Evidence of Soil Carbon Loss in the US Corn Belt. *Soil Science Society of America Journal*, **73**, 2078-2086.
- Shibu M, Leffelaar P, Van Keulen H, Aggarwal P (2010) LINTUL3, a simulation model for nitrogen-limited situations: Application to rice. *European Journal of Agronomy*, **32**, 255-271.
- Singels A, De Jager J (1991) Determination of optimum wheat cultivar characteristics using a growth model. *Agricultural Systems*, **37**, 25-38.
- Soltani A, Maddah V, Sinclair T (2013) SSM-Wheat: a simulation model for wheat development, growth and yield. *International Journal of Plant Production*, **7**, 711-740.

- 1 Sommer R, Piggitt C, Haddad A, Hajdibo A, Hayek P, Khalil Y (2012) Simulating the effects of zero tillage
2 and crop residue retention on water relations and yield of wheat under rainfed semiarid
3 Mediterranean conditions. *Field Crops Research*, **132**, 40-52.
- 4 Spitters Cjt, Schapendonk Ahcm (1990) Evaluation of breeding strategies for drought tolerance in potato
5 by means of crop growth simulation. *Plant and Soil*, **123**, 193-203.
- 6 Steduto P, Hsiao T, Raes D, Fereres E (2009) AquaCrop-The FAO Crop Model to Simulate Yield Response
7 to Water: I. Concepts and Underlying Principles. *Agronomy Journal*, **101**, 426-437.
- 8 Steduto P, Pocuca V, Caliendo A, Debaeke P (1995) An evaluation of the crop-growth simulation
9 submodel of epic for wheat grown in a Mediterranean climate with variable soil-water regimes.
10 *European Journal of Agronomy*, **4**, 335-345.
- 11 Stenger R, Priesack E, Barkle G, Sperr C (1999) Expert-N A tool for simulating nitrogen and carbon
12 dynamics in the soil-plant-atmosphere system. pp Page, New Zealand, Land Treatment
13 collective proceedings Technical Session.
- 14 Stockle C, Donatelli M, Nelson R (2003) CropSyst, a cropping systems simulation model. *European*
15 *Journal of Agronomy*, **18**, 289-307.
- 16 Taha Mh (2000) Soil fertility management in Egypt. Regional Workshop on Soil Fertility Management
17 Through Farmer Field Schools in the Near East, Amman, Jordan,, 2–5.
- 18 Tao F, Yokozawa M, Zhang Z (2009a) Modelling the impacts of weather and climate variability on crop
19 productivity over a large area: A new process-based model development, optimization, and
20 uncertainties analysis. *Agricultural and Forest Meteorology*, **149**, 831-850.
- 21 Tao F, Zhang Z (2010) Adaptation of maize production to climate change in North China Plain: Quantify
22 the relative contributions of adaptation options. *European Journal of Agronomy*, **33**, 103-116.
- 23 Tao F, Zhang Z (2013) Climate change, wheat productivity and water use in the North China Plain: A new
24 super-ensemble-based probabilistic projection. *Agricultural and Forest Meteorology*, **170**, 146-
25 165.
- 26 Tao F, Zhang Z, Liu J, Yokozawa M (2009b) Modelling the impacts of weather and climate variability on
27 crop productivity over a large area: A new super-ensemble-based probabilistic projection.
28 *Agricultural and Forest Meteorology*, **149**, 1266-1278.
- 29 Tavakkoli Ar, Oweis Ty (2004) The role of supplemental irrigation and nitrogen in producing bread wheat
30 in the highlands of Iran. *Agricultural Water Management*, **65**, 225-236.
- 31 Triboi E, Triboi-Blondel A, Martignac M, Falcimagne R (1996) Experimental device for studying post-
32 anthesis canopy functioning in relation to grain quality. In: *Proc 4th European Society of*
33 *Agronomy Congress, Amsterdam Academic Press, Wageningen, The Netherlands, pp68-69.* pp
34 Page.
- 35 Van Rees H, McClelland T, Hochman Z, Carberry P, Hunt J, Huth N, Holzworth D (2014) Leading farmers in
36 South East Australia have closed the exploitable wheat yield gap: Prospects for further
37 improvement. *Field Crops Research*, **164**, 1-11.
- 38 Wang E, Engel T (2000) SPASS: a generic process-oriented crop model with versatile windows interfaces.
39 *Environmental Modelling & Software*, **15**, 179-188.
- 40 Wang E, Robertson Mj, Hammer Gl *et al.* (2002) Development of a generic crop model template in the
41 cropping system model APSIM. *European Journal of Agronomy*, **18**, 121-140.
- 42 Webber H, Gaiser T, Oomen R *et al.* (2016) Uncertainty in future irrigation water demand and risk of
43 crop failure for maize in Europe. *Environmental Research Letters*, **11**, 074007.
- 44 Weir A, Bragg P, Porter J, Rayner J (1984) A winter wheat crop simulation model without water or
45 nutrient limitations. *The Journal of Agricultural Science*, **102**, 371-382.
- 46 Williams J (1995) *The EPIC model in: Computer Models of Watershed Hydrology*, Water Resources
47 Publications, Highlands Ranch, Colorado, USA.

- 1 Williams Jr, Jones Ca, Kiniry Jr, Spanel Da (1989) The EPIC crop growth model. Transactions of the ASAE,
2 **32**, 497-511.
- 3 Yan M, Cao W, C. Li Zw (2001) Validation and evaluation of a mechanistic model of phasic and
4 phenological development in wheat. Chinese Agricultural Science, **1**, 77-82.
- 5 Yin X, Van Laar Hh (2005) *Crop systems dynamics: an ecophysiological simulation model of genotype-by-*
6 *environment interactions*, Wageningen, The Netherlands, Wageningen Academic Publishers.

7